5-13-2022

Characterization of Quaternary stratigraphy in the Mississippi Sound to evaluate the influence of geologic heterogeneity on submarine groundwater transport and discharge

Zachary Peoples
Mississippi State University, zacharyp1@gmail.com

Characterization of Quaternary stratigraphy in the Mississippi Sound to evaluate the influence of geologic heterogeneity on submarine groundwater transport and discharge

By

Zachary Peoples

Approved by:

Adam Skarke (Major Professor)
Varun G. Paul
Alex Beebe
Andrew E. Mercer (Graduate Coordinator)
Rick Travis (Dean, College of Arts & Sciences)

A Thesis
Submitted to the Faculty of
Mississippi State University
in Partial Fulfillment of the Requirements
for the Degree of Master of Science
in Geology
in the Department of Geosciences

Mississippi State, Mississippi

May 2022

Name: Zachary Peoples

Date of Degree: May 13, 2022

Institution: Mississippi State University

Major Field: Geology

Major Professor: Adam Skarke

Title of Study: Characterization of Quaternary stratigraphy in the Mississippi Sound to evaluate the influence of geologic heterogeneity on submarine groundwater transport and discharge

Pages in Study: 91

Candidate for Degree of Master of Science

Submarine Groundwater Discharge (SGD) through seafloor sediments is gaining recognition as an important component of coastal water quality. Stratigraphic features creating geologic heterogeneity, such as incised paleochannels, may influence preferential pathways for SGD. The central Mississippi Sound is underlain by paleochannels that were incised into Pleistocene sediments while the area was subaerially exposed during the last glacial maximum and are now buried by transgressive Holocene deposits. In this thesis, newly collected chirp, previously published seismic reflection, and sediment core data are used to characterize the three-dimensional structure of the Holocene-Pleistocene contact. Results indicate that Pleistocene paleochannels cross-cut the study area, exhibiting depths from 7.3–23.4 m, widths from 0.2–2.5 km, infilling with higher acoustic impedance fluvial sediments, and burial by transgressive Holocene sediments. Results suggest that this shallow subsurface stratigraphy may mediate locations of SGD and aid in predicting SGD pathways and associated contaminant loading into the coastal ocean.

ACKNOWLEDGEMENTS

I would like to thank my advisor, Dr. Adam Skarke, for his time, constant support, advice, and guidance throughout my time at Mississippi State University. I would also like to thank Dr. Alex Beebe for recommending me for this program, Dr. Varun Paul for his encouragement and insight, and both for serving as members of my committee. I would also like to thank Jonathan Harris for serving as captain of our research vessel during data collection. Finally, I would like to thank everyone who helped me throughout this process, especially those closest to me. This research was funded by the United States Department of Treasury through the Mississippi Based RESTORE Act Center of Excellence (award number: 8006490-05.01).

TABLE OF CONTENTS

LIST OF FIGURES

CHAPTER I

INTRODUCTION

The hydrogeological research community has seen major advances in the last several decades in understanding the interaction of groundwater and ocean water through submarine groundwater discharge (Beusen et al., 2013; Rabouille et al., 2001; Taniguchi et al., 2019; Zektser and Loaiciga, 1993). Submarine groundwater discharge (SGD) is considered both the input of fresh groundwater from land derived sources into the ocean and the mixing and recycling of ocean-derived groundwater that infiltrates and returns to the surface water (Burnett et al., 2003). In locations where the water table in a coastal unconfined aquifer is higher than the mean sea level, the hydraulic gradient will result in terrestrial fresh groundwater discharging into the ocean. Seawater also intrudes into the aquifer, creating a zone where freshwater and saltwater mix (Breier et al., 2005; Robinson et al., 2018). Submarine groundwater discharge has been identified as a key source of continent-derived nutrients, solutes, and subsequent contaminants in marine environments (Kroeger and Charette, 2008; Moore, 1999; Taniguchi et al., 2019; Zhao et al., 2021).

While rivers are an obvious and easily gauged input into the ocean, submarine groundwater discharge has not been recognized until recently, due to the difficulty of observation and assessment as no exact gauging method exists. With recent advancements in techniques used to trace submarine groundwater and estimate discharge rate, there is greater recognition that terrestrial recharge and recycling of ocean-derived submarine groundwater results in substantial

flow through coastal sediments and delivery of solutes to the coastal ocean (Taniguchi et al., 2019). Because submarine groundwater discharge is now recognized as an important source of nutrients and contaminants, there is substantial interest in understanding and predicting where it occurs. This effort is complicated by the fact that groundwater transport through submarine aquifers is often spatially and temporally variable due to non-uniform hydraulic conductivity largely resulting from geologic heterogeneity (Bratton, 2007; Robinson et al., 2018; Russoniello et al., 2013; Sawyer et al., 2013). As recognition of the importance of submarine groundwater discharge has grown in the scientific community, so too has recognition that site-specific subsurface surveys are necessary to characterize shallow geologic heterogeneity and its potential influence on submarine groundwater conductivity (Taniguchi et al., 2019). Beneath Holocene sediments, ancient fluvial channel, or paleochannel, networks have been incised into the once exposed continental shelf, eroding and replacing sediments with coarse-grained channel deposits, which are then covered by finer-grained transgressive deposits. These finer-grained sediments act as a confining layer which may aid in preventing nearshore discharge and extend discharge further from shore, exposing marine life in these locations to contaminants that may be carried by the discharge.

Although several studies of coastlines and continental shelves have been successful in connecting paleochannel networks to SGD (Russoniello et al., 2013; Spalt et al., 2018; Viso et al., 2010), not all locations have been examined. To address this knowledge gap, this thesis investigates and maps the spatial heterogeneity of shallow sedimentary deposits in the central Mississippi Sound study area (Figure 1.1), with emphasis on understanding how shallow subsurface lithologic variability influences hydrologic conductivity and submarine groundwater discharge in the study area. Previous research efforts (Gal, 2018; Hollis, 2018; Adcock, 2019)

have successfully generated maps of Quaternary sedimentary paleovalley fill in adjacent areas of the Mississippi Sound.

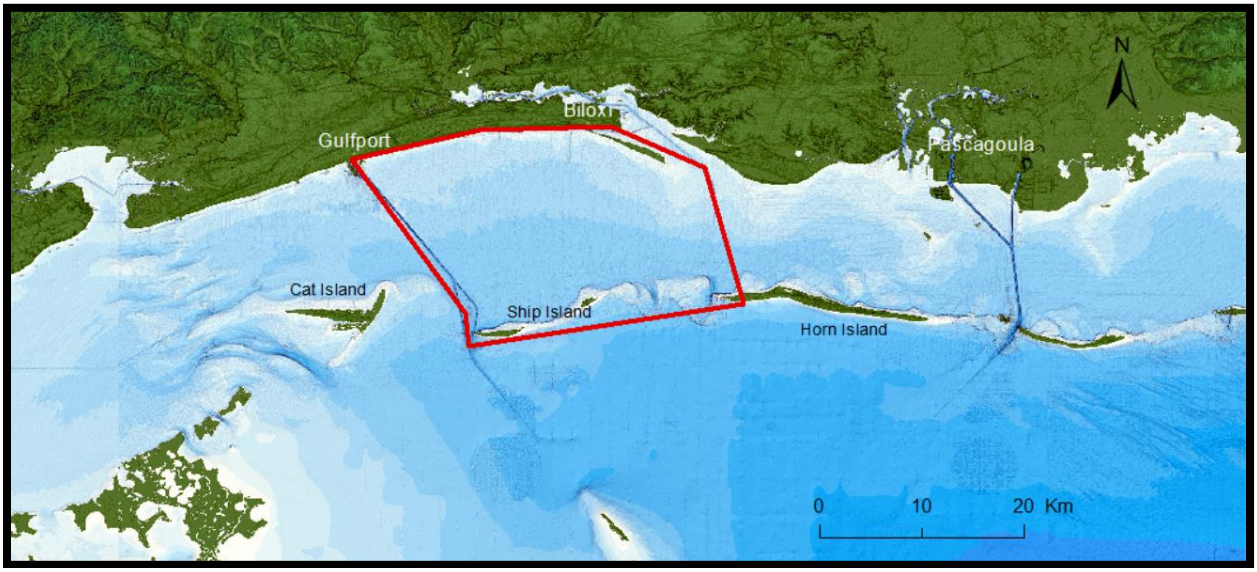

Figure 1.1 Location of study area, outlined in red, in the central Mississippi Sound.

CHAPTER II

BACKGROUND

2.1 Fluvial Geomorphology

Fluvial channels are landforms that discharge water and sediment downgradient, scaling in size due to variations in slope, velocity, width, depth, climate, tectonic activity, bed material grain size and texture, and the presence or absence of bank-stabilizing vegetation (Church, 2006; Dade and Friend, 1998; Leopold and Maddock, 1953; Posamentier and Vail, 1988; Williams, 1978). The balance of these variable conditions determines the propensity for aggradation or degradation (Church, 2006); channel beds aggrade when sediment supply exceeds bed load transport rates and degrade when transport rates exceed sediment supply (Blum and Törnqvist, 2000). Since alluvial channels are composed of sediments, the banks are erodible as well as the bed, leading to varying degrees of channel instability (Schumm, 1985). Depositional patterns, such as braided (shifting multi-channel), anabranching (stable multi-channel), meandering (sinuous single-channel), and straight (single-channel), are a function of the channel gradient, discharge, and sediment load type and amount (Church, 2006; Dade and Friend, 1998; Schumm, 1985). Typically, sediment grain size can be correlated to the gradient of the channel; channels with steep gradients have a higher water velocity, larger-grain bed loads, and an increase in the size of suspended sediments, conversely, near-base-level channels with a shallow gradient have a lower water velocity, smaller-grained bed loads, and much finer-grained suspended sediments (Leopold and Maddock, 1953; Posamentier and Vail, 1988; Rubey, 1952; Shulits, 1941).

Channels that transport suspended sediments with low sand and gravel bed loads through fine-grained, highly cohesive bank alluvium often exhibit a sinuous meander pattern, while channels with abundant, coarse sediment loads and highly unstable banks have a meandering or braided pattern (Church, 2006; Lunt and Bridge, 2004; Schumm, 1977, 1985).

These depositional patterns are dynamic and can shift in response to temporal changes of autogenic and allogenic boundary controls, where autogenic refers to internally-imposed fluctuations in processes and rates such as water or sediment supply, and allogenic refers to externally-imposed changes such as climate change and sea level rise and fall (Blum et al., 1995, 2013; Blum and Törnqvist, 2000; Starkel, 1991). A change in sea level, whether shortening or lengthening the longitudinal profile, has an effect on the channel gradient proportional to the magnitude of sea-level change (Posamentier and Vail, 1988); however, this effect is stronger near the base level of the profile (Blum, 1993; Shanley and McCabe, 1994; Törnqvist, 1998). Sea level rise along a continental margin results in the shortening of the channel, decreasing the distance over which sediments can be stored and usually flattening the channel slope (Blum and Törnqvist, 2000). However, sea-level decline will lengthen the channel by incising valleys across the newly exposed shelf, with subsequent transport of stored sediments seaward as more accommodation space is available (Allen and Posamentier, 1993; Blum, 1993, 2013; Dalrymple et al., 1994; Posamentier et al., 1992; Zaitlin et al., 1994), bypassing the new shelf (Blum, 1993; Talling, 1998) and depositing as a lowstand wedge further basinward (Mitchum, 1985).

2.2 Paleochannels and Submarine Groundwater Discharge

In the context of this thesis, geologic heterogeneity is considered the stratigraphic differing of Pleistocene units to the morphological effects of fluvial channels and their associated alluvium. Although limited work has been conducted to examine the effects of SGD (Beusen et

al., 2013; Cable et al., 1997; Essaid, 1990; Portnoy et al., 1998; Rabouille et al., 2001; Robinson and Gallagher, 1999; Taniguchi et al., 2019; Wicks and Herman, 1995; Zektser and Loaiciga, 1993), due to spatial and temporal variances and difficulties in assessment, even less has been conducted for the effects of paleochannels (Daniel et al., 1996; Mulligan et al., 2007; Russoniello et al., 2013; Spalt et al., 2018; Viso et al., 2010).

Paleochannels, or ancient fluvial channel valleys that are now a part of the stratigraphic record, exhibit varying characteristics between river systems due to geologic influences such as uplift and subsidence rates, the scale of the river system, controlling influences on sediment transfer and storage, and proximity to the river mouth and its migration due to eustatic sea level change (Blum et al., 2013; Blum and Törnqvist, 2000). The most common types of valleys are differentiated as bedrock and mixed-bedrock-alluvial valleys (where the channels directly impact bedrock and are in a long-term state of incision), coastal-plain valleys (extend from the upstream limits of sea level influence to the highstand shoreline and are fully alluvial), and cross-shelf paleovalleys (occur between highstand shorelines and the shelf margin and contain fluvial, estuarine, and shallow-marine deposits) (Blum et al., 2013). Paleochannels associated with cross-shelf paleovalleys are common features beneath the modern coastal plain sediments of the Gulf of Mexico and eastern United States (Harris et al., 2005; Thieler et al., 2014).

Since cross-shelf Pleistocene paleochannels are ubiquitous along the continental shelf in the Gulf of Mexico (Adcock, 2019; Anderson et al., 2004; Bartek et al., 2004; Coleman and Roberts, 1988; Fisk, 1947; Fisk et al., 1954; Flocks et al., 2015; Gal, 2018; Greene et al., 2007; Hollis, 2018, Kindinger, 1989; Kindinger et al., 1994; McBride et al., 2004; Spalt et al., 2018; Zaitlin et al., 1994), understanding the spatial effects of paleochannels on SGD is central to making accurate predictions of water balances for coastal aquifers. When fluvial channels are

incised across a newly exposed regressive surface, the channel fill is typically coarser-grained than the sediments that were incised (Allen, 1991; Allen and Posamentier, 1993; Dalrymple et al., 1992; Green, 2009; Mulligan et al., 2007; Zaitlin et al., 1994). After the period of maximum regression, transgressive deposition is initiated by a rise in sea level. Sedimentation rates on the submerged portion of the continental shelf are dependent on the rate of sea-level rise; thinner strata will be deposited where transgressive episodes are more rapid, and thicker strata where rise is slower (Anderson et al., 2016). Incised valleys on the continental shelf are filled with finer transgressive sediments if the channels are under-filled valleys, as opposed to an over-filled valley, which is filled entirely of fluvial sediments (Simms et al., 2006). During sea-level rise, fluvial sediment supply is commonly less than during times of maximum incision during the lowstand since the channel longitudinal profile is shortened, reducing accommodation space, resulting in a drowned-valley estuary at the seaward end of the incised valley (Blum et al., 2013; Dalrymple et al., 1994).

Transgressive sediments that have filled in the fluvial channels form a less-permeable sediment cap over the more porous fluvial fill (Allen, 1991; Foyle and Oertel, 1997; Green, 2009; Mulligan et al., 2007; Russoniello et al., 2013), impeding vertical flow and directing groundwater laterally through the porous channel sediments, preventing submarine groundwater discharge nearshore (Mulligan et al., 2007; Russoniello et al., 2013). Significant spatial distributions of SGD are possible where paleochannels have been incised across confining units, leading to seepage further from shore (Breier and Edmonds, 2007; Russoniello et al., 2013; Spalt et al., 2018).

2.3 Late Quaternary Sea Level

The late Quaternary sedimentary record is ordered into five chronostratigraphic stages (Figure 2.1) based on eustatic sea-level fluctuations and marine transgressive-regressive sequences (Bard et al., 1990a, 1990b, 1996; Fairbanks, 1989, 1992; Kindinger, 1988; Kindinger et al., 1989). These glacial and interglacial marine isotope stages (MIS) have been determined from the oxygen isotope ratio ($^{18}O/^{16}O$, or $\delta^{18}O_b$) of calcium carbonate ($CaCO_3$) shells of benthic foraminifera (Bouvier-Soumagnac and Duplessy, 1985; McCrea, 1950; Zeebe, 1999). This ratio is a function of both the isotopic composition and the water temperature of ancient oceans in which the shell was formed (Chappell et al, 1996; Emiliani, 1955; Lisiecki and Raymo, 2005; Waelbroeck et al., 2012; Wefer and Berger, 1991). When ocean water is evaporated, isotopic fractionation occurs, leaving the heavier ^{18}O and transporting the ^{16}O atmospherically poleward

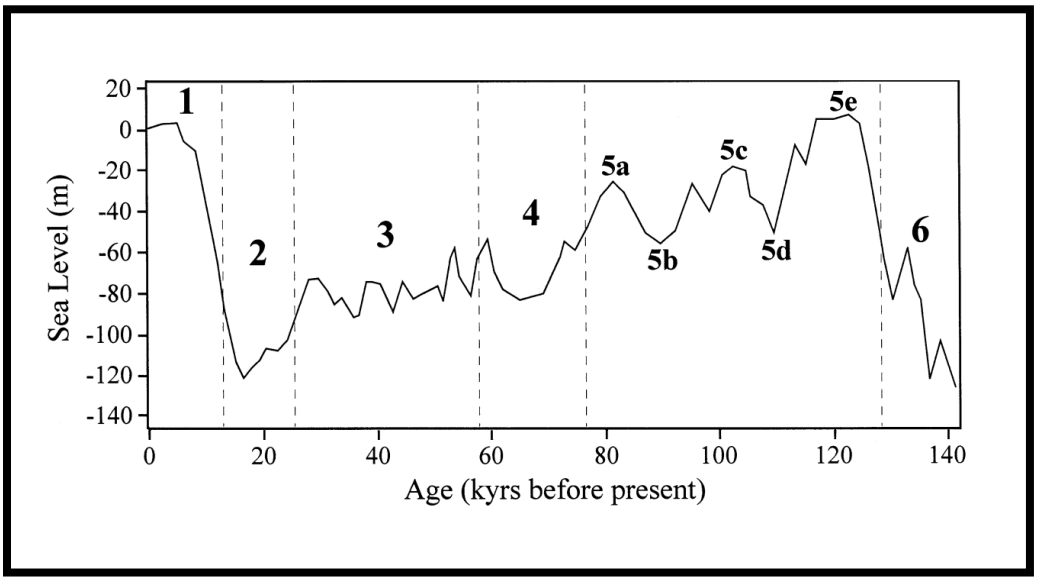

Figure 2.1 Eustatic sea level curve from Th-U dating of corals (from Chappell et al., 1996) with oxygen isotope stages separated by dashed lines (modified from Blum and Törnqvist, 2000).

to precipitate and accumulate as glaciers and ice sheets (Covey and Haagenson, 1984; Dansgaard, 1964). As more ^{16}O is locked into polar ice and sea level drops, organisms will incorporate the increasingly abundant ^{18}O in bioprecipitated shell material. Several complementary studies (Bard et al., 1990b; Chappell et al., 1996; Chen et al., 1991; Edwards et al., 1986; Stein et al., 1993) have used ^{230}Th–^{234}U and ^{234}U–^{238}U dating of corals to test the accuracy of the oxygen isotope ratio sea level calculations, finding them to be in good agreement and resolving some uncertainties with previous age calculations.

During the last interglacial highstand (MIS 5e) between ca. 131±1–112 ka (Bard et al., 1990b; Chen et al., 1991; Collins et al., 1993; Dia et al., 1992; Edwards et al., 1986; Helmens, 2014; Ludwig et al., 1996; Szabo et al., 1994; Zhu et al., 1993), eustatic sea level was ~2–8 m above the present mean level (Collins et al., 1993; Hearty and Kindler, 1997; Kopp et al., 2009; Otvos, 2018; Zhu et al., 1993). Around 122 ka, oxygen and carbon isotope records of benthic foraminifera from Ocean Drilling Project site 658 in the Eastern Atlantic show a short cold event and climate instability of a few hundred years at the peak of the interglacial period (Maslin and Tzedakis, 1996). This is supported by a coincident period of ash deposition triggered by catastrophic volcanism (Linsley, 1996) and U-series dating, which indicates that coral reef building starts at 127 ka and ends at 122 ka, the start of the cold event (Stirling et al., 1995). For the remainder of the MIS 5 period, substages MIS 5d–5a represent alternating cooler and warmer phases with subsequent sea level change between 113 and 76 ka (Richmond and Fullerton, 1986; Cutler et al., 2003): Substage MIS 5d relative sea level of –50 m (van Andel and Tzedakis, 1996); Substage MIS 5c relative sea level of –6 to –16 m (Bloom et al., 1974; Cabioch and Ayliffe, 2001; Dodge et al., 1983; Mesolella et al., 1969); Substage 5b relative sea level of –45 to –58 m (Cutler et al., 2003; van Andel and Tzedakis, 1996); Substage MIS 5a relative sea level of

–13 to –19 m (Bloom et al., 1974; Cabioch and Ayliffe, 2001; Dodge et al., 1983; Mesolella et al., 1969).

The first glacial maxima since the MIS 5e highstand occurred in MIS 4, ca. 70–60 ka, which reached full glacial conditions in Europe, the North Atlantic Ocean, and South America (Helmens, 2014; Larsen et al., 2009; Peltier, 2021), allowing some glaciers to reach maximum extent prior to 50 ka (Doughty et al., 2021; Ehlers et al., 2011; Gillespie and Molnar, 1995; Hughes et al., 2013; Kaufman et al., 2011; Peltier, 2021; Stauch et al., 2007). Sea levels declined from approximately –21 to –81 m during the MIS 5a–4 transition between ca. 71 and 65 ka (Cutler et al., 2003). Starting at this transition, until MIS 2, the newly exposed continental shelf starts to become incised by fluvial channels as eustatic sea level declines (Blum and Price, 1998; Törnqvist et al., 2000, 2003).

MIS 3, between ca. 59 to 29 ka (Voelker et al., 1998), was a mild interval (van Andel, 2002) of continued eustatic sea level decline between the two cold maxima with relative sea levels of approximately –45 to –85 m (Cabioch and Ayliffe, 2001; Chappell, 2002; Chappell et al., 1996; Cutler et al., 2003; Guilderson et al., 2000).

MIS 2, the period of the Last Glacial Maximum (LGM), occurred between ca. 28–12 ka (Lisiecki and Raymo, 2005; Martinson et al., 1987; Shackleton, 1987), with eustatic sea levels reaching a low of –80 to –127 m (Curray, 1965; Duncan et al., 2000; Guilderson et al., 2000; Johnson and Andrews, 1986; Shackleton, 1987; Skene et al., 1998; Yokoyama et al., 2000), dropping below the shelf edge (Törnqvist et al., 2006a). During this time, fluvial networks continued to erode and extend seaward, marking the height of incision and the creation of the MIS 2 sequence boundary (Anderson et al., 2016). At the peak of the LGM, between ca. 26.5–18 ka (Clark et al., 2009; Helmens, 2014; Hughes et al., 2013; Lunkka et al., 2001), glaciers that had

not previously reached maximum extent during MIS 4 would reach maximum extent during the LGM (Booth et al., 2003; Licciardi et al., 2004; Phillips et al., 2009; Porter, 2011; Vásquez-Selem and Heine, 2011).

MIS 1 marks the time period of drastic sea-level rise between ca. 18 ka–Present, transitioning from the Pleistocene Wisconsinan glacial period to the Holocene interglacial period (Anderson et al., 2016; Saucier, 1994). The early Holocene was a time of episodic retreat of ice sheets such as the West Antarctic Ice Sheet (Anderson et al., 2002; Lowe and Anderson, 2002) and the Antarctic Peninsula Ice Sheet (Heroy and Anderson, 2007). In the Gulf of Mexico, between ca. 10.5–8.2 ka, sea level rose from approximately –21 m to –15 m in the Mississippi Sound and Mobile Bay (Anderson et al., 2014; Otvos, 1982a, 2005b, 2018). The rapid sea-level rise in 8.2–8 ka is argued to be associated with the release of meltwaters from the Laurentide Ice Sheet (Blanchon and Shaw, 1995; Carlson et al., 2007) and the drainage of Lake Agassiz/Ojibway (Leverington et al., 2002; Törnqvist et al., 2005; Von Grafenstein et al., 1998). For 8–4 ka, a sea-level curve in the Gulf of Mexico has been established from basal peat samples, indicating –10 m to –3 m, respectively (Törnqvist et al., 2004, 2005, 2006b), which is similar to other depth findings of the time period (Anderson et al., 2016; Blum et al., 2001, 2002). For the time from 4 ka to Present, there are observations of sea-level rise ranging from 0.4–0.6 mm/yr (Anderson et al., 2014; Milliken et al., 2008) to 0.2 to 1.2 mm/yr (Clark et al., 1978; Fairbanks, 1992; Bard et al., 1996; Toscano and Macintyre, 2003).

2.4 Geologic Setting

The northern Gulf of Mexico coastal plain consists of a complex stratigraphic series resulting from cyclic periods of marine and terrestrial deposition from continuous sea level advance and retreat. Fine-grained sediments such as clay and silt are characteristic of shallow

marine, deltaic, and estuarine lower energy environments, while coarse-grained sediments such as sand and gravel are characteristic of nearshore, beach, and terrestrial fluvial environments. Transgressive and regressive sequences show repeated shoreline migration and evolution (Anderson et al., 2016; Sloss et al., 1949) throughout geologic history in response to mean sea level fluctuation associated with the change in global climate. In addition to controlling stratigraphic composition, shoreline migration greatly alters the hydrogeologic properties across marine marginal basins by reworking and redistributing previously deposited sediments. Subaerial surfaces are subjected to fluvial erosion (Galloway, 1989), while submerged sediments can be eroded by currents, wave action, sediment starvation, and mass wasting (Swift, 1968; Frazier, 1974). Collectively, these erosional processes create an unconformable contact between older and younger deposits (Blum et al., 2013; Galloway, 1989).

Near surface, late Quaternary stratigraphy along the Mississippi Gulf Coast consists of older (MIS 5 – MIS 3) Pleistocene sediments unconformably overlain by younger Holocene sediments deposited after the MIS 2 transgression (Kindinger et al., 1994; Otvos, 2001). This unconformable contact contains relict fluvial channels (Flocks et al., 2015; Mulligan et al., 2007; Spalt et al., 2018), or paleochannels, evidence of an exposed shelf from the mean sea level lowstand about 120 m below current mean sea level in MIS 2 (Curray, 1965; Kindinger et al., 1994), as a result of the LGM (Bartek et al., 2004; Swift, 1975; Waelbroeck et al., 2012; Woodruff et al., 2013; Yokoyama et al., 2000) (Figure 2.1). During this lowstand, rivers and streams flowing across the approximately 100–130 km of exposed shelf (Curray, 1965; Galicki and Schmitz, 2016; Shackleton, 1987) incised a network of fluvial channels (Bartek et al., 2004; Dalrymple et al., 1992, 1994; Greene et al., 2007; Mars et al., 1992; Rainwater, 1964) filled with coarse-grained fluvial sediments (Zaitlin et al., 1994) and then covered by progressively finer-

grained Holocene sediments from the subsequent sea-level rise and marine transgression into MIS 1 (Anderson et al., 2016; Kramer, 1990). Subsurface mapping of the northern Gulf of Mexico stratigraphy has identified multiple paleochannel networks incised during the major stages of glacial-interglacial periods of the late Quaternary (Adcock, 2019; Anderson et al., 2004; Bartek et al., 2004; Coleman and Roberts, 1988; Fisk, 1947; Fisk et al., 1954; Flocks et al., 2015; Gal, 2018; Greene et al., 2007; Hollis, 2018, Kindinger, 1989; Kindinger et al., 1994; McBride et al., 2004; Spalt et al., 2018; Zaitlin et al., 1994).

2.5 Regional and Study Area Setting

The Mississippi Sound is a bar-built estuarine system approximately 137 km long and 11–24 km wide, with a mean depth of 3 m, that extends from the mouth of the Pearl River to Mobile Bay. Its northern extent is defined by mainland tidal salt marshes and southern extent by the Mississippi Sound barrier-island system (Boone, 1973; Otvos, 2001; Priddy et al., 1955). Several rivers flow into the Mississippi Sound including the Pascagoula, Biloxi, Wolf, Jourdan, Pearl, and the Mobile River, which drains the fourth largest drainage basin in the U.S. in terms of flow (Isphording et al., 1989; Kindinger, 2014). Between the Pearl and Pascagoula River are several smaller streams that flow southeast and enter the Mississippi Sound through estuaries and bays (Upshaw et al., 1966).

In this microtidal, storm-dominated, slowly subsiding (~1.0–1.5 mm/yr), passive margin environment (Flocks, 2015; Ivins et al., 2005, 2007), the majority of coarse sediments are orthoquartzitic, originating from the weathering of the southern Appalachian igneous-metamorphic complex, which contain minerals characteristic of the Eastern Gulf Province (van Andel and Poole, 1960). However, the immediate source of coarse sediments in the study area is the erosion of Pre-Holocene deposits along the Alabama-Florida coast (Stone et al., 1992) and

the reworking of sediments deposited fluvially on the shelf during the Pleistocene glaciation (Rucker and Snowden, 1989). A westward long-shore current results in westward littoral drift of Eastern Gulf Province sediments along the coast and barrier islands (Cipriani and Stone, 2001), and restricts the eastward flow of sediments from the Mississippi River Delta (Mississippi Province) (Davies and Moore, 1970; van Andel and Poole, 1960). Although restricted, clay sediments of igneous origin, characteristic of the Mississippi River, have been found throughout the western Mississippi Sound (Milne and Shott, 1958; Priddy et al., 1955; Upshaw et al., 1966). While the sediments around the shore and barrier islands are generally well sorted quartzose sand, the seabed of the Sound is predominantly sandy mud (Ludwick, 1964) with silt and clay in the central portion (Upshaw et al., 1966).

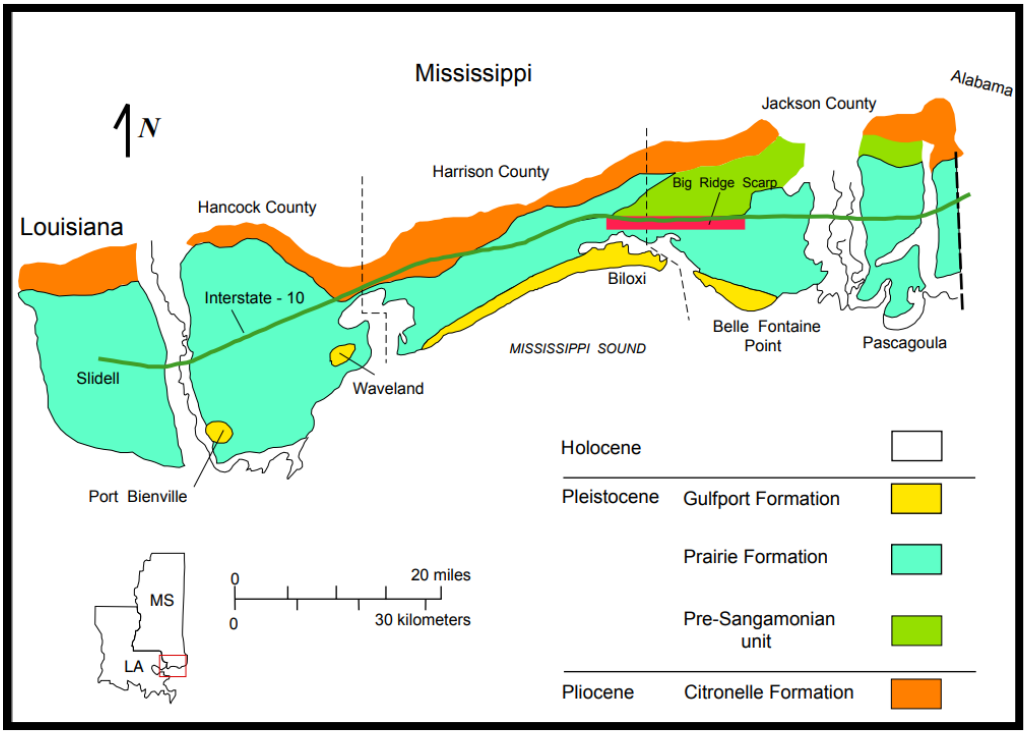

Figure 2.2 General locations of late Pleistocene units near the Mississippi coast and study area. The Biloxi Formation does not outcrop onto the land surface. (Otvos, 2001)

2.6 Stratigraphic Units

The Pleistocene units in the Mississippi Sound consist of a single complex of fluvial to marine sediments of late Pleistocene age, representing a single cycle of highstand sedimentation during the last interglacial episode (MIS 5), divided into the Gulfport, Biloxi, and Prairie Formations (Figure 2.2) (Gohn and Reinhardt, 2001; Otvos, 1982b, 1991a, 2001; Otvos and Howat, 1992). Although it has been suggested to classify these three formations into members of a single formation, Otvos (2001) argues that each unit differs in sediment characteristics, fossil content, if any, and that usually only two of three formations appear vertically together in any location.

2.6.1 Biloxi Formation

The Biloxi Formation is a late Pleistocene unit that represents a prograding, low-energy shoreline and offshore to lower shoreface, with marine to estuarine deposits (DuBar et al., 1991; Gohn and Reinhardt, 2001; Otvos, 1972, 1997, 2001), comprised of muddy sand, fine sandy mud, and silty very fine sand, and contains both macro and microfossils that provide an age dating of MIS 5 (Otvos and Howat, 1992; Otvos, 2001). Cores from Ocean Springs, Biloxi, Point aux Chenes, and Belle Fontaine Point, MS, show a thickness ranging from 2–28.5 m (Gohn et al., 2001; Otvos, 2001). The Biloxi Formation is marked by a basal erosional contact that is dark-greenish-gray to greenish-gray and an upper contact that is very pale orange (Gohn et al., 2001; Otvos, 2001). The Biloxi Formation underlies and interfingers with the Gulfport and Prairie Formations and extends seaward toward the Mississippi Sound.

2.6.2 Gulfport Formation

The Gulfport Formation, a late Pleistocene unit, which interfingers with the Biloxi Formation, displays evidence of aggradation, grading upward from muddy, poorly sorted sandy, relatively low-energy, nearshore deposits to subtidal shoal sands to finally eolian upper shoreface, foreshore, backshore and dune deposits (Gohn et al., 2001; Otvos, 2001). These deposits contain well-sorted fine to medium-quartz sand (Gohn et al., 2001; Otvos and Howat, 1992), have been found up to 21 m thick, are mostly barren of calcareous fossils, and are consistent with the sea level fall around 124–116 ka (MIS 5e–MIS 5d) in coastal Mississippi and northwestern Florida (Gohn and Reinhardt, 2001; Otvos, 2001).

2.6.3 Prairie Formation

Overlying the Gulfport Formation, the Prairie Formation represents the lowest shore-parallel Pleistocene unit (Otvos, 1991b) and underlies the coastwise Prairie terrace (Fisk, 1938). The lowest Prairie terrace reaches about +6–8 m (about +12–18 m inland from Quaternary regional uplift) in height, approximately 1 km wide at the narrowest, and up to 50 km wide along the Pearl River, near Louisiana (Otvos, 2001). Several studies have determined the age of the Prairie Formation to be between MIS 5 (Saucier, 1968, 1974, 1994), MIS 3 (Autin et al., 1991; Fisk, 1944, 1951), and ages of both MIS 5 to MIS 3 (Mange and Otvos, 2005; Otvos, 2005a), until 25 ka where the Peoria Loess begins to accumulate in the Lower Mississippi Valley (Bettis et al., 2003; Markewich et al., 1998; Otvos, 1975; Pye and Johnson, 1988). During this time, barrier strandplains prograded seaward from the edge of the Prairie Coastal Plain (Otvos, 1972, 1991a, 2001), filling large portions of valley margins with floodplain and coastal-plain deposits (Autin et al., 1991; Saucier, 1994). Muddy, clayey fine sands and moderately silty, fine and very fine sands, which are colored yellowish-gray, greenish-gray and gray with very pale orange, with

pale to medium-yellowish-orange oxidation near the surface (Greene et al., 2007), are predominant throughout this 4.5–12 m alluvial complex that wedges out landward against older units and interfingers with the Biloxi Formation (Otvos, 2001).

2.6.4 Holocene Sediments

After the peak of the LGM, as sea levels began to rise from 18 ka until 4 ka (Saucier, 1994), the preservation of coastal sediment deposits on the subaerially exposed surface was minimal as transgressive ravinement occurred (Anderson et al., 2016; McBride et al., 2004; Penland et al., 1988). Fluvial deposits that are topographically contained, such as channels and floodplains, and related delta, estuarine, and shore deposits, are more easily preserved during the transgressive episode and are comprised mostly of paleochannel fill (Simms et al., 2006; Thomas and Anderson, 1994). Otherwise, shoreface and tidal ravinement processes erode sediments, creating unconformable contacts where sediments are more easily eroded, leaving the stratigraphy largely fragmented except in paleochannel margins (Anderson et al., 2016; Simms et al., 2006; Thomas and Anderson, 1994).

It is generally accepted that the end of the Pleistocene epoch and the beginning of the Holocene occurred between 11.7–10 ka (Saucier, 1994; Walker et al., 2009), corresponding with a regime change of the Mississippi River from braided to meandering, found in the stratigraphic record, and seen near the coast in the sedimentary record as a chronological boundary (Saucier, 1994). Near the study area, the contact between Holocene and the underlying Pleistocene units is marked by an unconformity that is separated by a dark greenish-gray to medium gray sandy clay, fine sandy mud, and muddy medium-sand above, from a stiff, oxidized medium gray, dark greenish-gray to yellow-orange clay below (Greene et al., 2007; Otvos, 2001). These Holocene deposits now cover the majority of the Mississippi Sound and the northern Gulf of Mexico, in

intervals of approximately 6–20 m thick depending on the underlying unconformity/ravinement surface topography (Anderson et al., 2014; Gohn et al., 2001; Rucker et al., 1990), and create environments such as coastal wetland, lagoon, and deltaic deposits, mainland and barrier island strandplains, beach complexes, and alluvium (Otvos, 1994).

CHAPTER III

METHODS

3.1 Reflection Seismology

Because the incised paleochannels within the Holocene Pleistocene unconformity are covered with sediments and buried (6–20 m) in the subsurface, geophysical methods are the optimal method to image them. Geophysical seismic surveying has become an invaluable tool in allowing geologists to cost-effectively and rapidly collect data from the subsurface with a relatively high degree of resolution, without the need for direct observations. Although extracting core samples provides the highest resolution possible, the process of acquiring the cores requires more resources and time compared to that of seismic surveying on a large scale (Schock et al., 1992). Seismic reflection surveying allows for a spatially continuous observation and interpretation of subsurface features over a large area, while core samples only contain information relating to lithologic properties of the subsurface at discrete sample sites (Schock et al., 1992). For this research, core sample and seismic profile data are used together to enhance the interpretation of subsurface features. Specifically, core data are used to ground truth the lithologic properties of reflectors imaged in seismic profiles, including the reflectors interpreted to be the Pleistocene-Holocene unconformity.

Seismic reflection surveys require an acoustic source to transmit a seismic wave and a hydrophone receiver to capture the returning reflected wave. After the source creates the seismic wave, it travels through the underlying material (water for marine surveys and rock layers for

terrestrial surveys) until it comes in contact with a material or geologic feature with a different acoustic impedance than the material above it. A certain proportion of the wave is reflected based on the relative density between materials and the velocity of the seismic wave in each. This reflected energy travels back towards the surface where a receiver captures and records the data. The remaining source signal continues to propagate through the subsurface, creating reflectors at interfaces of differential acoustic impedance and losing energy until the wave becomes completely attenuated. The ratio of reflected to transmitted energy is known as the reflection coefficient, which is the ratio of the difference of acoustic impedance to the sum of the acoustic impedance of geologic units, and can be used to infer the physical characteristics of the reflecting surface. Coarser-grained sediments will have a higher reflection coefficient, whereas finer-grained sediments will have a lower reflection coefficient (Sanhaji and Guarin, 2013; Theuillon et al., 2008). The two-way travel time of the seismic wave from the source to the reflecting surface and back to the receiver is used to determine the range from the source and plot its relative depth beneath the seafloor (Červený, 2001; Mussett et al., 2000).

The depth of penetration for a seismic wave is determined by its frequency. The lower the frequency, the deeper the wave can travel, which is ideal for deep subsurface surveys. However, interfaces are not resolvable if they are less than one-half wavelength apart. Although low frequency (and thus higher wavelength) sources give the deepest range for surveys, they provide the lowest resolution for subsurface data. Alternatively, high frequency sources give the highest resolution data at the loss of depth penetration. Since Pleistocene paleochannels are observed in other study areas within the Mississippi Sound to be between ~5–25 m of depth (Adcock, 2019; Gal, 2018; Hollis, 2018; Rainwater, 1964), seismic reflection surveys should be used to collect

the highest resolution data possible as the shallow penetration depth will not be impacted by wave attenuation (Diogo et al., 2004).

Depending on the objective of the survey being conducted, whether penetrative depth or high-resolution data, there are a wide range of commonly used seismic sources, both naturally occurring and human engineered. Near the low frequency range ($<10^{-2}$–1 Hz), earthquakes provide the penetration required to survey through the earth's core. However, geologists often have time constraints and must use sources that release energy as needed. The mid frequency range (1–10^2 Hz) includes sources that are controlled and used for primarily terrestrial surveys. In the high frequency range (10^3–>10^5 Hz), these controlled devices are used exclusively for marine surveys that focus on the shallow subsurface where a higher resolution of data is required. For the purpose of this thesis, a high frequency source was used in order to obtain the highest resolution possible of the shallow subsurface.

Compressed High Intensity Radar Pulse (chirp) sub-bottom profilers are marine sonar systems which use a highly repeatable source pulse to acquire correlated data with up to 10 cm vertical resolution in the top 20–30 m of unconsolidated sediments (Bull et al., 1998; Gutowski et al., 2002). Chirp does this by transmitting frequency-modulated (FM) pulses over the band of 2–20 kHz (Schock, 2004) using a piezo-electric ceramic transducer that functions as both transmitter and receiver (Mosher and Simpkin, 1999). Reflection coefficients for chirp are calculated from amplitude information provided by single traces and polarity information provided by trace mixing (Bull et al., 1998). In the seismic profile, when examining collected chirp data, the areas with darker pixels indicate higher reflection coefficients, where lighter pixels indicate lower reflection coefficients (Figure 3.1).

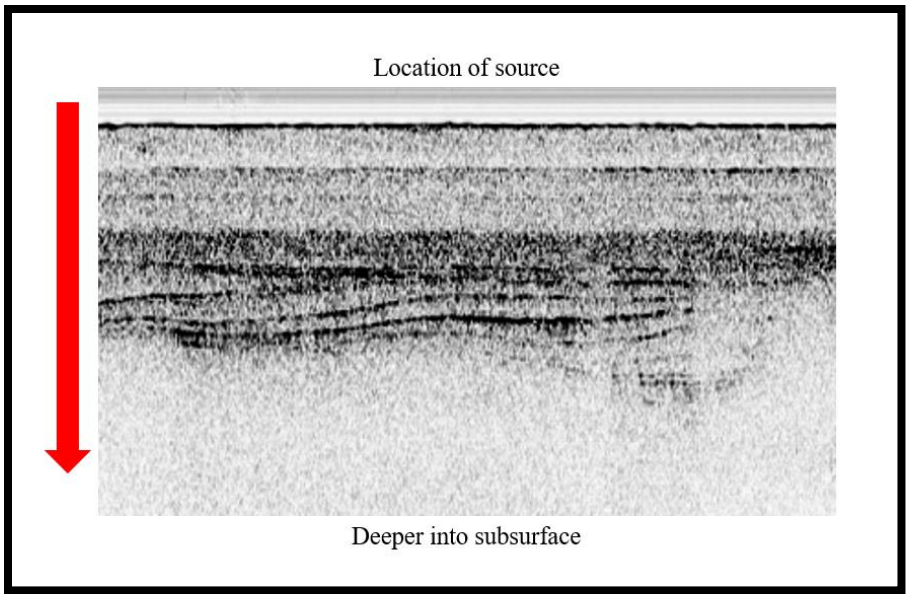

Figure 3.1 The produced seismic waves travel from the source downward into the subsurface (red arrow). Higher reflection coefficients are shown as darker pixels, and lower reflection coefficients are lighter pixels.

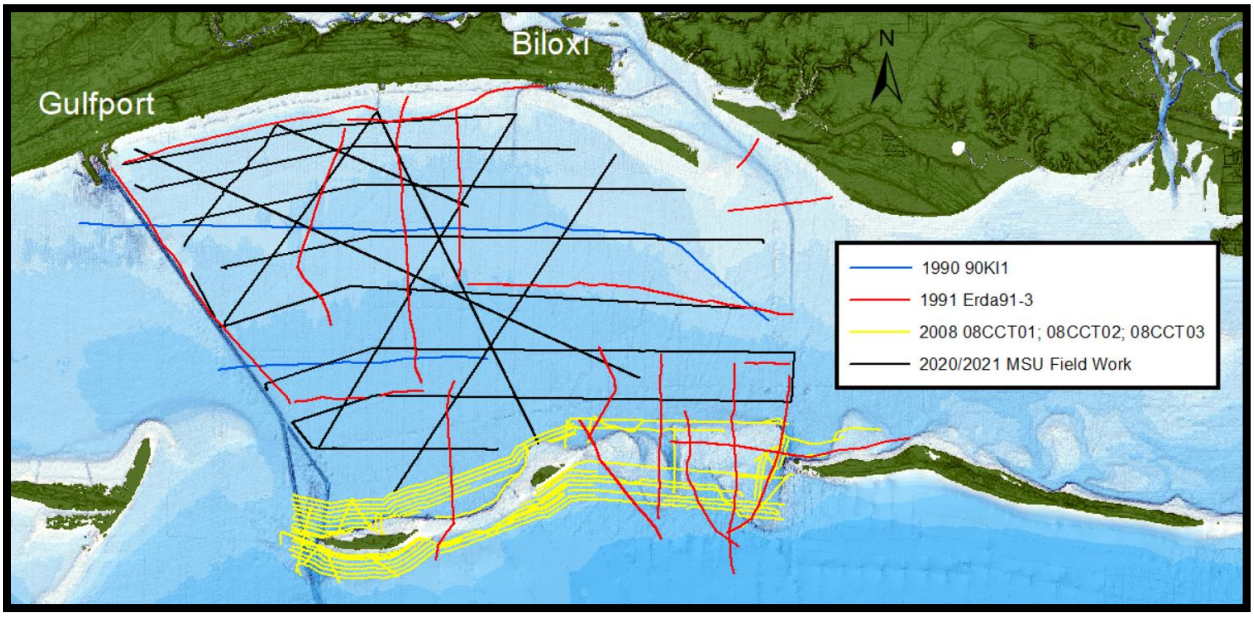

Figure 3.2 Collection of all seismic surveys used for this thesis.

3.2 Geophysical Data

In 1990, the U.S. Geological Survey (USGS) conducted geophysical survey 90KI1 to investigate the shallow subsurface geology of the Mississippi-Alabama-Florida shelf as part of a project to study coastal erosion and offshore sand resources (Sanford et al., 2016). Seismic data were collected through the use of an unnamed boomer system and hydrophone receiver; however, the amplitude of the reflected energy was recorded by an Edward P. Curley Lab (EPC) thermal plotter. Analog records have since been digitized through scanning at 200 dots per inch (dpi) using an IDEAL/Contex Crystal TX 40-inch (1394) large-format scanner and converted to TIFF format using WIDEimage software (version 2.8.1). These TIFF files were converted into SEGY files, resulting in ~44 km of seismic profile data used in this thesis (Figure 3.2).

Between September 12 and September 23, 1991, the USGS conducted cruise Erda 91-3, surveying portions of the Mississippi Sound west of Horn Island (Bosse et al., 2017). Seismic data were acquired from a Huntec boomer sled accompanied by a Benthos hydrophone receiver, with analog data plotted in real time using an electrostatic plotter. These now digitized analog images were provided as SEGY files and contribute ~148 km of seismic data in the study area used for this thesis (Figure 3.2).

In 2008, the USGS conducted geophysical surveys, cruises 08CCT01, 08CCT02, and 08CCT03, around Ship Island to create, in part, a complete modern topobathymetric map of the Mississippi barrier islands from Cat Island to Dauphin Island (Buster et al., 2017; DeWitt et al., 2012; Forde et al., 2011). Seismic reflection data were collected using a Chirp 512i Sub Bottom Profiler for cruise 08CCT01, and a Chirp 424 Sub Bottom Profiler for cruises 08CCT02 and 08CCT03. Together, data from the three cruises were able to contribute ~254 km of the seismic data used for this thesis (Figure 3.2).

Approximately 267 km of new chirp seismic data were collected (Figure 3.2), from November 10th –12th, 2020 and December 2nd –7th, 2021, using an EdgeTech SB-216S Full Spectrum Sub-Bottom Tow Vehicle, operating at 2–10 kHz frequency modulated range, 1–2 m depth below sea level, powered by an EdgeTech 3100P Portable Sub-Bottom Processor. These profiles were recorded as SEGY format files and later processed with Chesapeake Technologies' SonarWiz software.

3.3 Sediment Cores

This thesis uses core data from two sources to identify the relative elevation of the Pleistocene-Holocene unconformable contact throughout the Mississippi Sound to aid in seismic profile interpretation. The first set of cores were taken from the Mississippi Department of Environmental Quality (MDEQ) historic cores website (geology.deq.ms.gov/coastal/Core_ historic_cores.htm) (Figure 3.3). Core log images showing the Pleistocene-Holocene contact are shown in Appendix A, Figures A.1–A.30. Cores from the Mississippi Sound (MS and P) and Barrier Islands (BI and IS) show the Pleistocene-Holocene contact at depth, and the cores from Harrison County (HR) show the contact at the surface or near the surface. These core logs contain contact depths, in feet, many showing evidence of the unconformity: yellowish to orange stained fine sandy mud, evidence of oxidation, below a dark-greenish gray to greenish-gray fine sandy mud, which is consistent with observations made by Greene et al. (2007) and Otvos (2001).

The second source of sediment core logs is given by Rainwater (1964). Borings from the Mississippi Sound were taken along a line from Beauvoir to Ship Island for a proposed causeway connecting Ship Island to the mainland. Core samples were given to Rainwater, who described the lithologies and plotted the Pleistocene contact (Figure 3.4). A seismic data survey line was

collected during this study to closely match the line of cores that were collected and given to Rainwater (Figure 3.4). Results show that the newly collected data closely resemble the unconformable contact noted by Rainwater, mainly from Core A to Core M (Figure 3.5). Rainwater notes that the contact is much more difficult to determine as the core locations extend seaward, which is consistent with collected seismic profile data, in which the contact is not distinguishable near the same location as the core's area of uncertainty (Figure 3.5). These sediment core logs give contact depths at which to best interpret the seismic data in all profiles.

Figure 3.3 Locations of MDEQ historic cores in relation to the study area. Mississippi Sound (MS) locations are shown in red, Barrier Island (BI) locations are shown in yellow, and Harrison County (HR) locations are shown in blue.

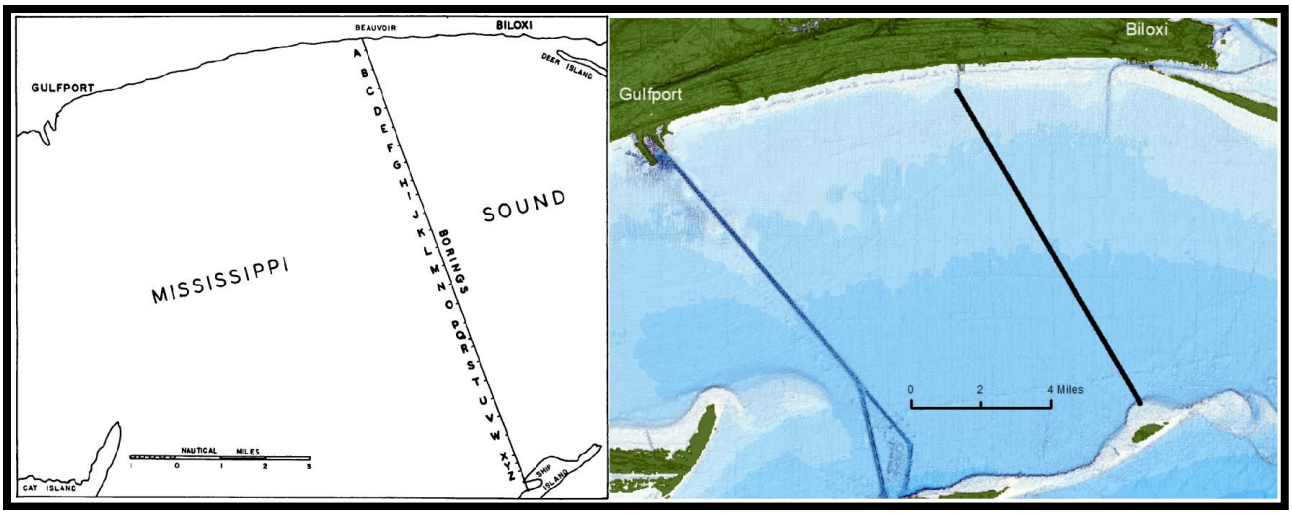

Figure 3.4 Locations of boring sites along the line from the mainland to Ship Island from Rainwater, 1964 (left), and line 20211205150644-CH1-to-20211205165419-CH1 collected for this study closely matching the boring site path (right).

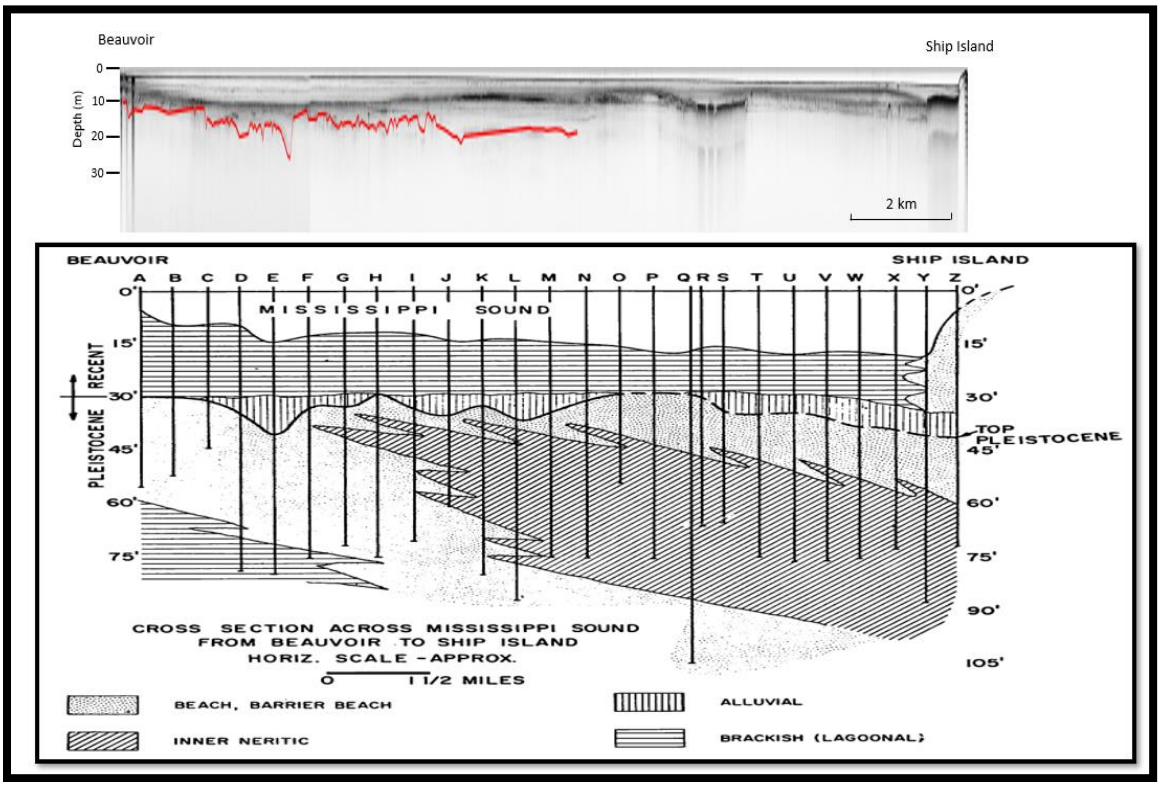

Figure 3.5 Seismic profile data line 20211205150644-CH1-to-20211205165419-CH1 with interpreted Pleistocene-Holocene contact from this study (top), and Pleistocene-Holocene contact interpreted by Rainwater, (1964) from core samples (bottom).

3.4 Data Processing

All seismic data were imported as SEGY files and processed with SonarWiz, version 7.06.06, which allows seismic profiles to be viewed and reflector elevations to be digitized. The determined locations of paleochannel reflectors were supported by contact locations taken from sediment core logs and stratigraphic evidence of incised channels based on reflector structure and intensity. Seismic profiles were then bottom-tracked and aligned to a Biloxi, MS bathymetry grid.

To create an image of the topography of the unconformable Pleistocene-Holocene contact, all digitized reflector elevation data were exported to ArcGIS to be processed with the Topo to Raster interpolation method. This method of interpolation uses an iterative finite difference interpolation technique to ensure the drainage structure remains connected for correct representation of ridges and streams from input data without losing surface continuity of other interpolation methods, such as Kriging and Spline (Hutchinson et al., 2011).

CHAPTER IV

RESULTS

Interpolation of the digitized reflectors that were determined from sediment core and reflector structure and intensity to be the unconformable Pleistocene-Holocene contact shows evidence of a network of connected incised paleochannels within the unconformable Holocene-Pleistocene surface (Figure 4.1). Visual analysis of the marked paleochannels shows channel morphologies ranging from wide with flat channel bottoms to narrow V-shaped channels with steep sides (Figures 4.2 & 4.3–4.9). A majority of seismic profiles contain evidence of these paleochannels, reaching depths of 7.3–23.4 m and widths up to 2.5 km. Throughout these channel incisions, sediment infill can be seen as thinly layered and, in some instances, exhibiting large scale foreset bedding (Figures 4.10 & 4.11). Due to coarse grained sand deposits around Ship Island, several of the profiles contain shallow and highly reflective multiples, rendering much of the data unusable (Figures 4.2 & 4.12).

Adhering to uniformitarianism, modern coastal channel drainage patterns in the region were used to aid in the interpretation of the interpolated surface. Interpretation of the paleochannel drainage surface (Figure 4.13) was determined by the interpolated channel area size and connectivity of lower elevation areas.

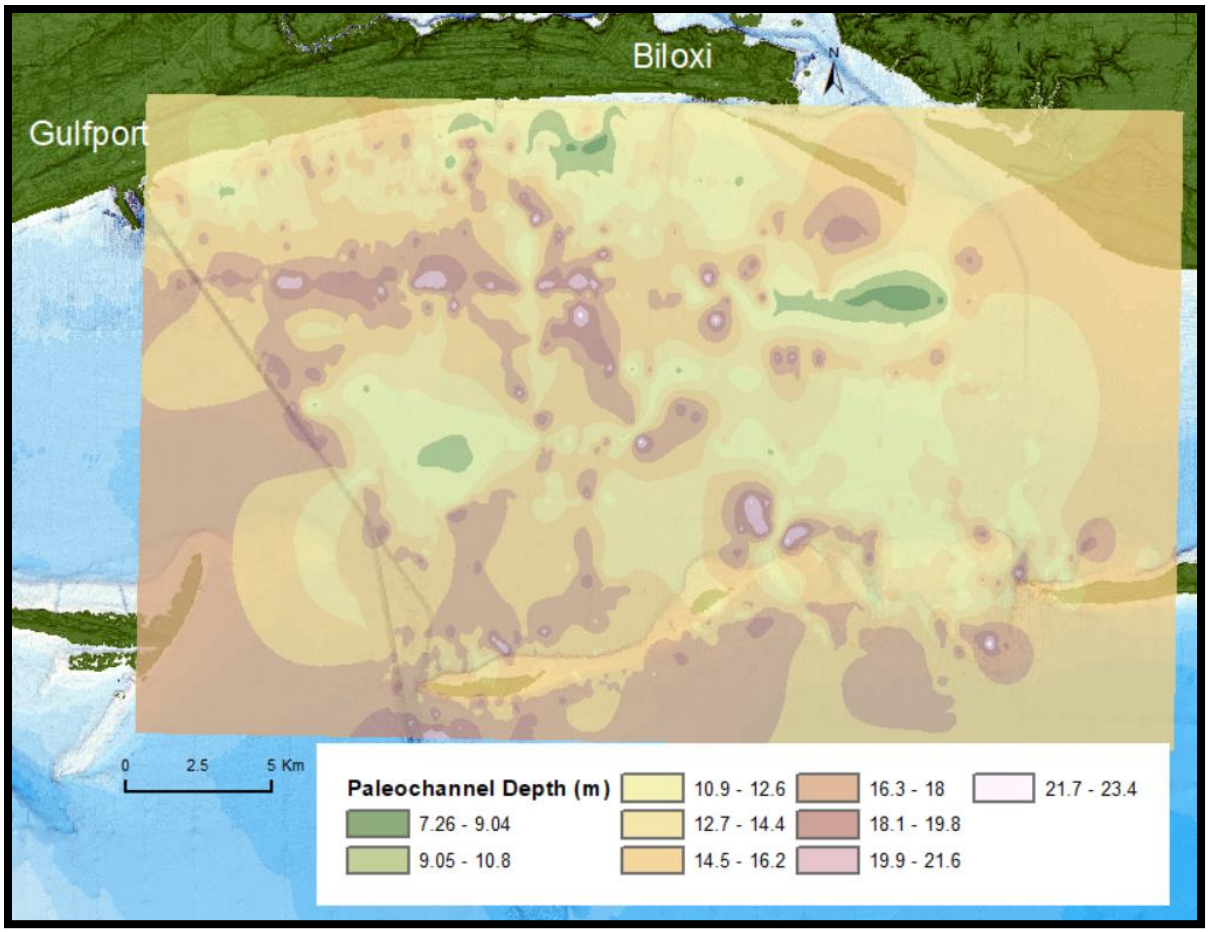

Figure 4.1 Interpolated surface generated with Topo to Raster in ArcGIS.

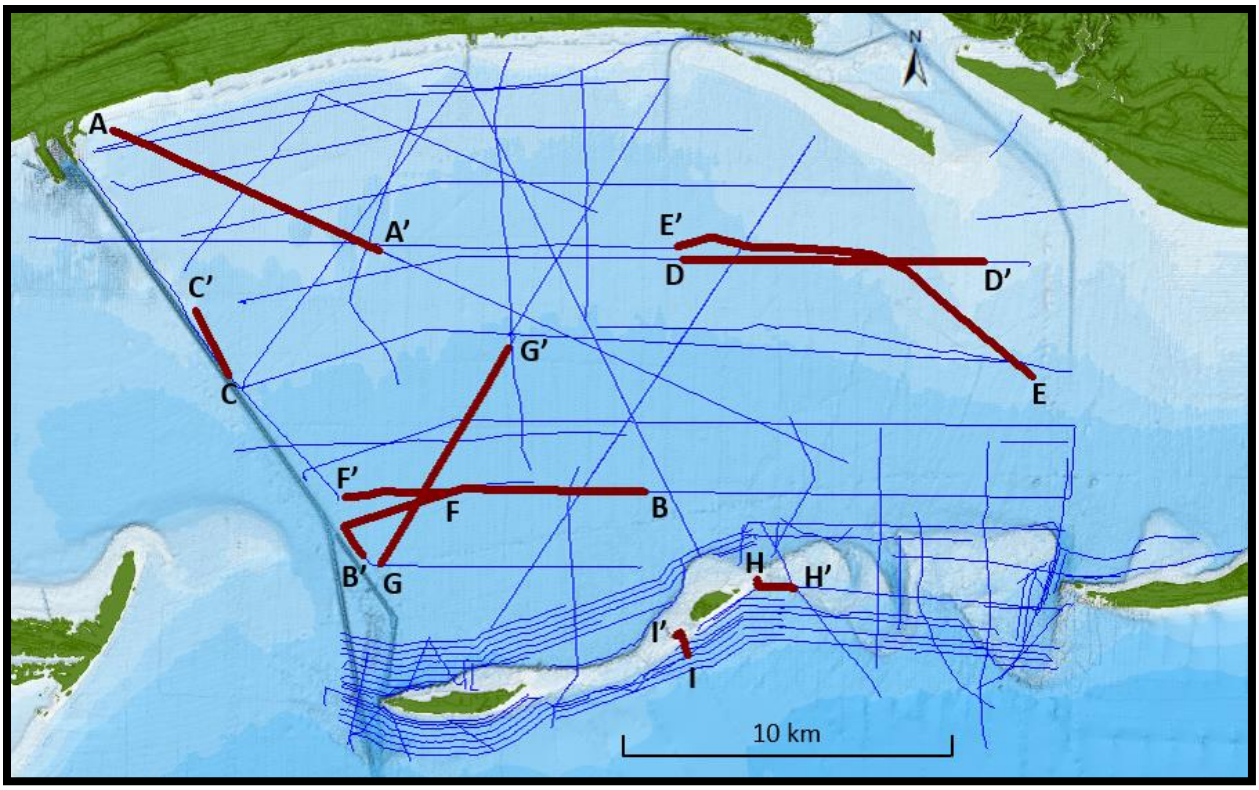

Figure 4.2 Interpolated surface overlain with seismic survey lines showing locations of individual seismic profiles. Lines A to G are seismic profiles and lines H and I are seismic profiles with reflection multiples near Ship Island.

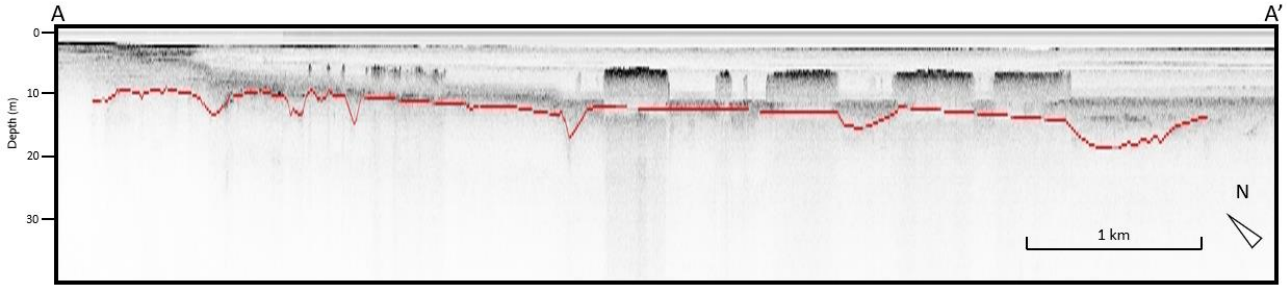

Figure 4.3 Seismic profile for line 20211004214001-CH1. Pleistocene-Holocene unconformity is marked in red and exhibits paleochannels.

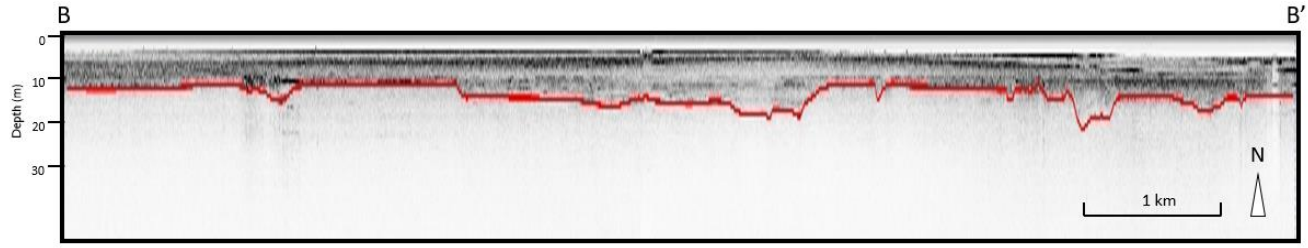

Figure 4.4 Seismic profile for line 20211005191355-CH1. Pleistocene-Holocene unconformity is marked in red and exhibits paleochannels.

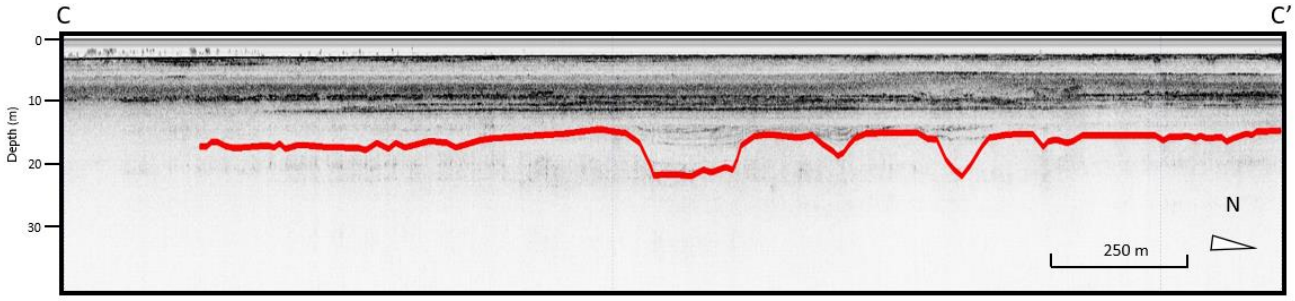

Figure 4.5 Seismic profile for line 20211005120129-CH1. Pleistocene-Holocene unconformity is marked in red and exhibits paleochannels.

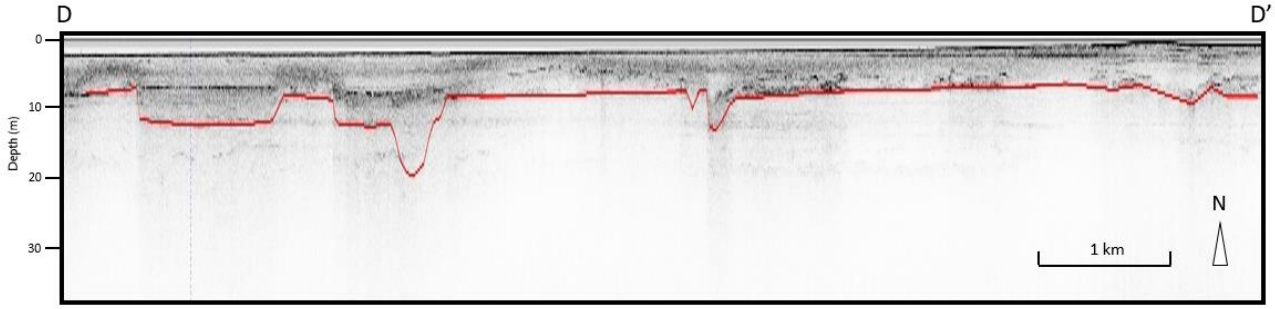

Figure 4.6 Seismic profile for line 20220211005053934-CH1-to-20211005073517-CH1. Pleistocene-Holocene unconformity is marked in red and exhibits paleochannels.

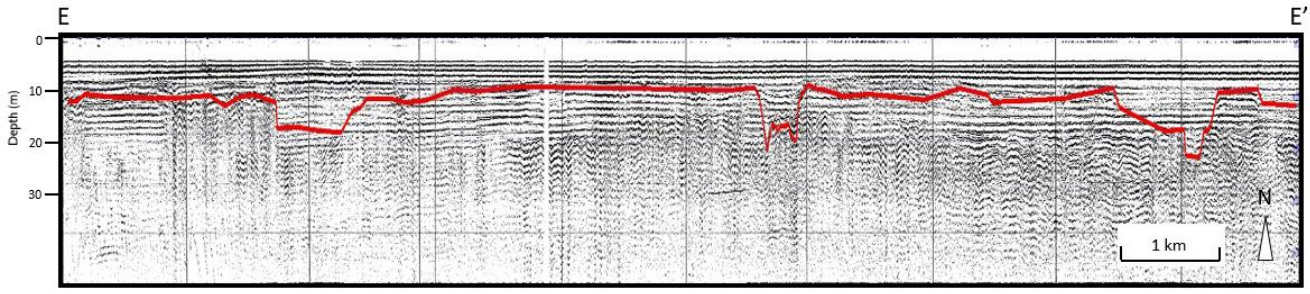

Figure 4.7 Seismic profile for line 90KI1_5(b)-CH1. Pleistocene-Holocene unconformity is marked in red and exhibits paleochannels.

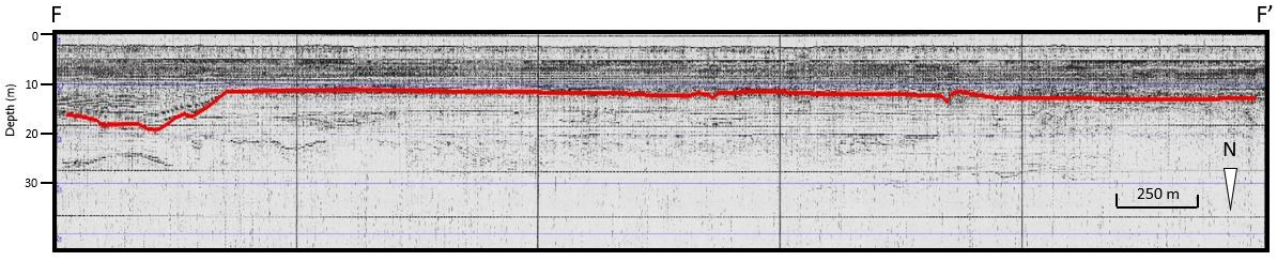

Figure 4.8 Seismic profile for line Erda91-3-SEGY_9b-CH1. Pleistocene-Holocene unconformity is marked in red and exhibits paleochannels. This paleochannel's margins are not fully seen as this seismic profile begins in the middle of the channel.

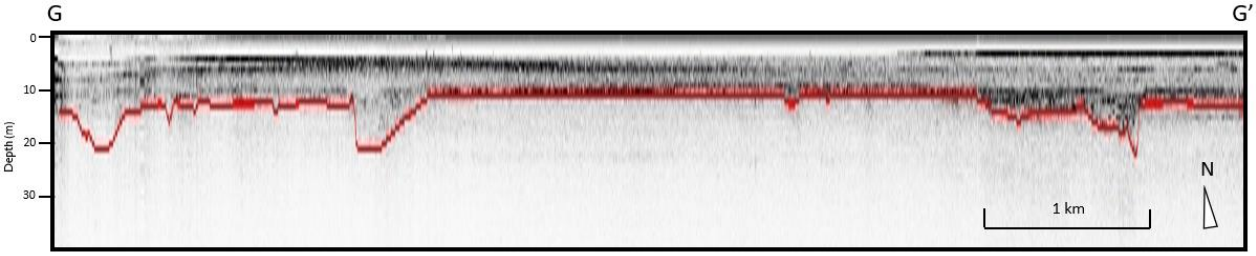

Figure 4.9 Seismic profile for line 20211205175559-CH1. Pleistocene-Holocene unconformity is marked in red and exhibits paleochannels.

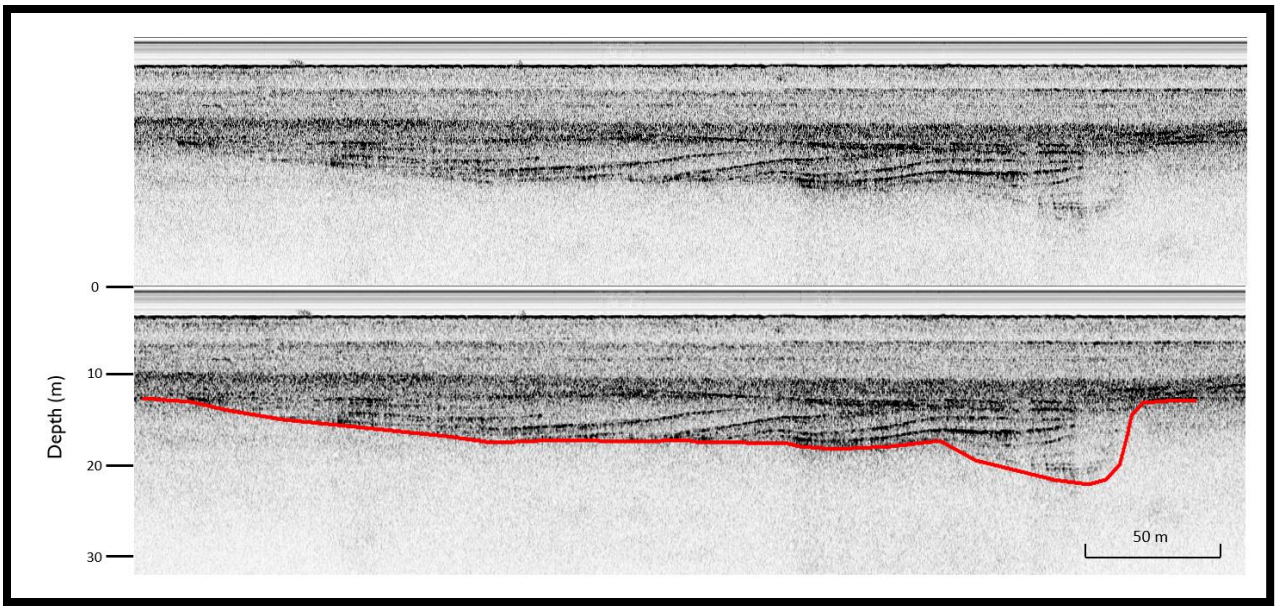

Figure 4.10 An example of channel infill thinly layered and with foreset beds in a paleochannel cross-section from line 20211205175559-CH1. Red line indicates channel margins.

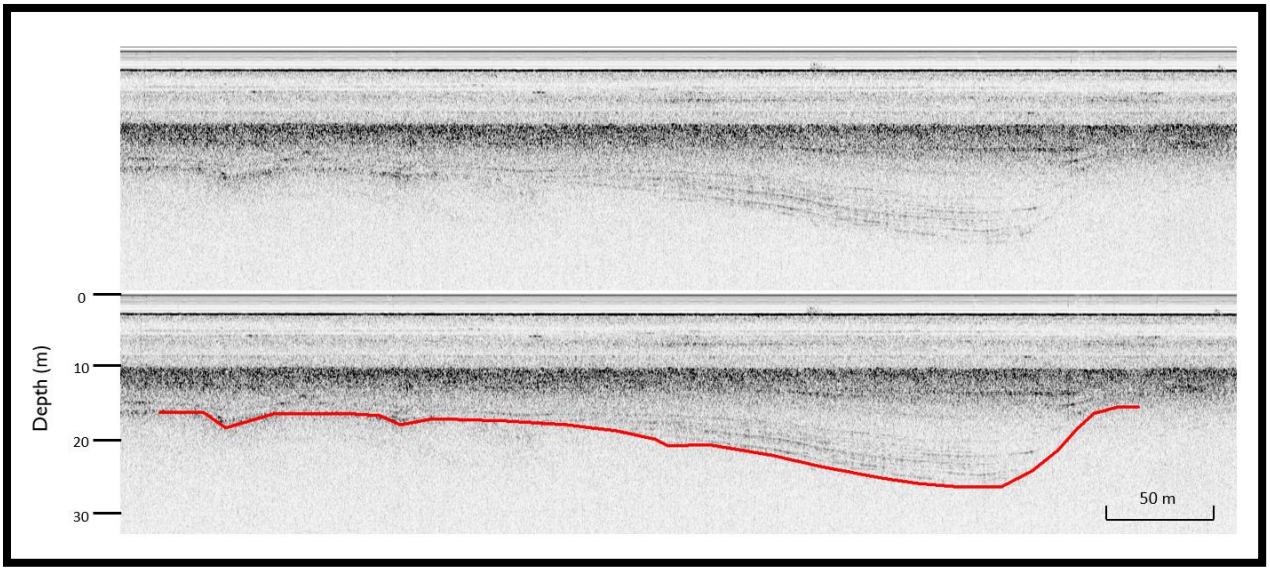

Figure 4.11 An example of channel infill thinly layered in a paleochannel cross section from line 20211205150644-CH1-to-20211205165419-CH1. Red line indicates channel margins.

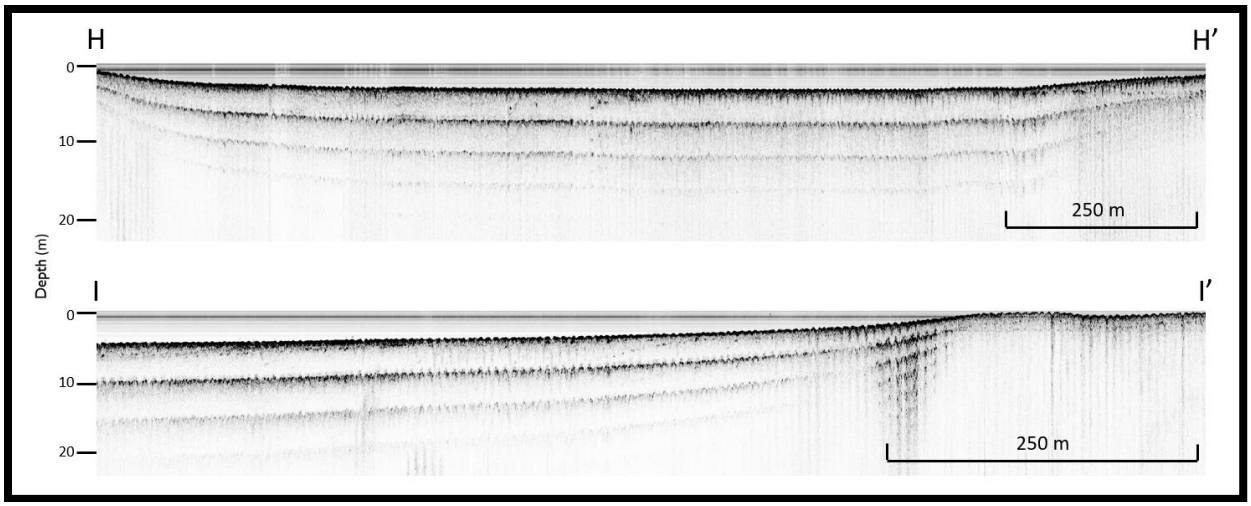

Figure 4.12 Seismic profiles of data collected in proximity of Ship Island, lines 08c553-CH1 (H-H') and 08c644-CH1 (I-I'). These profiles show reflection multiples.

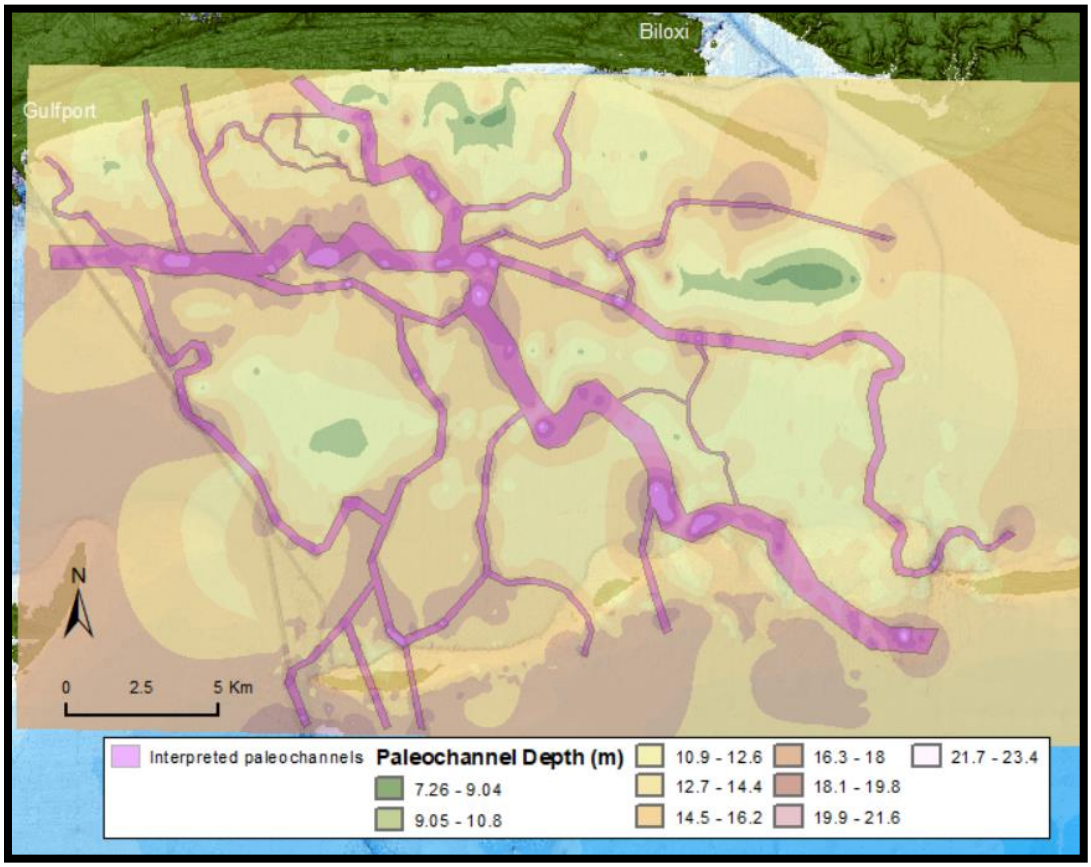

Figure 4.13 Shows interpreted paleochannel locations from interpolated Pleistocene-Holocene unconformable surface.

CHAPTER V

DISCUSSION

The results indicate a branching Pleistocene paleochannel drainage network present within the study area, beneath Holocene sediments, that were incised starting at ~120 ka and ending at ~8–10 ka, when glacial melting of the LGM returned the eustatic sea level to near present level. The Biloxi, Gulfport, and Prairie Formations, which represent a shift from estuarian to beach deposits, were subaerially exposed as the shoreline retreated. Subsequently, the exposed surface experienced fluvial incision as streams and rivers extended channels toward the semi-continuously declining shoreline. Many of the paleochannels observed in this thesis exhibit wide channel margins close to or over 1 km, point bars with foreset beds, a channel thalweg, and cut banks, suggesting that these channels were meandering in depositional pattern. (Figures 4.3–4.9; 4.10 & 4.11). There are, however, many V-shaped, steep sided, shallow channels present in the seismic profiles (Figures 4.3 & 4.5), possibly created as overflow channels from increased continental runoff as glacial melt occurred, resulting in much younger channels as opposed to the meandering channels.

As the eustatic sea level declined, and the elongation of existing channels occurred, the accommodation space and slope of the channels increased (as noted in the Fluvial Geomorphology section), effectively causing deeper incision of previously existing fluvial channels. Conversely, as the eustatic sea level rose, channels shortened and were subjected to aggradation, which is visible in Figures 4.10 & 4.11. Reflectors in both cases show highly

detailed, thin stratigraphic layering that comprises a large majority of the channel area. As the channels in the study area were subjected to channel shortening and the flow velocity decreased, coarse-grained sediments were no longer able to be transported, resulting in thick channel deposits. During the rise, the channel mouth would form a deltaic or estuarian depositional environment, widening channels and protecting the coarse sediment deposits. As the transgression occurred, the remaining portion of the channel was infilled with finer-grained sediments, fining further as the transgression continued landward. Portions of the exposed surface not protected by channel margins were more vulnerable to transgressive ravinement, creating the unconformity between Pleistocene and Holocene sediments seen today.

The interpreted Pleistocene drainage surface (Figure 4.13) shows wider channel margins indicating main channel locations and narrow channels representing smaller streams and tributaries. The direction of flow over the area follows the main channel orientation, northwest to southeast. The two larger channels form a confluence near the center of the study area and continue toward the southeast. Many of the channels exhibit meandering patterns.

Presently, transgressive Holocene sediments that are deposited over the Pleistocene deposits are continuously reworked within the Mississippi Sound and the Gulf Coast. These transgressive deposits fine upward, where coarser fine-grained sediments were deposited near the Pleistocene deposits and the continued rise of the sea level allowed finer-grains to finally settle (Figure 5.1). These finer-grained sediments have created a less-permeable layer over the much coarser-grained fluvial channel deposits. As terrestrial groundwater hydraulic head seeks mean sea level, these paleochannels may act as conduits for submarine groundwater to be discharged further from shore since groundwater will preferentially flow through the coarse-grained channel infill as opposed to other surrounding stratigraphic features of smaller grain sizes. The fine-

grained, less permeable layer above the paleochannel will act to keep the groundwater from discharging nearshore, extending the influence of fresh groundwater into the coastal system. Synthesis of these results with isotopic tracer data and subsurface resistivity observations collected by collaborators, working under the same grant that funded this research, will be used to further investigate the impact of paleochannels and associated stratigraphic heterogeneity on submarine groundwater discharge processes.

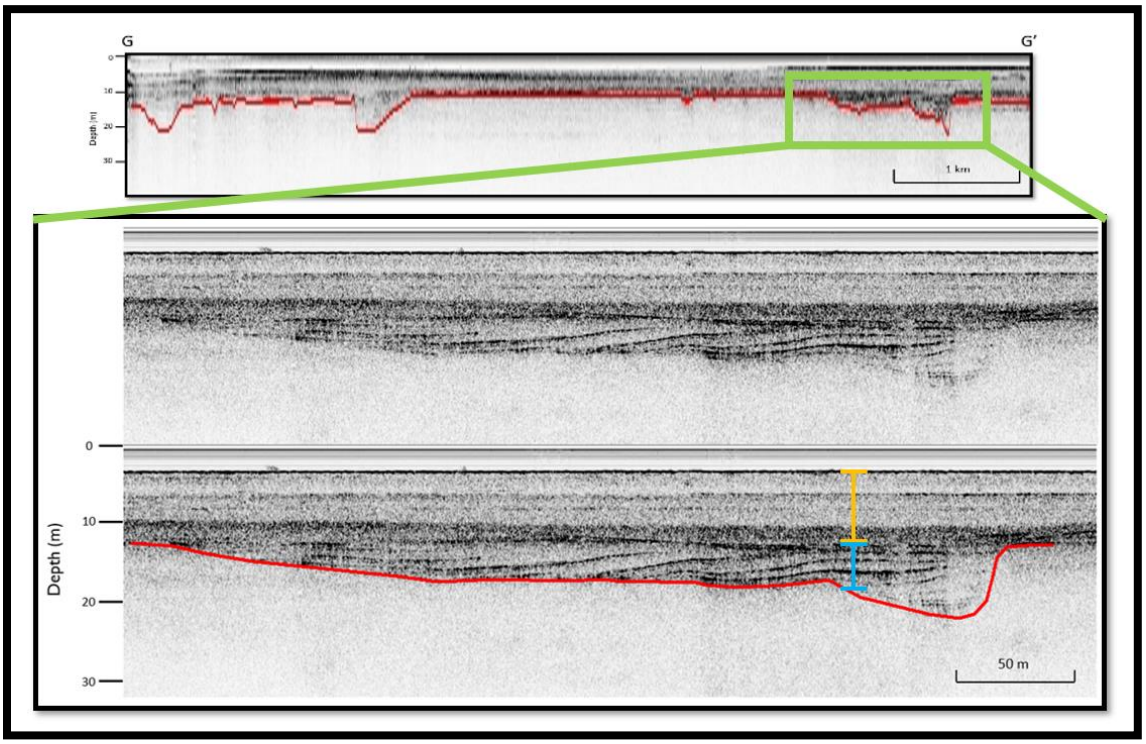

Figure 5.1 Paleochannel cross-section from line 20211205175559-CH1. Green outline indicates the area of examination for bottom image. Yellow line indicates transgressive sediments, which fine upwards. The sediments near the base of yellow line show a higher acoustic impedance, indicating a composition of coarser grains. The blue line indicates area of channel infill which reflects the most energy and contains the coarsest grains. Red lines indicate channel margins.

CHAPTER VI

CONCLUSION

This thesis combines newly and previously collected seismic reflection data from the study area in the central Mississippi Sound to characterize the shallow subsurface Pleistocene-Holocene unconformity. The results indicate that a paleochannel drainage network was created from fluvial incision during the Last Glacial Maximum and associated eustatic sea level decline, and is now covered with Holocene sediments.

Submarine groundwater discharge input into coastal water bodies is difficult to measure and its discharge locations are difficult to predict largely due to heterogeneous hydrogeologic properties in the subsurface. For the study area, stratigraphic features such as paleochannels and related channel infill are possible conduits for submarine groundwater discharge further from shore. Understanding the stratigraphic framework of an area is crucial in determining areas that may experience higher rates of discharge. Marine life adjacent to areas with higher flow potential, such as paleochannel networks, are at risk of exposure to fresh groundwater and possible contaminants. By knowing the locations of paleochannels, more informed decisions can be made by officials in determining wildlife conservation and commercial practices.

This thesis aims to provide an increased understanding of the subsurface heterogeneities within the study area. Further refinement of the study area examined could be attained through the collection and application of more seismic data and sediment cores to better interpolate the Pleistocene-Holocene unconformity, therefore more accurately determining paleochannel

locations and potential SGD. Since the understanding of spatial variability of SGD is not well known for many areas, more research should be conducted where the terrestrial input of freshwater and subsequent contamination can have a significant environmental impact.

NOTE

This project was paid for with federal funding from the Department of the Treasury under the Resources and Ecosystems Sustainability, Tourist Opportunities, and Revived Economies of the Gulf Coast States Act of 2012 (RESTORE Act). The statements, findings, conclusions, and recommendations are those of the author(s) and do not necessarily reflect the views of the Department of the Treasury.

REFERENCES

Adcock, D., 2019. Stratigraphic characterization of the Pleistocene paleodrainage network in the western Mississippi Sound. Theses and Dissertations. 4073. https://scholarsjunction.msstate.edu/td/4073

Allen, G.P., 1991. Sedimentary processes and facies in the Gironde estuary: a recent model of macrotidal estuarine systems. In: Smith, D.G.; Reinson, G.E.; Zaitlin, B.A., and Rahmani, R.A. (eds.), Clastic Tidal Sedimentology. Calgary, Alberta: Canadian Society of Petroleum Geologists, Memoir 16, 29–40.

Allen, G.P., and Posamentier, H.W., 1993. Sequence stratigraphy and facies model of an incised valley fill: Gironde Estuary, France: Journal of Sedimentary Petrology, 63, 378–391. doi.org/10.1306/D4267B09-2B26-11D7-8648000102C1865D

Anderson, J.B., Shipp, S.S., Lowe, A.L., Wellner, J.S., and Mosola, A.B., 2002. The Antarctic Ice Sheet during the Last Glacial Maximum and its subsequent retreat history: Areview: Quaternary Science Reviews, 21, 49–70, doi: 10.1016/S0277-3791(01)00083-X.

Anderson, J.B., Rodriguez, A., Abdulah, K.C., Fillon, R.H., Banfield, L.A., McKeown, H.A., and Wellner, J.S., 2004. Late Quaternary Stratigraphic Evolution of the Northern Gulf of Mexico margin: A Synthesis, in Anderson, J.B. and Fillion, R.H. (eds.), Late Quaternary Stratigraphic Evolution of the Northern Gulf of Mexico Margin: Society of Economic Paleontologists and Mineralogists, Special Publication 79, 1–23.

Anderson, J.B., Wallace, D.J., Simms, A.R., Rodriguez, A.B., and Milliken, K.T., 2014. Variable response of coastal environments of the northwestern Gulf of Mexico to sea-level rise and climate change: implications for future change. Mar. Geol., 352, 348–366. doi.org/10.1016/j.margeo.2013.12.008

Anderson, J.B., Wallace, D.J., Simms, A.R., Rodriguez, A.B., Weight, R.W., and Taha, Z.P., 2016. Recycling Sediments Between Source and Sink During a Eustatic Cycle: Case Study of Late Quaternary Northwestern Gulf of Mexico Basin. Earth-Science Reviews 153, 111–138. doi.org/10.1016/j.earscirev.2015.10.014

Autin, W.J., Burns, S.F., Miller, B.J., Saucier, R.T., and Snead, J.I., 1991. Quaternary geology of the Lower Mississippi Valley, in Morrison, R.B., ed., Quaternary nonglacial geology: Conterminous U.S.: Boulder, Colorado, Geological Society of America, The Geology of North America, K-2, 547–582.

Bard, E., Hamelin, B., Fairbanks, R.G., and Zindler, A., 1990a. Calibration of the ^{14}C timescale over the past 30,000 years using mass spectrometric U-Th ages from Barbados corals. Nature, 345, 405–409. doi: 10.1038/345405a0

Bard, E., Hamelin, B., and Fairbanks, R.G., 1990b. U-Th ages obtained by mass spectrometry in corals from Barbados: sea level during the past 130,000 years. Nature 346, 456–458. doi: 10.1038/346456a0

Bard, E., Hamelin, B., Arnold, M., Montaggioni, L., Cabioch, G., Faure, G., and Rougerie, F., 1996. Sea-level record from Tahiti corals and the timing of deglacial meltwater discharge. Nature, 382, 241–244, doi: 10.1038/382241a0

Bartek, L.R., Cabote, B.S., Young, T., and Schroeder, W., 2004. Sequence stratigraphy of a continental margin subjected to low-energy and low-sediment supply environmental boundary conditions: late Pleistocene-Holocene deposition offshore Alabama, U.S.A., in Anderson, J.B., Fillon, R.H. (Eds.), Late Quaternary Stratigraphic Evolution of the Northern Gulf of Mexico Margin. Society for Sedimentary Geology, Special Publication 79, 85–109.

Bettis, E.A., III, Muhs, D.R., Roberts, H.M., and Wintle, A.G., 2003. Last Glacial loess in the conterminous USA: Quaternary Science Reviews, 22, 1907–1946. doi: 10.1016/S0277-3791(03)00169-0.

Beusen, A.H.W., Slomp, C.P., and Bouwman, A.F., 2013. Global land–ocean linkage: Direct inputs of nitrogen to coastal waters via submarine groundwater discharge. Environmental Research Letters, 8, 6. doi.org/10.1088/1748-9326/8/3/034035

Blanchon, P., and Shaw, J., 1995. Reef drowning during the last deglaciation: Evidence for catastrophic sea-level rise and ice-sheet collapse. Geology, 23, 1, 4–8. doi: 10.1130/0091-7613(1995)023<0004:RDDTLD>2.3.CO;2.

Bloom, A.L., Broecker, W.S., Chappell, J.M.A., Matthews, R.K., and Mesolella, K.J., 1974. Quaternary sea-level fluctuations on a tectonic coast: New $^{230}Th/^{234}U$ dates from the Huon Peninsula, New Guinea. Quaternary Research, 4, 185–205.

Blum, M.D., 1993. Genesis and architecture of incised valley fill sequences: a late Quaternary example from the Colorado River, Gulf coastal plain of Texas, in Weimer, P., and Posamentier, H.W., eds., Siliciclastic Sequence Stratigraphy: Recent Developments and Applications: American Association of Petroleum Geologists, Memoir 58, 259–283. doi.org/10.1306/M58581C10

Blum, M.D., and Price, D.M., 1998. Quaternary alluvial plain construction in response to glacio-eustatic and climatic controls, Texas Gulf Coastal Plain, in Shanley, K.W., and McCabe, P.J., eds., Relative Role of Eustasy, Climate, and Tectonism in Continental Rocks: Society for Sedimentary Geology Special Publication 59, 31–48. doi.org/10.2110/pec.98.59.0031

Blum, M.D., and Törnqvist, T.E., 2000. Fluvial responses to climate and sea-level change: a review and look forward. Sedimentology 47, 2–48.

Blum, M.D., Morton, R.A., and Durbin, J.M., 1995. “Deweyville” terraces and deposits of the Texas Gulf Coastal Plain. Transactions of the Gulf Coast Association of Geological Societies, 45, 53–60.

Blum, M.D., Misner, T.J., Collins, E.S. Scott, D.B., Morton, R.A., and Aslan, A., 2001. Middle Holocene sea-level rise and highstand at +2m. Texas Gulf Coast. Journal of Sedimentary Research, 71, 581–588. doi.org/10.1306/112100710581

Blum, M.D., Carter, A.E., Zayac, T., and Goble, R., 2002. Middle Holocene sea-level and evolution of the Gulf of Mexico coast. Journal of Coastal Research, 36, 65–80. doi.org/10.2112/1551-5036-36.sp1.65

Blum, M.D, Martin, J., Milliken, K., and Garvin, M., 2013. Paleovalley systems: insights from Quaternary analogs and experiments. Earth-Sci. Rev. 116, 128–169.

Boone, P.A., 1973. Depositional Systems of the Alabama, Mississippi and Western Florida Coastal Zone, Gulf Coast Association of Geological Societies, Transactions, 23, 266–277.

Booth, D.B., Troost, K.G., Clague, J.J., and Waitt, R.B., 2003. The Cordilleran ice sheet. In: A.R. Gillespie, S.C. Porter, B.F. Atwater (Eds.), The Quaternary Period in the United States, Developments in Quaternary Science, 1, Elsevier, Amsterdam, 17–43.

Bosse, S.T., Flocks, J.G., and Forde, A.S., 2017. Digitized analog boomer seismic-reflection data collected during U.S. Geological Survey cruises Erda 90-1_HC, Erda 90-1_PBP, and Erda 91-3 in Mississippi Sound, June 1990 and September 1991: U.S. Geological Survey Data Series 1047. doi.org/10.3133/ds1047

Bouvier-Soumagnac, Y., and Duplessy J.C., 1985. Carbon and oxygen isotopic composition of planktonic foraminifera from laboratory culture, plankton tows and recent sediment: Implications for the reconstruction of paleoclimatic conditions and of the global carbon cycle. Journal of Foraminiferal Research, 15, 302–320. doi.org/10.2113/gsjfr.15.4.302

Bratton, J.F., 2007. The importance of shallow confining units to submarine groundwater flow. In: A new Focus on Groundwater-Seawater Interactions. Wallingford, UK: International Association of Hydrological Sciences, 28–36.

Breier, J.A., Breier, C.F., and Edmonds, H.N., 2005. Detecting submarine groundwater discharge with synoptic surveys of sediment resistivity, radium, and salinity. Geophysical Research Letters, 32 (23). doi.org/10.1029/2005GL024639

Breier, J.A., and Edmonds, H.N., 2007. High Ra-226 and Ra-228 activities in Nueces Bay, Texas indicate large submarine saline discharges. Marine Chemistry, 103(1–2), 131–145. doi.org/10.1016/j.marchem.2006.06.015

Bull, J.M., Quinn, R., and Dix, J.K., 1998. Reflection Coefficient Calculation from Marine High Resolution Seismic Reflection (Chirp) Data and Application to an Archaeological Case Study. Marine Geophysical Researches, 20, 1–11. doi: 10.1023/A:1004373106696.

Burnett, W.C., Bokuniewicz, H., Huettel, M., Moore, W. S., and Taniguchi, M., 2003. Groundwater and pore water inputs to the coastal zone. Biogeochemistry, 66, 3–33. doi.org/10.1023/B:BIOG.0000006066.21240.53

Buster, N.A., Brenner, O.T., and Flocks, J.G., 2017. Historical and recent coastal bathymetry data nearshore Ship, Horn, and Petit Bois Islands, Mississippi: U.S. Geological Survey data release. doi.org/10.5066/F7028QFV

Cabioch, G., and Ayliffe, L.K., 2001. Raised coral terraces at Malakula, Vanauatu, southwest Pacific, indicate high sea level during Marine Isotope Stage 3. Quaternary Research, 56, 357–365. doi.org/10.1006/qres.2001.2265

Cable, J.E., Burnett, W.C., and Chanton, J.P., 1997. Magnitude and variations of groundwater seepage along a Florida marine shoreline. Biogeochemistry, 38, 189–205. doi.org/10.1023/A:1005756528516

Carlson, A.E., Clark, P.U., Raisbeck, G.M., and Brook, E.J., 2007. Rapid Holocene deglaciation of the Labrador sector of the Laurentide Ice Sheet. Journal of Climate, 20, 5126–5130. doi: 10.1175/JCLI4273.1

Červený, V., 2001. Seismic Rays and Travel Times. In Seismic Ray Theory. Cambridge: Cambridge University Press, 99–233. doi:10.1017/CBO9780511529399.004

Chappell, J., 2002. Sea level changes forced ice breakouts in the Last Glacial cycle: new results from coral terraces. Quaternary Science Reviews, 21, 1229–1240. doi.org/10.1016/S0277-3791(01)00141-X

Chappell, J., Omura, A., Ezat, T., McCulloch, M., Pandolfi, J., Ota, Y., and Pillans, B., 1996. Reconciliation of late Quaternary sea levels derived from coral terraces at Huon Peninsula with deep-sea oxygen isotope records. Earth and Planetary Science Letters 141, 227–236. doi.org/10.1016/0012-821X(96)00062-3

Chen, J.H., Curran H.A., White B., and Wasserburg, G.J., 1991. Precise chronology of the last interglacial period: ^{234}U–^{230}Th data from fossil coral reefs in the Bahamas. Geol. Soc. Am. Bulletin, 103, 82–97. doi.org/10.1130/00167606(1991)103<0082:PCOTLI>2.3.CO;2

Church, M., 2006. Bed material transport and the morphology of alluvial river channels. Annual Review of Earth and Planetary Sciences, 34, 325–354.

Cipriani, L.E., and Stone, G.W., 2001. Net longshore sediment transport and textural changes in beach sediments along the southwest Alabama and Mississippi barrier islands, U.S.A. Journal of Coastal Research, 17, 443–458.

Clark, J.A., Farrell, W.E., and Peltier, W.R., 1978, Global changes in postglacial sea level: A numerical calculation: Quaternary Research, 9, 265–287. doi: 10.1016/0033-5894(78)90033-9.

Clark, P.U., Dyke, A.S., Shakun, J.D., Carlson, A.E., Clark, J., Wohlfarth, B., Mitrovica, J.X., Hostetler, S.W., and McCabe, A.M., 2009. The last glacial maximum. Science, 325 (5941), 710–714. doi:10.1126/science.1172873

Coleman, J.M. and Roberts, H.H., 1988. Sedimentary development of the Louisiana continental shelf related to sea level cycles: Part II—seismic response. Geo-Marine Letters 8, 109–119. https://doi.org/10.1007/BF02330968

Collins, L.B., Zhu, Z.R., Wyrwoll, K., Hatcher, B.G., Playford, P.E., Chen, J.H., Eisenhauer, A., and Wasserburg, G.J., 1993. Late Quaternary evolution of coral reefs on a cool-water carbonate margin: the Abrolhos Carbonate Platforms, southwest Australia. Marine Geology 110: 203–212. https://doi.org/10.1016/0025-3227(93)90085-A

Covey, C., and Haagenson, P.L., 1984. A model of oxygen isotope composition of precipitation: Implications for paleoclimate data, Journal of Geophysical Research, 89(D3), 4647–4655. doi:10.1029/JD089iD03p04647

Curray, J.R., 1965. Sediments and history of the Holocene transgression, continental shelf, northwest Gulf of Mexico, In: Wright, H.E., Jr., and Frey, D.G., eds., The Quaternary of the United States: Princeton, New Jersey, Princeton University Press, 723–735.

Cutler, K.B., Edwards, R.L., Taylor, F.W., Cheng, H., Adkins, J., Gallup, C.D., Cutler, P.M., Burr, G.S., and Bloom, A.L., 2003. Rapid sea-level fall and deep-ocean temperature change since the last interglacial period. Earth and Planetary Science Letters, 206, 253–271. doi:10.1016/S0012-821X(02)01107-X

Dade, W.B., and Friend, P.F., 1998. Grain-size, sediment transport regime, and channel slope in alluvial rivers. Journal of Geology 106, 661–675. doi.org/10.1086/516052

Dalrymple, R.W., Zaitlin, B.A., And Boyd, R., 1992. Estuarine facies models: conceptual basis and stratigraphic implications: Journal of Sedimentary Petrology, 62, 1130–1146. doi.org/10.1306/D4267A69-2B26-11D7-8648000102C1865D

Dalrymple, R.W., Boyd, R., and Zaitlin, B.A., 1994. History of research, types and internal organization of incised-valley systems: introduction to volume, in Dalrymple, R.W., Boyd, R., and Zaitlin, B.A., eds., Incised-Valley Systems: Origin and Sedimentary Sequences: SEPM, Special Publication 51, 1–10. doi.org/10.2110/pec.94.12.0003

Daniel III, C.C., Miller, R.D., and Wrege, B.M., 1996. Application of geophysical methods to the delineation of paleochannels and missing confining units above the Castle Hayne aquifer at the US Marine Corps Air Station Cherry Point, North Carolina. US Geological Survey, Water-Resources Investigations Report 95–4252. doi.org/10.3133/wri954252

Dansgaard, W., 1964. Stable isotopes in precipitation, Tellus, 16:4, 436–468. doi: 10.3402/tellusa.v16i4.8993

Davies, D.K. and Moore, W.R., 1970. Dispersal of Mississippi Sediment in the Gulf of Mexico. SEPM Journal of Sedimentary Research, 40. doi: 10.1306/74d71f41-2b21-11d7-8648000102c1865d

DeWitt, N.T., Flocks, J.G., Pendleton, E.A., Hansen, M.E., Reynolds, B.J., Kelso, K.W., Wiese, D.S., and Worley, C.R., 2012. Archive of single beam and swath bathymetry data collected nearshore of the Gulf Islands National Seashore, Mississippi, from West Ship Island, Mississippi, to Dauphin Island, Alabama: Methods and data report for USGS cruises 08CCT01, 08CCT02, July 2008 and 09CCT03 and 09CCT04, June 2009: U.S. Geological Survey Data Series 675. doi.org/10.3133/ds675

Dia, A.N., Cohen, A.S., O'Nions, R.K., and Shackleton, N.J., 1992. Seawater Sr isotope variation over the past 300 ka and influence of global climate cycles. Nature, 356, 786. doi.org/10.1038/356786a0

Diogo, L.A., le Diagon, F.M.M., and Prado, R.L., 2004. Bedrock imaging using post-critical shallow seismic reflection data. Journal of Applied Geophysics, 57(1), 1–9. doi.org/10.1016/j.jappgeo.2004.08.006

Dodge, R.E., Fairbanks, R.G., Benninger, L.K., and Maurrasse, F., 1983. Pleistocene sea levels from the raised coral reefs of Haiti. Science, 219, 1423–1425.

Doughty, A.M., Kaplan, M.R., Peltier, C., and Barker, S., 2021. A maximum in global glacier extent during MIS 4. Quaternary Science Reviews, 261. doi: 10.1016/j.quascirev.2021.106948

DuBar, J.R., Ewing, T.E., Lundelius, Jr., E.L., Otvos, E.G., and Winker, C.D., 1991. Quaternary geology of the Gulf of Mexico coastal plain. In: Morrison, R.B., ed., Quaternary Nonglacial Geology, Conterminous U.S.: Geological Society of America, The Geology of North America, K-2, 583–610. doi.org/10.1130/DNAG-GNA-K2.583

Duncan, J.M., Goff, J.A., Austin Jr., J.A., and Fulthorpe, C.C., 2000. Tracking the last sea-level cycle: seafloor morphology and shallow stratigraphy of the latest Quaternary New Jersey middle continental shelf. Marine Geology 170, 395–421.

Edwards, R., Chen, J.H., and Wasserburg, G.J., 1986. ^{238}U-^{234}U-^{230}Th-^{232}Th systematics and the precise measurement of time over the past 500,000 years. Earth and Planetary Science Letters 81, 175–192. doi: 10.1016/0012-821X(87)90154-3

Ehlers, J., Gibbard, P.L., and Hughes, P.D., 2011. Quaternary Glaciations – Extent and Chronology: A Closer Look, Developments in Quaternary Science, 15, Elsevier, Amsterdam.

Emiliani, C., 1955. Pleistocene temperatures. Journal of Geology, 63, 538–578. jstor.org/stable/30080906

Essaid, H.I., 1990. A multilayered sharp interface model of coupled freshwater and saltwater flow in coastal systems: model development and application. Water Resources Research, 26(7), 1431–1454. doi: 10.1029/WR026i007p01431

Fairbanks, R.G., 1989. A 17,000-year glacio-eustatic sea-level record: Influence of glacial melting rates on the Younger Dryas event and deep-ocean circulation. Nature, 342, 637–642, doi: 10.1038/342637a0

Fairbanks, R.G., 1992. Barbados sea level and Th/U 14C calibration. IGBP Pages/World Data Center for Paleoclimatology Data Contribution Series #92-0202. NOAA/NGDC Paleoclimatology Program, Boulder Colorado.

Fisk, H.N., 1938, Pleistocene exposures in western Florida Parishes, Louisiana, in Contributions to the Pleistocene history of the Florida Parishes of Louisiana: Louisiana Geological Survey Bulletin 12, 3–26.

Fisk, N.H., 1944, Geological Investigation of the Alluvial Valley of the Lower Mississippi River: Vicksburg, Mississippi River Commission.

Fisk, H.N., 1947. Geology of the Mississippi Valley Region, Tulsa Geological Society Digest, 15, 50–55.

Fisk, N.H., 1951. Loess and Quaternary geology of the Lower Mississippi Valley: The Journal of Geology, 59, 333–356, doi:10.1086/625872

Fisk, H.N., McFarlane Jr., E., Kolb, C.R., Wilbert Jr., L.J., 1954. Sedimentary Framework of the Mississippi Delta, Journal of Sedimentary Petrology, 24, no. 2, 76–99.

Flocks, J.G., Kindinger, J.L., and Kelso, K.W., 2015. Geologic control on the evolution of the inner shelf morphology offshore of the Mississippi barrier islands, northern Gulf of Mexico, USA. Cont. Shelf Res. 101. doi.org/10.1016/j.csr.2015.04.008

Forde, A.S., Dadisman, S.V., Flocks, J.G., DeWitt, N.T., Reynolds, B.J., and Wiese, D.S., 2011. Archive of digital CHIRP sub-bottom profile data collected during USGS cruise 08CCT02 and 08CCT03, Mississippi Gulf Islands, July and September 2008: U.S. Geological Survey Data Series 569. doi.org/10.3133/ds569

Foyle, A.M., and Oertel, G.F., 1997. Transgressive systems tract development and incised valley fills within a Quaternary estuary shelf system: Virginia inner shelf, USA. Marine Geology, 137, 227–249. doi.org/10.1016/S0025-3227(96)00092-8

Frazier, D.E., 1974. Depositional episodes: their relationship to the strati-graphic framework in the Gulf Basin: University of Texas, Bureau of Economic Geology, Circular 74–1, 28.

Gal, N., 2018. Holocene Formation and Evolution of Horn Island, Mississippi, USA. Masters thesis. 603. https://aquila.usm.edu/masters_theses/603

Galicki, S., and Schmitz, D.W., 2016. Roadside Geology of Mississippi. Mountain Press Publishing Company, Missoula, MT.

Galloway, W., 1989. Genetic Stratigraphic Sequences in Basin Analysis I: Architecture and Genesis of Flooding-Surface Bounded Depositional Units. AAPG Bulletin, 73. 10.1306/703C9AF5-1707-11D7-8645000102C1865D.

Gillespie, A., and Molnar, P., 1995. Asynchronous maximum advances of mountain and continental glaciers. Reviews of Geophysics, 33, 311–364. doi: 10.1029/95RG00995

Gohn, G.S., and Reinhardt, J., 2001. A. Stratigraphy of Subsurface Neogene and Quaternary Sediments in Southern Jackson County, Mississippi. In: Gohn, G.S., ed., 2001, Stratigraphic and Paleontologic studies of the Neogene and Quaternary sediments in southern Jackson County, Mississippi: U.S. Geological Survey Open-File Report 01-415-A. pubs.usgs.gov/of/2001/of01-415/

Gohn, G.S., Reinhardt, J., Bybell, L.M., Rubin, M., and Garrison, Jr., J.A., 2001. B. Physical Stratigraphy, Calcareous Nannofossil Biostratigraphy, and Depositional History of the Quaternary Sediments in the USGS-Belle Fontaine No. 1 Core, Jackson County, Mississippi. In: Gohn, G.S., ed., 2001. Stratigraphic and paleontologic studies of the Neogene and Quaternary sediments in southern Jackson County, Mississippi: U.S. Geological Survey Open-File Report 01-415-B. pubs.usgs.gov/of/2001/of01-415/

Green, A.N., 2009. Palaeo-drainage, incised valley fills and transgressive systems tract sedimentation of the northern KwaZulu-Natal continental shelf, South Africa, SW Indian Ocean. Marine Geology, 263, 46–63. doi.org/10.1016/j.margeo.2009.03.017

Greene Jr., D.L., Rodriguez, A.B., and Anderson, J.B., 2007. Seaward- branching coastal-plain and piedmont incised-valley systems through multiple sea-level cycles: Late Quaternary examples from Mobile Bay and Mississippi Sound, U.S.A. J. Sediment. Res. 77, 139–158. doi.org/10.2110/jsr.2007.016

Guilderson, T., Burckle, L., and Hemming, S., 2000. Late Pleistocene sea level variations derived from the Argentine Shelf Geochemistry Geophysics Geosystems, 1. doi.org/10.1029/2000GC000098

Gutowski, M., Bull, J., Henstock, T., Dix, J., Hogarth, P., Leighton, T., and White, P., 2002. Chirp sub-bottom profiler source signature design and field testing. Marine Geophysical Researches, 23, 481–492. 10.1023/B:MARI.0000018247.57117.0e

Harris, M.S., Gayes, P.T., Kindinger, J.L., Flocks, J.G., Krantz, D.E., and Donovan, P., 2005. Quaternary geomorphology and modern coastal development in response to an inherent geologic framework: An example from Charleston, South Carolina. Journal of Coastal Research, 21(1), 49–64. doi.org/10.2112/00-015.1

Hearty, P.J., and Kindler, P., 1997. The stratigraphy and surficial geology of New Providence and surrounding islands, Bahamas. Journal of Coastal Research, 13, 798–812.

Helmens, K.F., 2014. The Last Interglacial-Glacial cycle (MIS 5e–2) re-examined based on long proxy records from central and northern Europe. Quaternary Science Review, 86, 115–143. doi.org/10.1016/j.quascirev.2013.12.012

Heroy, D.C., and Anderson, J.B., 2007. Radiocarbon constraints on Antarctic Peninsula ice sheet retreat following the Last Glacial Maximum: Quaternary Science Reviews, 26, 3286–3297, doi: 10.1016/j.quascirev.2007.07.012.

Hollis, R, 2018. Late Quaternary Evolution and Stratigraphic Framework Influence on Coastal Systems along the North-Central Gulf of Mexico, USA. Masters thesis. 598. https://aquila.usm.edu/masters_theses/598

Hughes, P.D., Gibbard, P.L., and Ehlers, J., 2013. Timing of glaciation during the last glacial cycle: evaluating the concept of a global 'Last Glacial Maximum'(LGM). Earth-Science Reviews, 125, 171–198. doi.org/10.1016/j.earscirev.2013.07.003

Hutchinson, M.F., Xu, T., and Stein, J.A., 2011. Recent Progress in the ANUDEM Elevation Gridding Procedure. In: Geomorphometry 2011, edited by T. Hengel, I.S. Evans, J.P. Wilson and M. Gould, 19–22. Redlands, California, USA. See: http://geomorphometry.org/HutchinsonXu2011.

Isphording, W.C., Imsand, F.D., and Flowers, G.C., 1989. Physical Characteristics and Aging of Gulf Coast Estuaries, Gulf Coast Association of Geological Societies Transactions, 39, 387–401.

Ivins, E.R., Blom, R.G., Wu, X., and Dokka, R., 2005. Late Pleistocene sedimentation increase in the Gulf of Mexico and modeling of time-dependent long-wavelength flexural subsidence. American Geophysical Union, Fall Meeting 2005.

Ivins, E.R., Dokka, R.K., and Blom, R.G., 2007. Post-glacial sediment load and subsidence in coastal Louisiana. Geophysical Research Letters 34, 1–5. doi:10.1029/2007GL030003.

Johnson, R.G., and Andrews, J.T., 1986. Glacial terminations in the oxygen isotope record of deep sea cores: hypothesis of massive Antarctic ice-shelf destruction. Palaeogeogr. Palaeoclimatol. Palaeoecol. 53, 107–138.

Kaufman, D.S., Young, N.E., Briner, J.P., and Manley, W.F., 2011. Alaska Palaeo-Glacier Atlas (Version 2). In: Ehlers, J., Gibbard, P.L., and Hughes, P.D., 2011. Quaternary Glaciations — Extent and Chronology: A Closer Look, Developments in Quaternary Science, 15, Elsevier, Amsterdam, 427–445. doi.org/10.1016/B978-0-444-53447-7.00033-7

Kindinger, J.L., 1988. Seismic Stratigraphy of the Mississippi-Alabama Shelf and Upper Continental Slope, Marine Geology, 83, 79–94.

Kindinger, J.L, Penland, S., Williams, S.J., and Suter, J.R., 1989. Inner Shelf Deposits of the Louisiana-Mississippi-Alabama Region, Gulf of Mexico. Transactions- Gulf Coast Association of Geological Societies, 39, 413–420.

Kindinger, J., Balson, P., and Flocks, J., 1994. Stratigraphy of the Mississippi-Alabama shelf and the Mobile River incised valley system. In: Dalrymple, R., Boyd, R., Zaitlin, B. (Eds.), Incised-Valley Systems: Origin and Sedimentary Sequences, 51. SEPM (Society of Sedimentary Geology) Special Publication, Tulsa, OK, USA, 83–95.

Kindinger, J.L., Miselis, J.L., and Buster, N.A., 2014. The shallow stratigraphy and sand resources offshore from Cat Island, Mississippi: U.S. Geological Survey Open-File Report 2014–1070, 74. doi.org/10.3133/ofr20141070.

Kopp, R.E., Simons, F.J., Mitrovica, J.X., Maloof, A.C., and Oppenheimer, M., 2009. Probabilistic assessment of sea level during the last interglacial stage. Nature, 462, 863–868. doi.org/10.1038/nature08686

Kramer, K.A., 1990. Late Pleistocene to Holocene Geologic Evolution of the Grande Batture Headland Area, Jackson County, Mississippi, 1990. Mississippi State University: Mitchell Library Special Collections.

Kroeger, K.D., and Charette, M.A., 2008. Nitrogen biogeochemistry of submarine groundwater discharge. Limnol. Oceanogr., 53 (3), 1025–1039.

Larsen, N.K., Knudsen, K.L., Krohn, C.F., Kronborg, C., Murray, A.S. and Nielsen, O.B., 2009. Late Quaternary ice sheet, lake and sea history of southwest Scandinavia – a synthesis. Boreas, 38, 732–761. doi.org/10.1111/j.1502-3885.2009.00101.x

Leopold, L.B., and Maddock, T., 1953. The Hydraulic Geometry of Stream Channels and Some Physiographic Implications, USGS Professional Paper, 252, 1–57.

Leverington, D.W., Mann, J.D., and Teller, J.T., 2002. Changes in the bathymetry and volume of glacial Lake Agassiz between 9200 and 7700 ^{14}C yr B.P. Quaternary Research, 57, 244–252. doi.org/10.1006/qres.2001.2311

Licciardi, J.M., Clark, P.U., Brook, E.J., Elmore, D., and Sharma, P., 2004. Variable responses of western US glaciers during the last termination. Geology, 32, 81–84. doi.org/10.1130/G19868.1

Linsley, B.K., 1996. Oxygen-isotope record of sea-level and climate variations in the Sulu Sea over the past 150,000 years. Nature, 380, 234–237. doi.org/10.1038/380234a0

Lisiecki, L.E., and Raymo, M.E., 2005. A Pliocene–Pleistocene stack of 57 globally distributed benthic δ18O records. Paleoceanography, 20, 1–17. doi: 10.1029/2004PA001071

Lowe, A.L., and Anderson, J.B., 2002. Late Quaternary advance and retreat of the West Antarctic Ice Sheet in Pine Island Bay: Antarctica: Quaternary Science Reviews, 21, 1879–1897, doi: 10.1016/S0277-3791(02)00006-9.

Ludwick, J.C., 1964. Sediments of the northeastern Gulf of Mexico. In: Miller, R.L., (ed.), Papers in Marine Geology: Shepard Commemorative Volume: MacMillan: New York, 204–238.

Ludwig, K.R., Muhs, D.R., Simmons, K.R., Halley, R.B., and Shinn, E.A., 1996. Sea-level records at ~80 ka from tectonically stable platforms: Florida and Bermuda. Geology 24, 211–214. doi.org/10.1130/0091-7613(1996)024<0211:SLRAKF>2.3.CO;2

Lunkka, J.P., Saarnisto, M., Gey, V., Demidov, I., and Kiselova, V., 2001. Extent and age of the Last Glacial Maximum in the southeastern sector of the Scandinavian Ice Sheet. Global Planet. Change 31, 407–425. doi.org/10.1016/S0921-8181(01)00132-1

Lunt, I.A., and Bridge, J.S., 2004. Evolution and deposits of a gravelly braid bar, Sagavanirktok River, Alaska. Sedimentology 51, 415–432. doi.org/10.1111/j.1365-3091.2004.00628.x

Mange, M.A., and Otvos, E.G., 2005. Gulf Coastal Plain evolution in West Louisiana: Heavy mineral provenance and Pleistocene alluvial chronology. Sedimentary Geology, 82, 1–4, 29–57, doi:10.1016/j.sedgeo.2005.07.015.

Markewich, H.W., Wysocki, D.A., Pavich, M.J., Rutledge, E.M., Millard Jr., H.T., Rich, F.J., Maat, P.B., Rubin, M., and McGeehin, J.P., 1998. Paleopedology plus TL, ^{10}Be, and ^{14}C dating as tools in stratigraphic and paleoclimatic investigations, Mississippi River Valley USA Quaternary International, 51-52, 143–167. doi.org/10.1016/S1040-6182(97)00041-4

Mars, J.C., Shultz, A.W., and Schroeder, W.W., 1992. Stratigraphy and Holocene evolution of Mobile Bay in southwestern Alabama: Gulf Coast Association of Geological Societies, Transactions, 42, 529–542.

Martinson, D.G., Pisias, N.G., Hays, J.D., Imbrie, J., Moore, T.C., and Shackleton, N.J., 1987. Age dating and the orbital theory of the ice ages: development of a high resolution 0–300,000 year chronostratigraphy. Quaternary Research, 27, 1–29. doi.org/10.1016/0033-5894(87)90046-9

Maslin, M.M., and Tzedakis, C., 1996. Sultry Last Interglacial gets sudden chill. EOS. 77, 353–354. doi.org/10.1029/96EO00243

McBride, R.A., Moslow, T.F., Roberts, H.H., and Diecchio, R.J., 2004. Late Quaternary Geology of the Northeastern Gulf of Mexico Shelf: Depositional History, and Ancient Analogues of a Major Shelf Sand Sheet of the Modern Transgressive Systems Tract, in Anderson, J.B. and Fillion, R.H. (eds.), Late Quaternary Stratigraphic Evolution of the Northern Gulf of Mexico Margin, Society of Economic Paleontologists and Mineralogists (SEPM), Special Publication, 79, 55–83.

McCrea, J.M., 1950. On the isotopic chemistry of carbonates and a paleotemperature scale. Journal of Chemical Physics, 18, 849–857. doi.org/10.1063/1.1747785

Mesolella, K.J., Matthews, R.K., Broecker, W.S., and Thurber D.L., 1969. The astronomical theory of climatic change: Barbados data. Journal of Geology, 77, 250–274.

Milliken, K.T., Anderson, J.B., and Rodriguez, A.B., 2008. A new composite Holocene sea-level curve for the northern Gulf of Mexico. In: Anderson, J.B., Rodriguez, A.B. (Eds.), Response of Upper Gulf Coast Estuaries to Holocene Climate Change and Sea-Level Rise. Geological Society of America, Boulder, 1–11.

Milne, I.H., and Shott, W.L., 1958. Clay mineralogy of recent sediments from the Mississippi Sound area: Fifth National Conference on Clays and Clay Minerals, Publication 566, 253–265.

Mitchum, R.M., 1985. Seismic stratigraphic expression of submarine fans. American Association of Petroleum Geologists Memoir 39, Tulsa, Oklahoma, 117–136. doi.org/10.1306/M39449C7

Moore, W.S., 1999. The subterranean estuary: A reaction zone of groundwater and sea water. Marine Chemistry, 65(1–2), 111–125. doi.org/10.1016/S0304-4203(99)00014-6

Mosher, D.C., and Simpkin, P., 1999. Status and trends of marine high-resolution seismic reflection profiling: data acquisition. Geosci. Can., 26, 174–188.

Mulligan, A.E., Evans, R.L., and Lizarralde, D., 2007. The role of paleochannels in groundwater/seawater exchange. Journal of Hydrology, 335(3–4), 313–329. doi.org/10.1016/j.jhydrol.2006.11.025

Mussett, A.E., Khan, M.A., and Button, S., 2000. Looking into the Earth: An Introduction to Geological Geophysics: Cambridge, Cambridge University Press. doi: 10.1017/CBO9780511810305

Otvos, E.G., 1972. Pre-Sangamon beach ridges along the northeastern Gulf Coast: Gulf Coast Association of Geological Societies Transactions, 22, 223–228.

Otvos E.G., 1975. Southern limit of Pleistocene loess, Mississippi Valley. Southeastern Geology, 17, 27–38.

Otvos, E.G., 1982a. Santa Rosa Island, Florida Panhandle, origin of a composite barrier island. Southeastern Geology, 23, 15–24.

Otvos, E.G., 1982b. Coastal Geology of Mississippi, Alabama and adjacent Louisiana areas, Guidebook, Field Trip June 5-6, 1982, The New Orleans Geological Society, 66.

Otvos, E.G., 1991a. Northeastern Gulf Coast Quaternary, section in Quaternary geology of the Gulf of Mexico Coastal Plain, in Morrison, R.B., ed., Quaternary nonglacial geology; Conterminous U.S.: Boulder, Colorado, Geological Society of America, The Geology of North America, K-2, 588–594.

Otvos, E.G., 1991b. Houston ridge, SW Louisiana - end link in the late Pleistocene Ingleside barrier chain? Prairie Formation newly defined: Southeastern Geology, 31, 235–249.

Otvos, E.G., 1994. Mississippi's revised Neogene stratigraphy in northern Gulf context. Gulf Coast Association of Geological Societies Transactions, 44, 542–554.

Otvos, E.G., 1997. Biloxi sands and the Biloxi Formation - A footnote in "stratigraphic archeology": Mississippi Geology, 18, 1, 4–5.

Otvos, E.G., 2001. H. Mississippi Coast: Stratigraphy and Quaternary Evolution in the Northern Gulf Coastal Plain Framework. U.S. Geological Survey Open-file Report 01-415-H.

Otvos, E.G., 2005a. Numerical chronology of Pleistocene coastal plain and valley development; extensive aggradation during glacial low sea-levels: Quaternary International, 135, 91–113, doi: 10.1016/j.quaint.2004.10.026.

Otvos, E.G., 2005b. Coastal barriers, Gulf of Mexico: Holocene evolution and chronology. Jour. Coast. Res. Rhodes Fairbridge Festschr. Vol. Spec. Issue 42, 141–163.

Otvos, E.G., 2018. Coastal barriers, northern Gulf-Last Eustatic Cycle; genetic categories and development contrasts. A review. Quaternary Science Reviews 193, 212–243.

Otvos, E.G., and Howat, W.E., 1992. Late Quaternary coastal units and marine cycles: Correlations between northern Gulf sectors: Gulf Coast Association of Geological Societies Transactions, 42, 571–586.

Peltier C., Kaplan, M.R., Birkel, S.D., Soteres, R.L., Sagredo, E.A., Aravena, J.C., Araos, J., Moreno, P.I., Schwartz, R., and Schaefer, J.M., 2021. The large MIS 4 and long MIS 2 glacier maxima on the southern tip of South America. Quaternary Science Reviews, 262. doi: 10.1016/j.quascirev.2021.106858

Penland, S.P., Boyd, R., and Suter, J.R., 1988. The transgressive depositional systems of the Mississippi River delta plain: A model for barrier shoreline and shelf sand development. Journal of Sediment Research, 58(6), 932–949. doi.org/10.1306/212F8EC2-2B24-11D7-8648000102C1865D

Phillips, F.M., Zreda, M., Plummer, M.A., Elmore, D., and Clark, D.H., 2009. Glacial geology and chronology of Bishop Creek and vicinity, eastern Sierra Nevada, California. Geological Society of America Bulletin, 121, 1013–1033. doi.org/10.1130/B26271.1

Porter, S.C., 2011. Glaciation of Hawaii. In: J. Ehlers, P.L. Gibbard, P.D. Hughes. Quaternary Glaciations - Extent and Chronology: A Closer Look. Developments in Quaternary Science, 15, Elsevier, Amsterdam, 463–466.

Portnoy, J.W., Nowicki, B.L., Roman, C.T., and Urish, D.W., 1998. The discharge of nitrate-contaminated groundwater from developed shoreline to marsh-fringed estuary. Water Resources Research 34 (11), 3095–3104. doi: 10.1029/98WR02167

Posamentier, H.W., and Vail, P.R., 1988. Eustatic control on clastic deposition II – sequence and system tract models. In: Wilgus, C.K., Hastings, B.S., Kendall, C.G.C., Posamentier, H.W., Ross, C.A., Van Wagoner, J.C. (Eds.), Sea-Level Changes: An Integrated Approach: SEPM Special Publication, 42, 125–154.

Posamentier, H.W., Allen, G.P., James, D., and Tesson, M., 1992. Forced regressions in a sequence stratigraphic framework: concepts, examples, and exploration significance. AAPG Bulletin 76, 1687–1709.

Priddy, R.R., Crisler, Jr., R.M., Sebren, C.P., Powell, J.D., and Burford, H., 1955. Sediments of Mississippi Sound and inshore waters. University, Miss. 1955.

Pye, K., and Johnson, R., 1988. Stratigraphy, geochemistry, and thermoluminescence ages of Lower Mississippi Valley loess Earth Surface Processes and Landforms, 13, 103–124. doi:10.1002/esp.3290130203

Rabouille, C., Mackenzie, F.T., and Ver, L.M., 2001. Influence of the human perturbation on carbon, nitrogen, and oxygen biogeochemical cycles in the global coastal ocean. Geochimica et Cosmochimica Acta, 65(21), 3615–3641. doi.org/10.1016/S0016-7037(01)00760-8

Rainwater, E.H., 1964. Late Pleistocene and recent history of Mississippi Sound between Beauvoir and Ship Island: Mississippi Geological Survey Bulletin. No. 103, 32–61.

Richmond, G.M., and Fullerton, D.S., 1986. Introduction to Quaternary glaciations in the United States. Quaternary Science Reviews, 5, 3–10.

Robinson, M.A., and Gallagher, D.L., 1999. A model of ground water discharge from an unconfined coastal aquifer. Ground Water, 37(1), 80–87. doi.org/10.1111/j.1745-6584.1999.tb00960.x

Robinson, C.E., Xin, P., Santos, I.R., Charette, M.A., Li, L., and Barry, D.A., 2018. Groundwater dynamics in subterranean estuaries of coastal unconfined aquifers: Controls on submarine groundwater discharge and chemical inputs to the ocean. Advances in Water Resources, 115, 315–331. doi.org/10.1016/j.advwatres.2017.10.041

Rubey, W.W., 1952. Geology and mineral resources of the Hardin and Brussels quadrangles (in Illinois): U.S. Geological Survey Professional Paper 218, 179. doi.org/10.3133/pp218

Rucker, J.B. and Snowden, J.O., 1989. Relict progradational beach ridge complex on Cat Island in Mississippi Sound. Transactions Gulf Coast Association of Geological Societies, 39, 531–539.

Rucker, J.B., Snowden, J.O., Lambert, D.N., and Kramer, K., 1990. Sub-bottom acoustic reconnaissance survey of sediments in eastern Mississippi Sound. In: Tanner, W.F. (ed.) Coastal Sediments and Processes. Proceedings, Ninth Symposium on Coastal Sedimentology, 101–111.

Russoniello, C.J., Fernandez, C., Bratton, J.F., Banaszak, J.F., Krantz, D.E., Andres, A S., Konikow, L.F., and Michael, H.A., 2013. Geologic effects on groundwater salinity and discharge into an estuary. Journal of Hydrology, 498, 1–12. doi.org/10.1016/j.jhydrol.2013.05.049

Sanford, J.M., Harrison, A.S., Wiese, D.S., and Flocks J.G., 2016. Archive of Digitized Analog Boomer Seismic Reflection Data Collected from the Mississippi-Alabama-Florida Shelf During Cruises Onboard the R/V Kit Jones, June 1990 and July 1991. U.S. Geological Survey Data Series 429. pubs.usgs.gov/ds/429/index.html

Sanhaji M., and Guarin, H., 2013. High-resolution seismic reflection coefficient calculation using a chirp sub-bottom profiler. IEEE/OES Acoustics in Underwater Geosciences Symposium, 1–3. doi:10.1109/RIOAcoustics.2013.6684005

Saucier, R.T., 1968. New chronology for braided stream surface formation in the Lower Mississippi Valley. Southeastern Geology, 9, 65–76.

Saucier, R.T., 1974. Quaternary geology of the Lower Mississippi Valley: Arkansas Archeological Survey. Research Series, 6, 1–26.

Saucier, R.T., 1994. Geomorphology and Quaternary Geologic History of the Lower Mississippi Valley. Vicksburg, Mississippi River Commission, 364.

Sawyer, A.H., Shi, F., Kirby, J.T., and Michael, H.A., 2013. Dynamic response of surface water-groundwater exchange to currents, tides, and waves in a shallow estuary. Journal of Geophysical Research: Oceans, 118, 1749–1758. doi.org/10.1002/jgrc.20154

Schock, S.G., LeBlanc, L.A., and Parda, S., 1992. Sediment Classification Using the Chirp Sonar. Offshore Technology Conference. doi: 10.4043/6851-MS

Schock, S.G., 2004. A method for estimating the physical and acoustic properties of the sea bed using chirp sonar data. IEEE Journal of Oceanic Engineering, 29, 4, 1200–1217. doi: 10.1109/JOE.2004.841421

Schumm, S.A., 1977. The Fluvial System. New York: Wiley-Interscience, 338.

Schumm, S.A., 1985. Patterns of alluvial rivers. Annual Review of Earth and Planetary Sciences, 13, 5–27. doi.org/10.1146/annurev.ea.13.050185.000253

Shackleton, N.J., 1987. Oxygen isotopes, ice volume and sea level. Quaternary Science Reviews 6, 183–190.

Shanley, K.W., and McCabe, P.J., 1994. Perspectives on the sequence stratigraphy of continental strata. American Association of Petroleum Geologists, Bulletin, 78, 544–568. doi.org/10.1306/BDFF9258-1718-11D7-8645000102C1865D

Shulits, S., 1941. Rational equation of river-bed profile: Am. Geophys. Union Trans., 22, 622–631. doi.org/10.1029/TR022i003p00622

Simms, A.R., Anderson, J.B., Taha, Z.P., and Rodriguez, A.B., 2006. Overfilled versus underfilled incised valleys: lessons from the Quaternary Gulf of Mexico. In: Dalrymple, R., Leckie, D., Tillman, R. (Eds.), Incised Valleys in Time and Space. SEPM Special Publication 85, 117–139. doi.org/10.2110/pec.06.85.0117

Skene, I.J., Piper, D.J.W., Aksu, A.E., and Syvitski, J.P.M., 1998. Evaluation of the global oxygen, isotope curve as a proxy for Quaternary sea level by modeling of delta progradation. Journal of Sedimentary Research, 68, 1077–1092.

Sloss, L.L., Krumbein, W.C., and Dapples, E.C., 1949. Integrated facies analysis. In: Longwell, C.R., ed., Sedimentary Facies in Geologic History: Geological Society of America, Memoir 39, 91–124.

Spalt, N., Murgulet, D., and Hu, X., 2018. Relating estuarine geology to groundwater discharge at an oyster reef in Copano Bay, TX. Journal of Hydrology, 564, 785–801. doi.org/10.1016/j.jhydrol.2018.07.048

Starkel, L., 1991. Long-distance correlation of fluvial events in the temperate zone. In: Starkel, L., Gregory, K.J., and Thornes, J.B., Temperate Palaeohydrology: Fluvial Processes in the Temperate Zone During the Last 15,000 Years, 473–495.

Stauch, G., Lehmkuhl, F., and Frechen, M., 2007. Luminescence chronology from the Verkhoyansk Mountains (North-Eastern Siberia). Quaternary Geochronology, 2, 255–259. doi.org/10.1016/j.quageo.2006.05.013

Stein, M., Wasserburg, G.J., Aharon, P., Chen, J.H., Zhu, Z.R., Bloom, A., and Chappell, J., 1993. TIMS U-series dating and stable isotopes of the last interglacial event in Papua New Guinea. Geochemica et Cosmochemica Acta 57, 2541–2554. doi: 10.1016/0016-7037(93)90416-T

Stirling, C.H., Esat, T.M, McCulloch, M.T., and Lambeck, K., 1995. High-precision U-series dating of corals from Western Australia and implications for the timing and duration of the last interglacial, Earth and Planetary Science Letters, 135, 115–130. doi.org/10.1016/0012-821X(95)00152-3

Stone, G.W., Stapor, F.W., Jr., May, J.P., and Morgan, J.P., 1992. Multiple sediment sources and a cellular, non-integrated, long-shore drift system: Northwest Florida and southeast Alabama coast, U.S.A. Marine Geology, 105, 141–154.

Swift, D.J.P., 1968. Coastal erosion and transgressive stratigraphy. Journal of Geology, 76, 444–456.

Swift, D.J., 1975. Barrier-island genesis: evidence from the central Atlantic shelf, eastern U.S.A. Sedimentary Geology 14, 1–43. doi:10.1016/0037-0738(75)900159

Szabo, B.J., Ludwig, K.R., Muhs, D.R., and Simmons, K.R., 1994. Thorium-230 ages of corals and duration of the Last Interglacial sea-level high stand on Oahu, Hawaii. Science 266, 93–96. doi: 10.1126/science.266.5182.93

Talling, P.J., 1998. How and where do incised valleys form if sea-level remains above the shelf edge? Geology, 26, 87–90. doi.org/10.1130/00917613(1998)026<0087:HAWDIV> 2.3.CO;2

Taniguchi, M., Dulai, H., Burnett, K.M., Santos, I. R., Sugimoto, R., Stieglitz, T., Kim, G., Moosdorf, N., and Burnett, W.C., 2019. Submarine Groundwater Discharge: Updates on Its Measurement Techniques, Geophysical Drivers, Magnitudes, and Effects. Front. Environ. Sci. 7, 141. doi: 10.3389/fenvs.2019.00141

Theuillon, G., Stéphan, Y., and Pacault, A., 2008. High-Resolution Geoacoustic Characterization of the Seafloor Using a Subbottom Profiler in the Gulf of Lion. IEEE Journal of Oceanic Engineering, 33, 240–254. doi:10.1109/JOE.2008.926958

Thieler, E.R., Foster, D.S., Himmelstoss, E.A., and Mallinson, D.J., 2014. Geologic framework of the northern North Carolina, USA inner continental shelf and its influence on coastal evolution. Marine Geology, 348, 113–130. doi.org/10.1016/j.margeo.2013.11.011

Thomas, M.A., and Anderson J.B., 1994. Sea-level controls on the facies architecture of the Trinity/Sabine incised-valley system, Texas continental shelf. In: Dalrymple R., Boyd R., Zaitlin B.A., editors. Incised-valley systems. Special Publication 51. Tulsa, OK: Society of Economic Paleontologists and Mineralogists. 63–82. doi.org/10.2110/pec.94.12

Törnqvist, T.E., 1998. Longitudinal profile evolution of the Quaternary Rhine–Meuse river system during the last deglaciation: Interplay of climate change and glacioeustasy?: Terra Nova, 10, 11–15.

Törnqvist, T.E., Wallinga, J., Murray, A.S., De Wolf, H., Cleveringa, P., and De Gans, W., 2000. Response of the Rhine-Meuse system (west-central Netherlands) to the last Quaternary glacio-eustatic cycles: A first assessment: Global and Planetary Change, 27, 89–111, doi:10.1016/S0921-8181(01)00072-8.

Törnqvist, T.E., Wallinga, J., and Busschers, F.S., 2003. Timing of the last sequence boundary in a fluvial setting near the highstand shoreline—Insights from optical dating: Geology, 31, 279–282, doi: 10.1130/0091-7613(2003)031<0279:TOTLSB>2.0.CO;2.

Törnqvist, T.E., Gonzalez, J.L., Newsom, L.A., van der Borg., K., de Jong, A.F.M., and Kurnik, C.W., 2004. Deciphering Holocene sea-level history on the U.S. Gulf Coast: A high-resolution record from the Mississippi Delta: Geological Society of America Bulletin, 116, 1026–1039. doi.org/10.1130/B2525478.1

Törnqvist, T.E., Bick, S.J., Gonzalez, J.L., van der Borg, K., and de Jong, A.F.M., 2005. Tracking the sea-level signature of the 8.2 ka cooling event: New constraints from the Mississippi Delta: Geophysical Research Letters, 31, 1–4. doi.org/10.1029/2004GL021429

Törnqvist, T.E., Wortman, S.R., Mateo, Z.R.P., Milne, G.A., and Swenson, J.B., 2006a. Did the last sea level lowstand always lead to cross-shelf valley formation and source-to-sink sediment flux?: Journal of Geophysical Research, 111. doi:10.1029/2005JF 00042

Törnqvist, T.E., Bick, S.J., van der Borg, K., and de Jong, A.F.M., 2006b. How stable is the Mississippi Delta?: Geology, 34, 697–700, doi: 10.1130/G22624.1.

Toscano, M.A., and Macintyre, I.G., 2003. Corrected western Atlantic sea-level curve for the last 11,000 years based on calibrated ^{14}C dates from Acropora palmate framework and intertidal mangrove peat. Coral Reefs, 22, 257–270, doi: 10.1007/s00338-003-0315-4.

Upshaw, C.F., Creath, W.B., and Brooks, F.L., 1966. Sediments and microfauna off the coast of Mississippi and adjacent states: Mississippi Geological Economic and Topographic Survey Bulletin, No. 106, 9–72.

van Andel, T.H., 2002. The climate and landscape of the middle part of the Weichselian glaciation in Europe: the stage 3 project. Quaternary Research, 57, 2–8. doi.org/10.1006/qres.2001.2294

van Andel, T.H. and Poole, D.M., 1960. Sources of recent sediments in the northern Gulf of Mexico. Journal of Sedimentary Petrology, 30 (1), 91–122.

van Andel, T.H., and Tzedakis, P.C., 1996. Paleolithic landscapes of Europe and environs, 150,000–25,000 years ago: an overview. Quaternary Science Reviews, 15, 481–500.

Vásquez-Selem, L., and Heine, K., 2011. Late Quaternary glaciation in Mexico. In: J. Ehlers, P.L. Gibbard, P.D. Hughes (Eds.), Quaternary Glaciations — Extent and Chronology: A Closer Look, Developments in Quaternary Science, 15, Elsevier, Amsterdam, 849–862.

Viso, R., McCoy, C., Gayes, P., and Quafisi, D., 2010. Geological controls on submarine groundwater discharge in Long Bay, South Carolina (USA). Continental Shelf Research 30, 335–341. doi: 10.1016/j.csr.2009.11.014

Voelker, A.H.L., Sarnthein, M., Grootes, P., Erlenkeuser, H., Laj, C., Mazaud, A., Nadeau, M.J., and Schleicher, M., 1998. Correlation of marine ^{14}C ages from the Nordic Seas with the GISP2 isotope record: implications for ^{14}C calibration beyond 25 ka BP. Radio-carbon, 40, 517–534. doi: 0.1017/s0033822200018397

Von Grafenstein, U., Erlenkeuser, H., Müller, J., Jouzel, J., and Johnsen, S., 1998. The cold event 8200 years ago documented in oxygen isotope records of precipitation in Europe and Greenland, Clim. Dyn., 14, 73–81. doi: 10.1007/s003820050210

Waelbroeck, C., Labeyrie, L., Michel, E., Duplessy, J.C., McManus, J., Lambeck, K., Balbon, E., and Labracherie, M., 2012. Sea-level and deep-water temperature changes derived from benthic foraminifera isotopic records. Quaternary Science Reviews 21, 295–305. doi.org/10.1016/S0277-3791(01)00101-9

Walker, M., Johnsen, S., Rasmussen, S.O., Popp, T., Steffensen, J.P., Gibbard, P., Hoek, W., Lowe, J., Andrews, J., Björck, S., Cwynar, L.C., Hughen, K., Kershaw, P., Kromer, B., Litt, T., Lowe, D.J., Nakagawa, T., Newnham, R., and Schwander, J., 2009. Formal definition and dating of the GSSP (Global Stratotype Section and Point) for the base of the Holocene using the Greenland NGRIP ice core, and selected auxiliary records. Journal of Quaternary Science, 24, 3–17. doi.org/10.1002/jqs.1227

Wefer, G., and Berger, W.H., 1991. Isotope paleontology: growth and composition of extant calcareous species. Marine Geology, 100, 207–248. doi.org/10.1016/0025-3227(91) 90234-U

Wicks, C.M., and Herman, J.S., 1995. The effect of zones of high porosity and permeability on the configuration of the saline–freshwater mixing zone. Ground Water, 33(5), 733–740. doi.org/10.1111/j.1745-6584.1995.tb00019.x

Williams, G.P., 1978. Bankfull discharge of rivers. Water Resources Research, 14, 1141–1154. doi: 10.1002/esp.1337

Woodruff, J.D., Irish, J.L., and Camargo, S.J., 2013. Coastal flooding by tropical cyclones and sea-level rise. Nature, 504, 44–52. doi: 10.1038/nature12855

Yokoyama, Y., Lambeck, K., De Deckker, P.P.J., and Fifield, L.K., 2000. Timing of the last glacial maximum from observed sea-level minima. Nature 406, 713–716. doi: 10.1038/35083629

Zaitlin, B.A., Dalrymple, R.W., and Boyd, R., 1994. The stratigraphic organization of incised valley systems associated with relative sea level change, in Dalrymple, R.W., Boyd, R., and Zaitlin, B.A., eds., Incised-Valley Systems: Origin and Sedimentary Sequences: SEPM, Special Publication 51, 45–60.

Zeebe, R.E., 1999. An explanation of the effect of seawater carbonate concentration on foraminiferal oxygen isotopes. Geochimica et Cosmochimica Acta. 63 (13–14), 2001–2007. doi: 10.1016/S0016-7037(99)00091-5

Zektser, I.S.S., and Loaiciga, H.A., 1993. Groundwater fluxes in the global hydrologic cycle: Past, present and future. Journal of Hydrology, 144(1-4), 405–427. doi.org/10.1016/0022-1694(93)90182-9

Zhao, S., Xu, B., Yao, Q., Burnett, W.C., Charette, M.A., Su, R., Lian, E., and Yu, Z., 2021. Nutrient-rich submarine groundwater discharge fuels the largest green tide in the world. Science of the Total Environment, 770. doi: 10.1016/j.scitotenv.2020.144845

Zhu, Z.R., Wyrwoll, K., Collins, L.B., Chen, J.H., Wasserburg, G.J. and Eisenhauer, A., 1993. High-precision U-series dating of Last Interglacial events by mass spectrometry: Houtman Abrolhos Islands, Western Australia. Earth Planetary Science Letters 118, 281–293. doi.org/10.1016/0012-821X(93)90173-7

APPENDIX A

SEDIMENT CORES

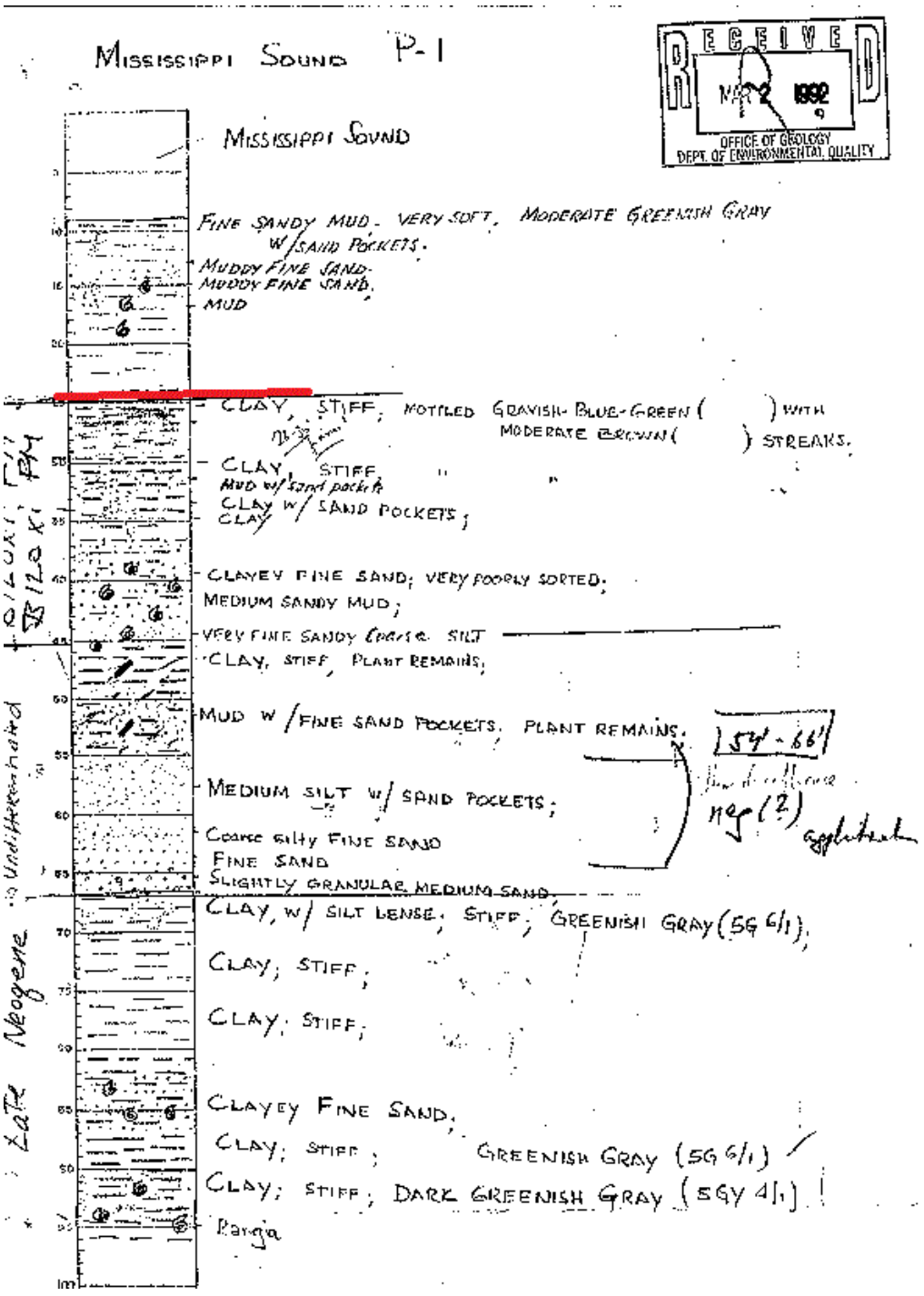

Figure A.1 Mississippi Sound core log MS1 provided by the MDEQ. Red line shows Pleistocene-Holocene contact.

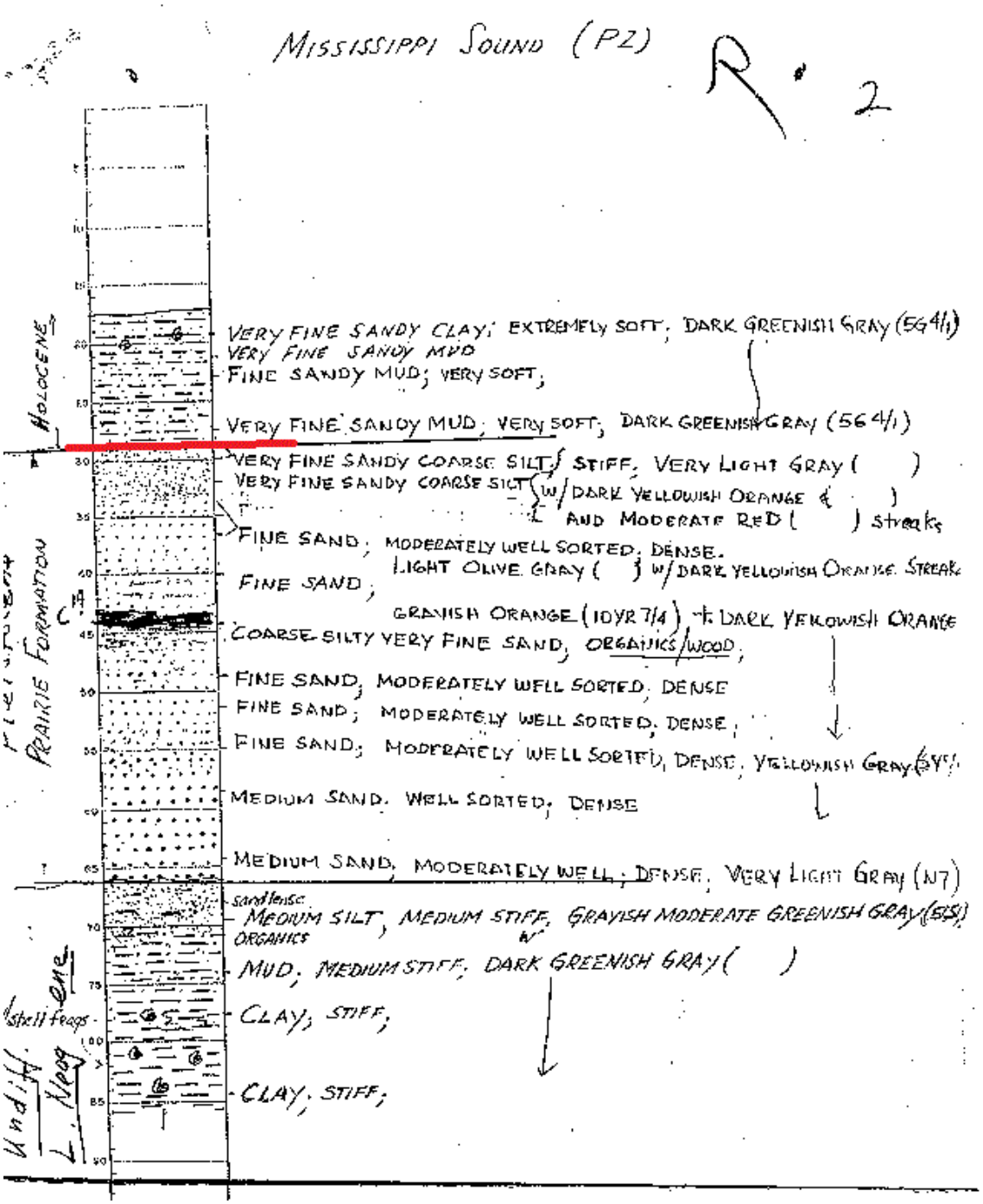

Figure A.2 Mississippi Sound core log MS2 provided by the MDEQ. Red line shows Pleistocene-Holocene contact.

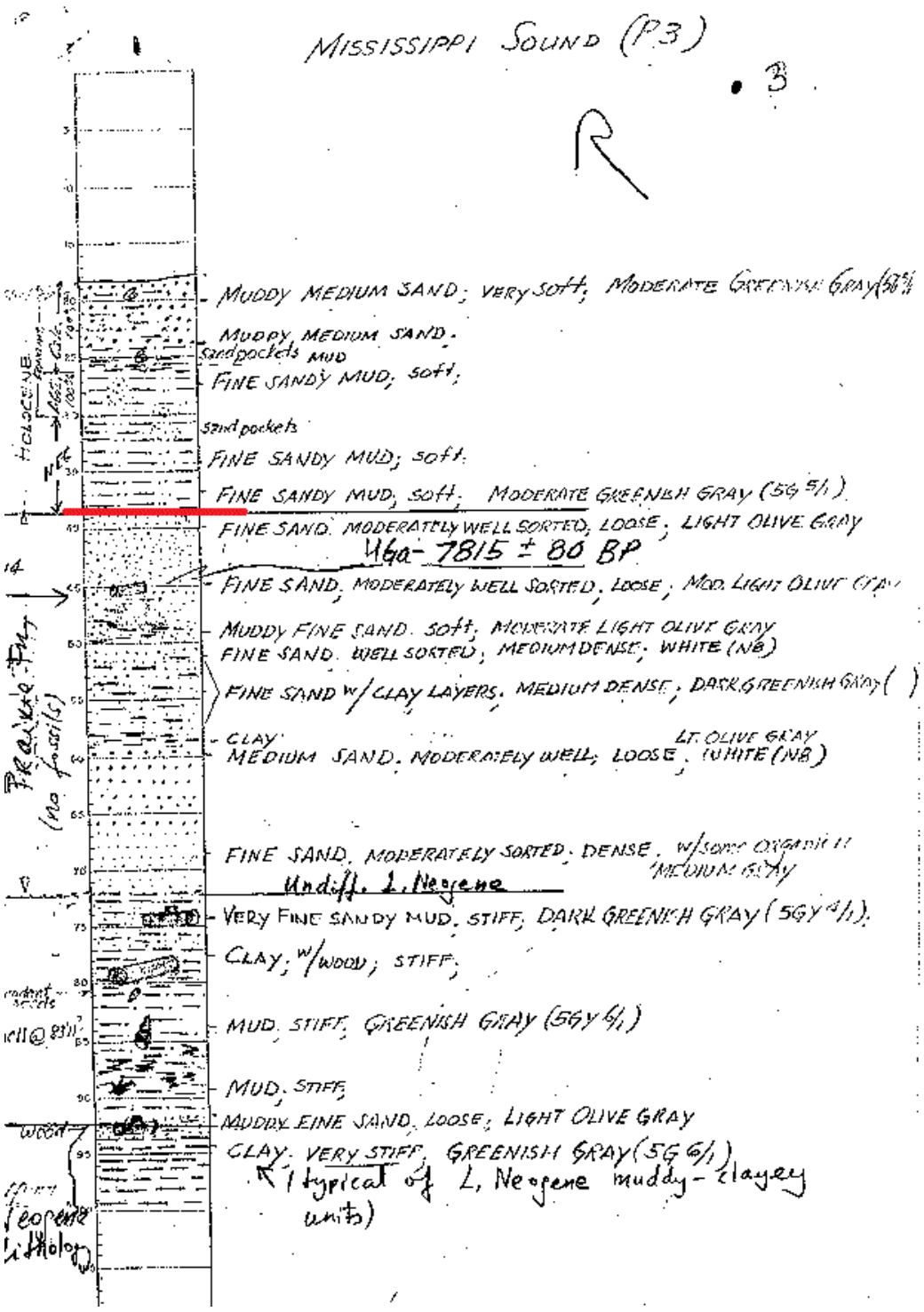

Figure A.3 Mississippi Sound core log MS3 provided by the MDEQ. Red line shows Pleistocene-Holocene contact.

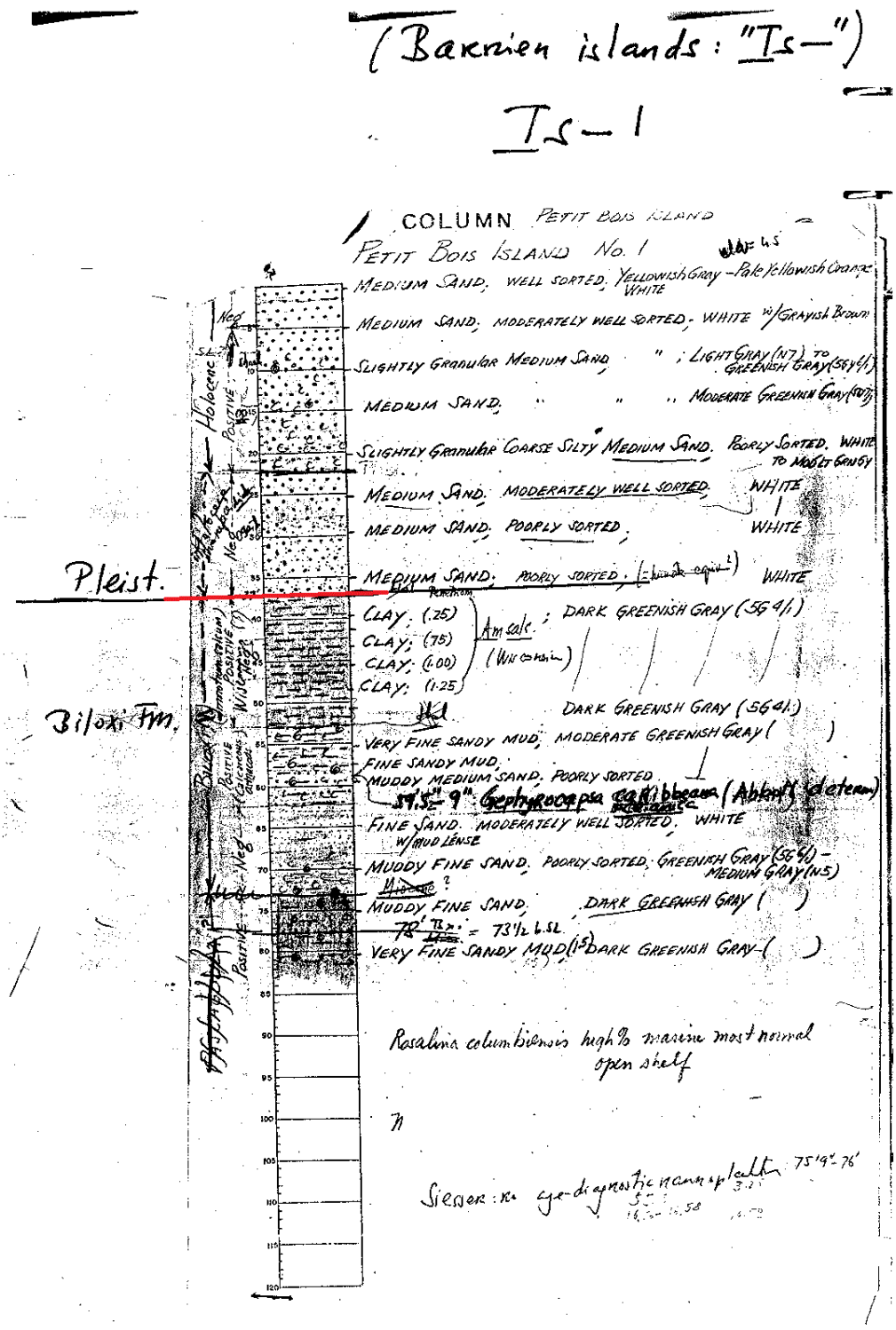

Figure A.4 Mississippi Sound core log BI1 provided by the MDEQ. Red line shows Pleistocene-Holocene contact.

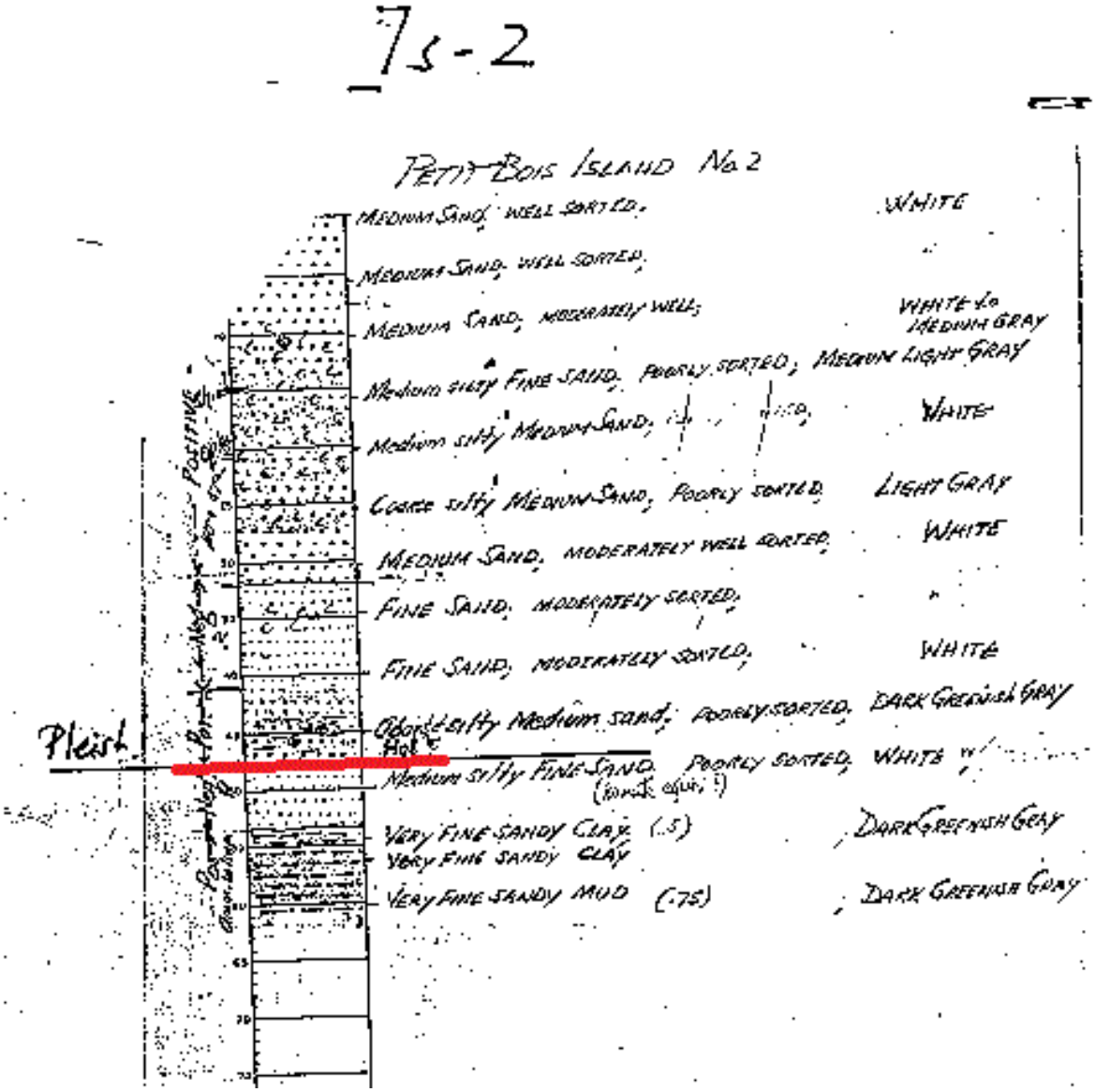

Figure A.5 Mississippi Sound core log BI2 provided by the MDEQ. Red line shows Pleistocene-Holocene contact.

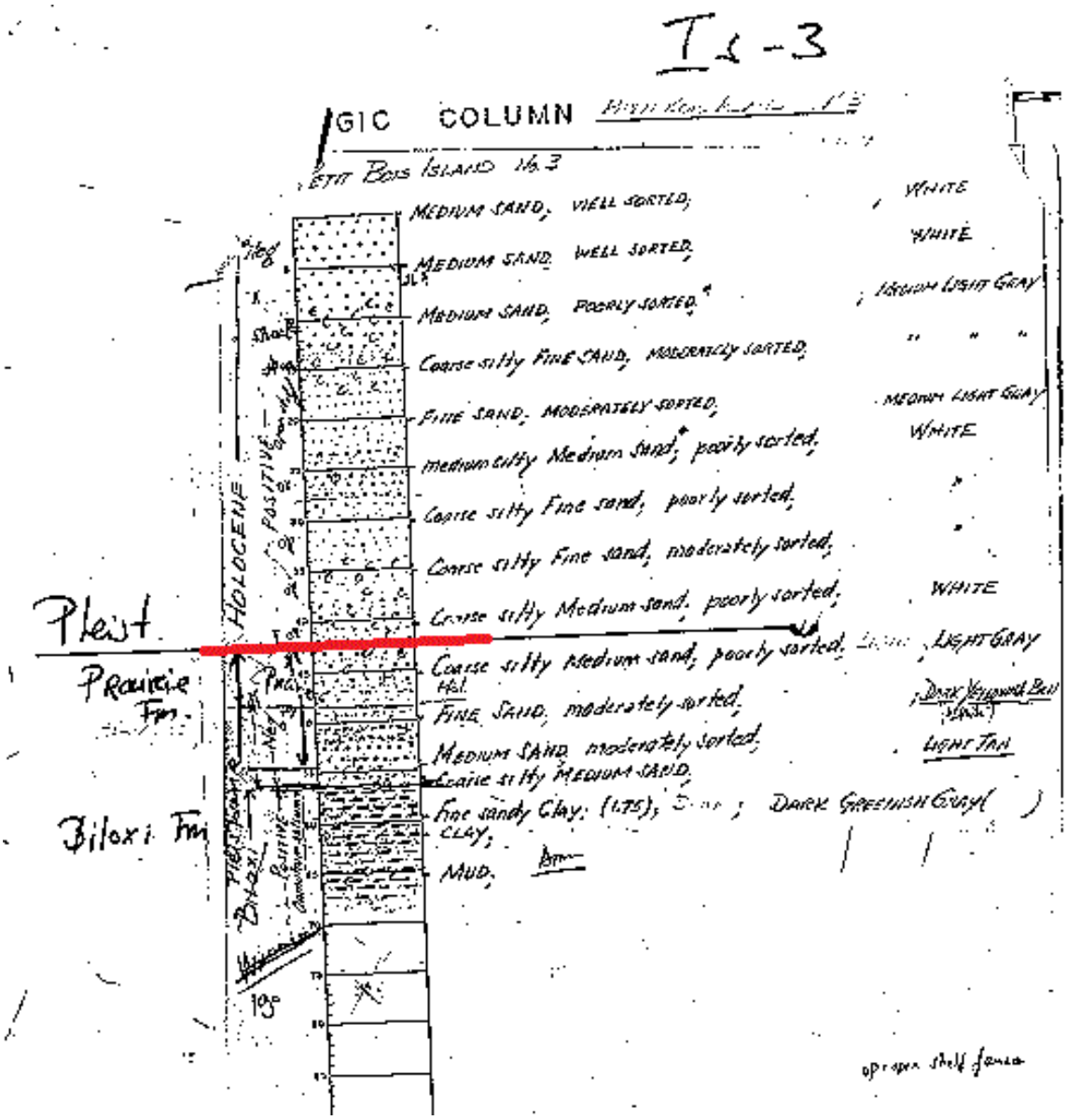

Figure A.6 Mississippi Sound core log BI3 provided by the MDEQ. Red line shows Pleistocene-Holocene contact.

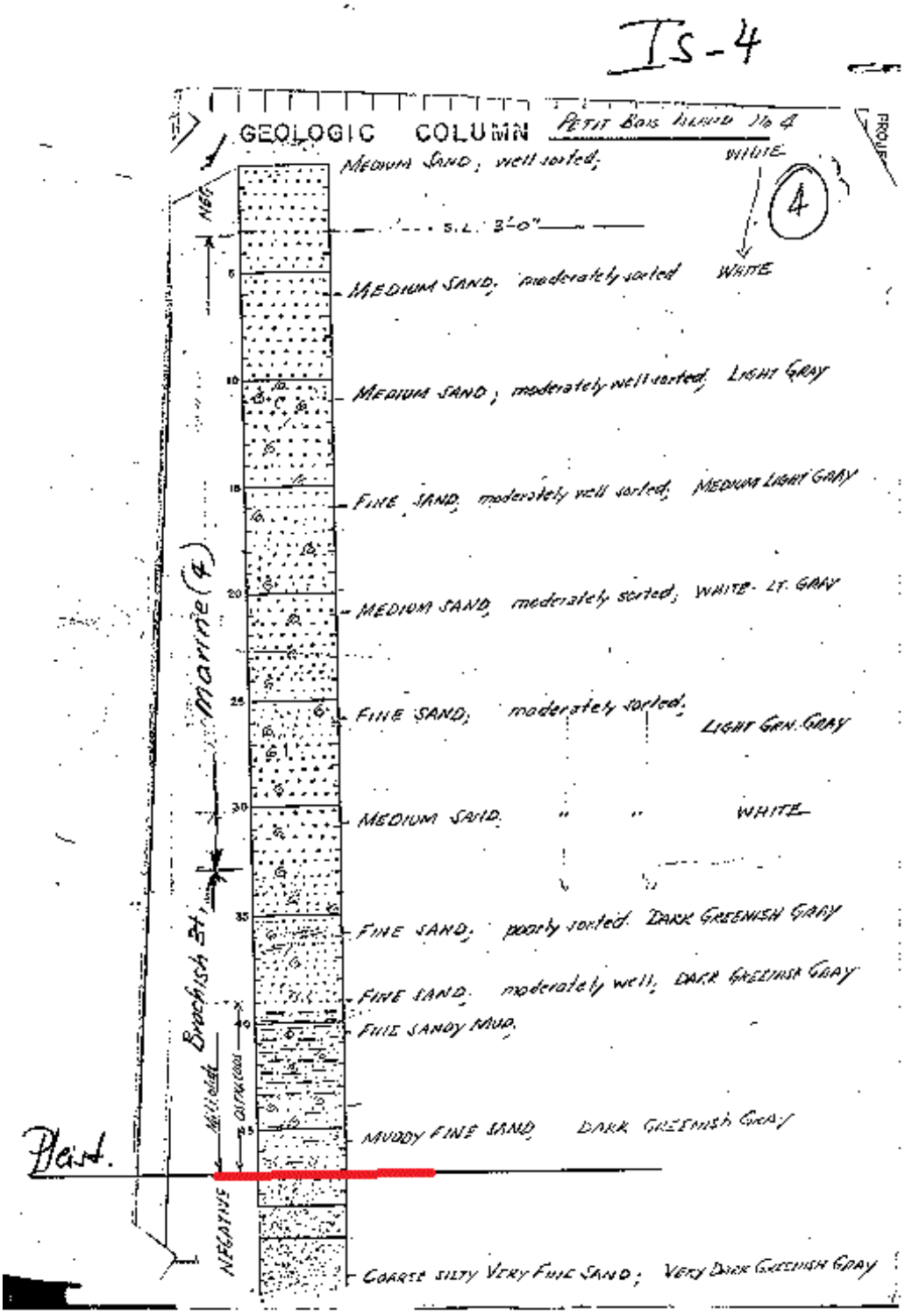

Figure A.7 Mississippi Sound core log BI4 provided by the MDEQ. Red line shows Pleistocene-Holocene contact.

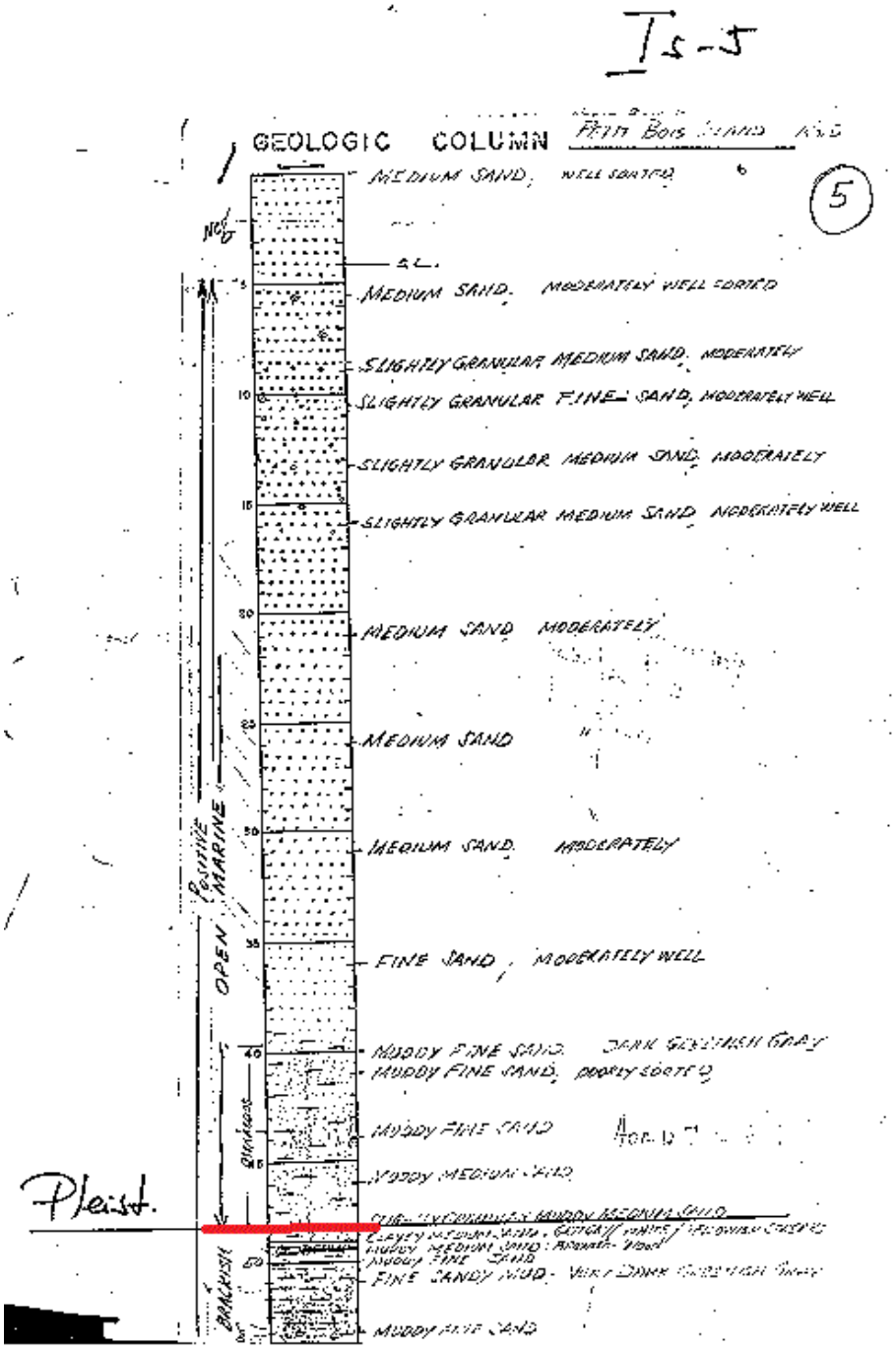

Figure A.8 Mississippi Sound core log BI5 provided by the MDEQ. Red line shows Pleistocene-Holocene contact.

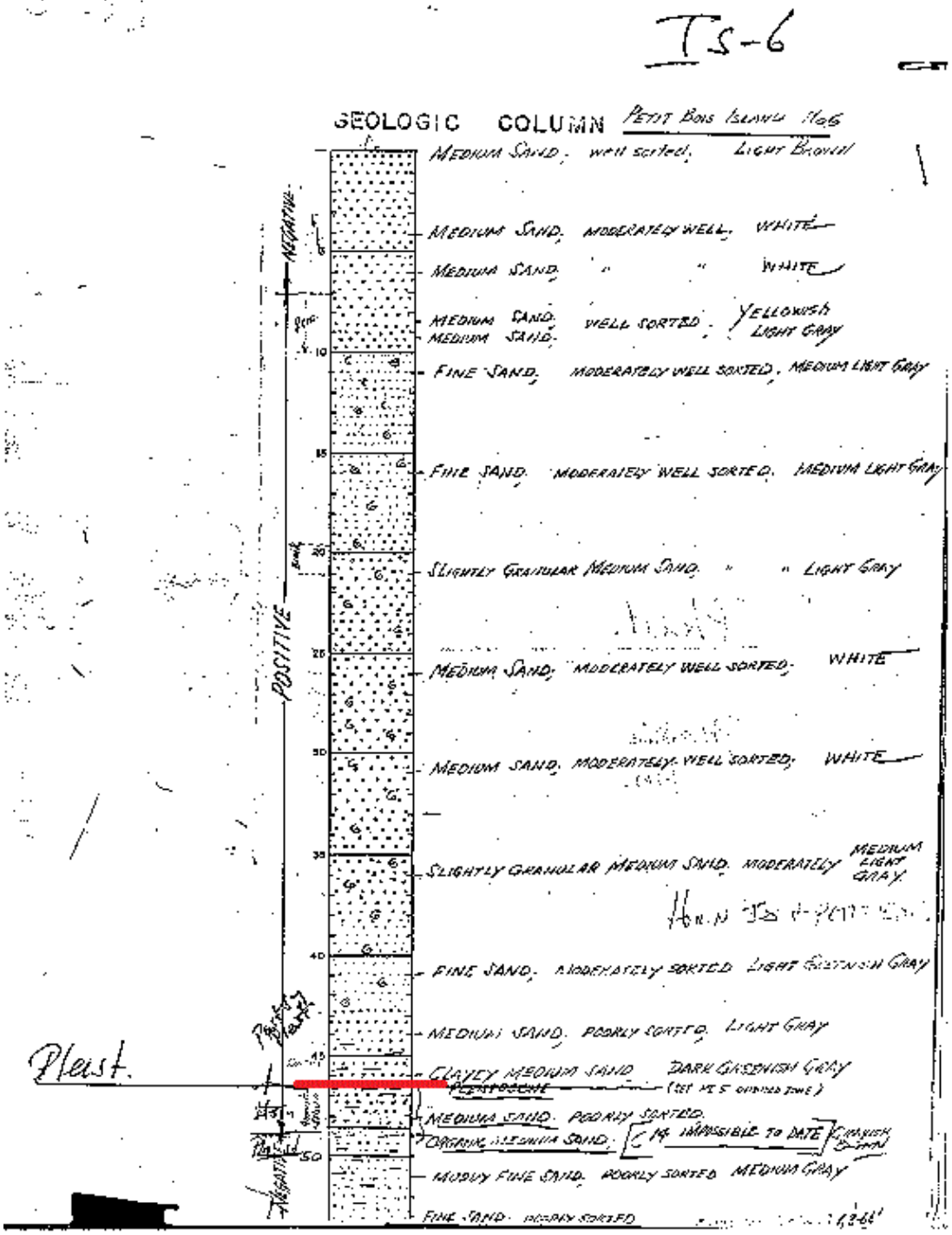

Figure A.9 Mississippi Sound core log BI6 provided by the MDEQ. Red line shows Pleistocene-Holocene contact.

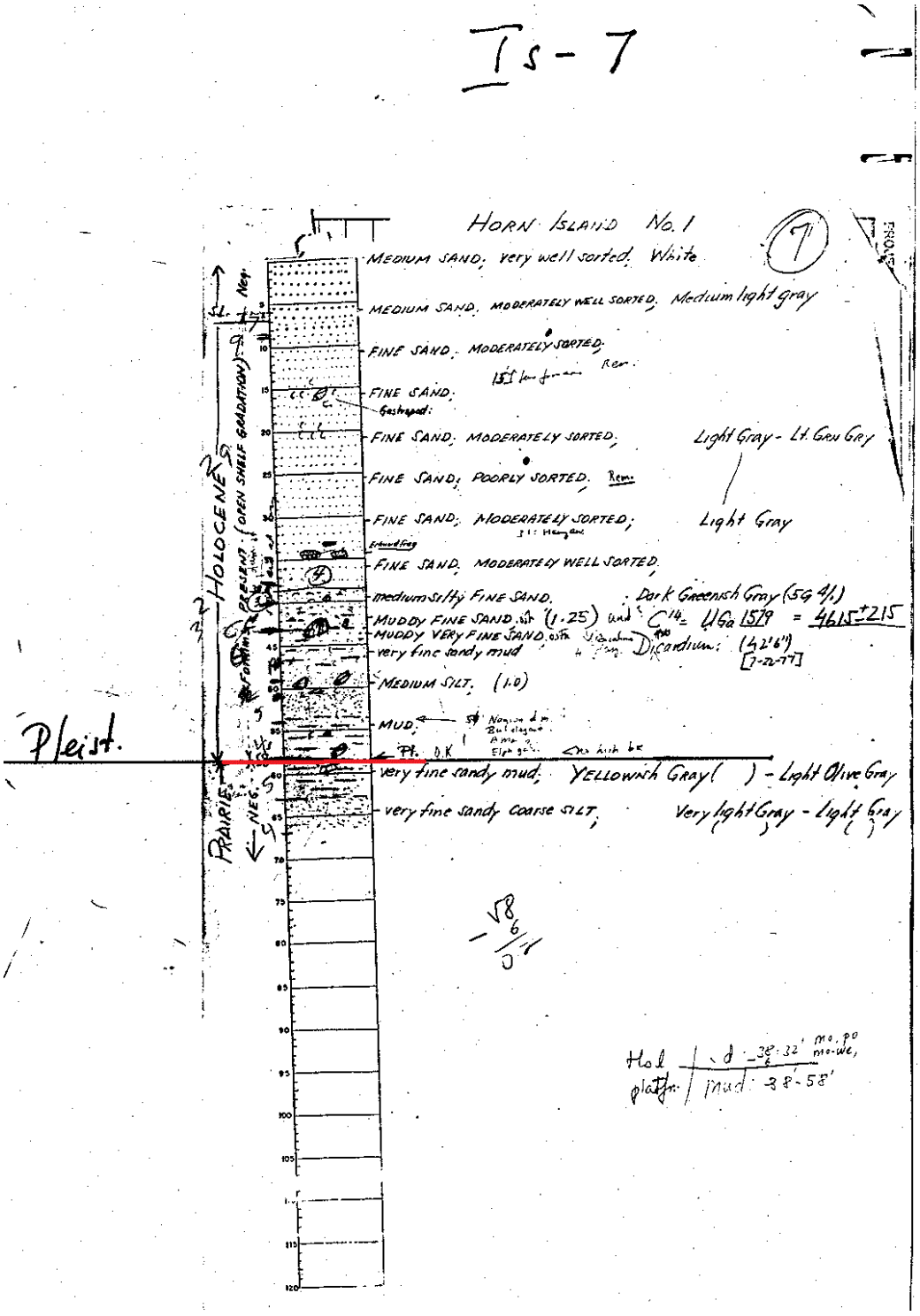

Figure A.10 Mississippi Sound core log BI7 provided by the MDEQ. Red line shows Pleistocene-Holocene contact.

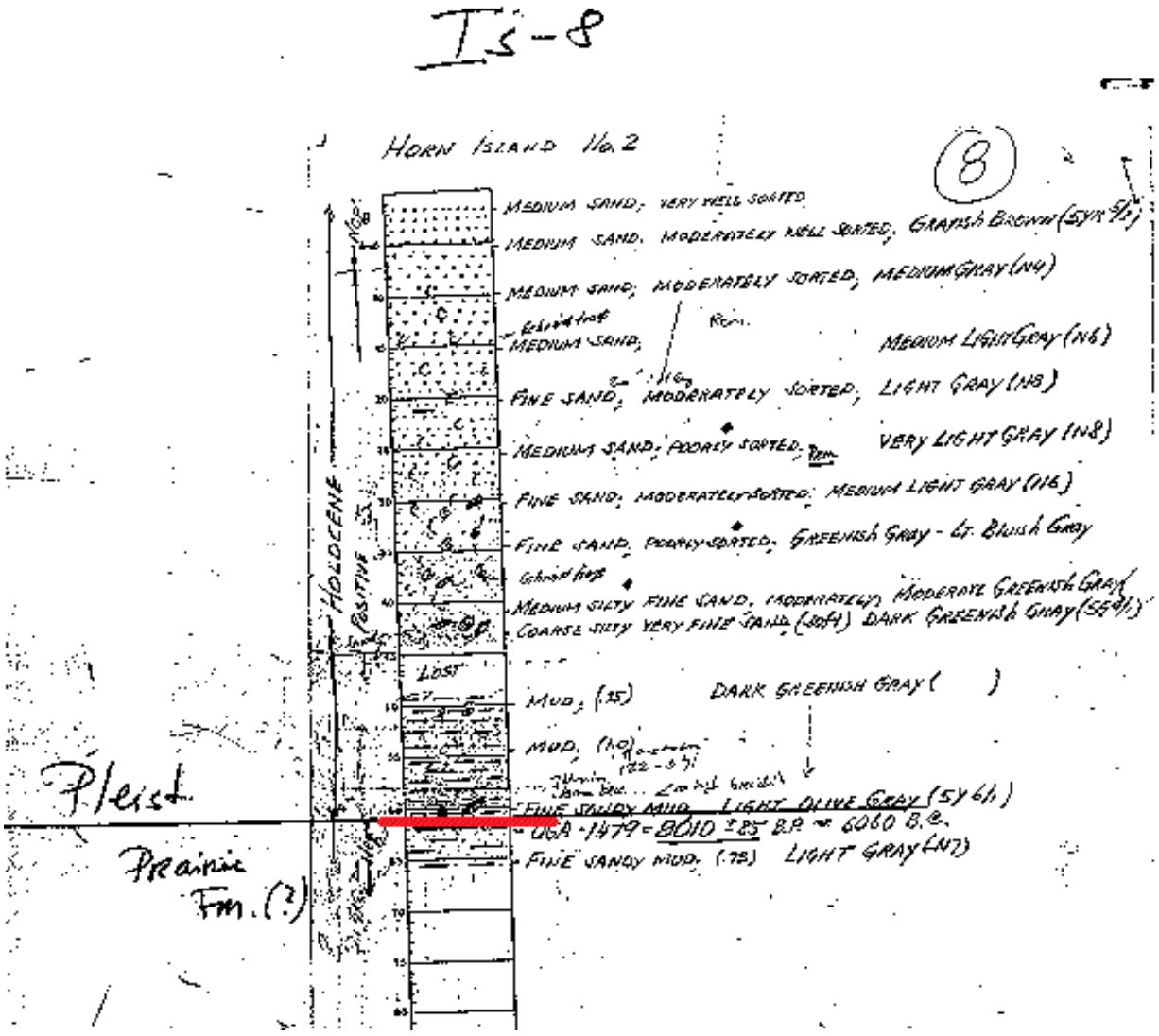

Figure A.11 Mississippi Sound core log BI8 provided by the MDEQ. Red line shows Pleistocene-Holocene contact.

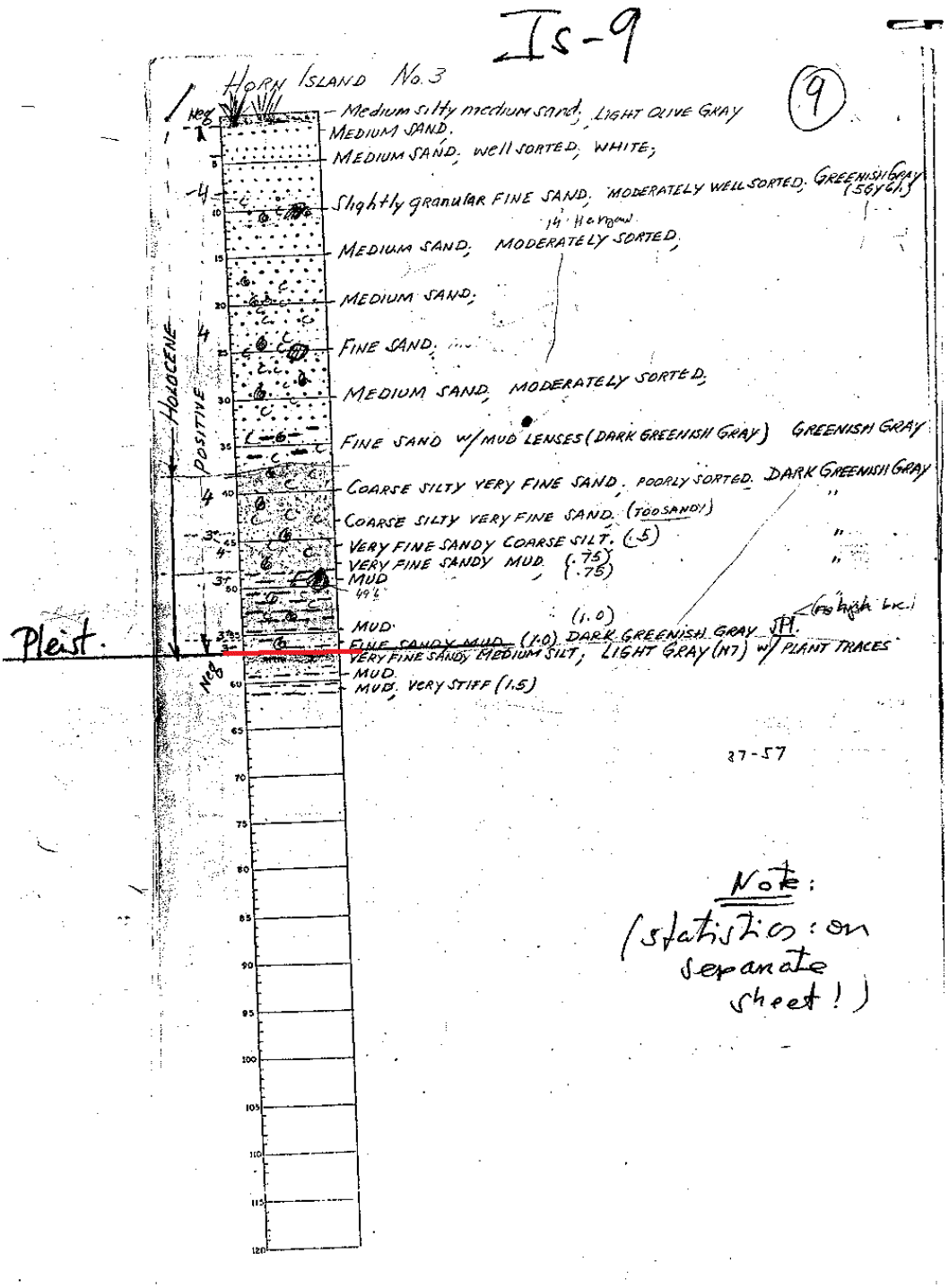

Figure A.12 Mississippi Sound core log BI9 provided by the MDEQ. Red line shows Pleistocene-Holocene contact.

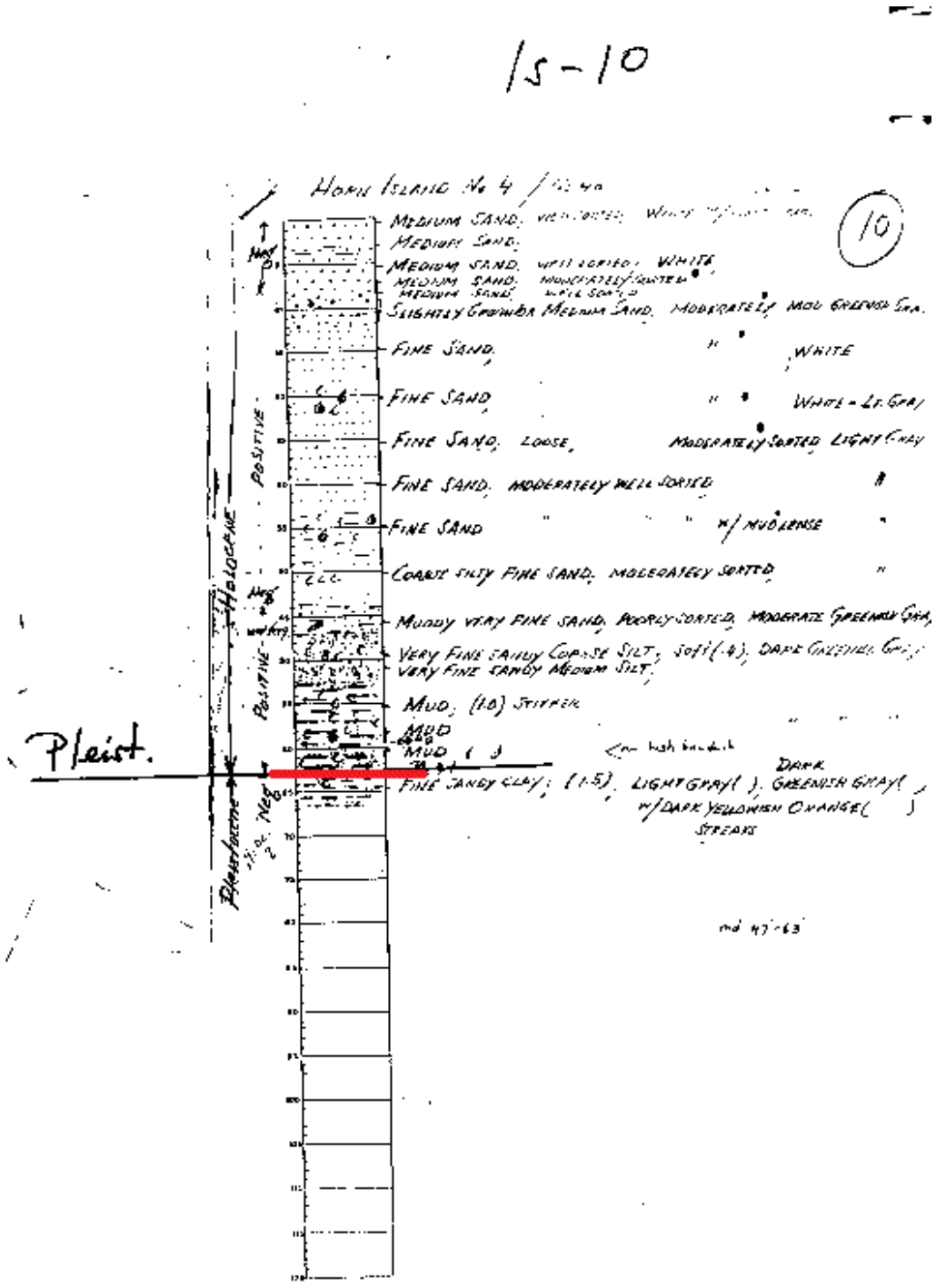

Figure A.13 Mississippi Sound core log BI10 provided by the MDEQ. Red line shows Pleistocene-Holocene contact.

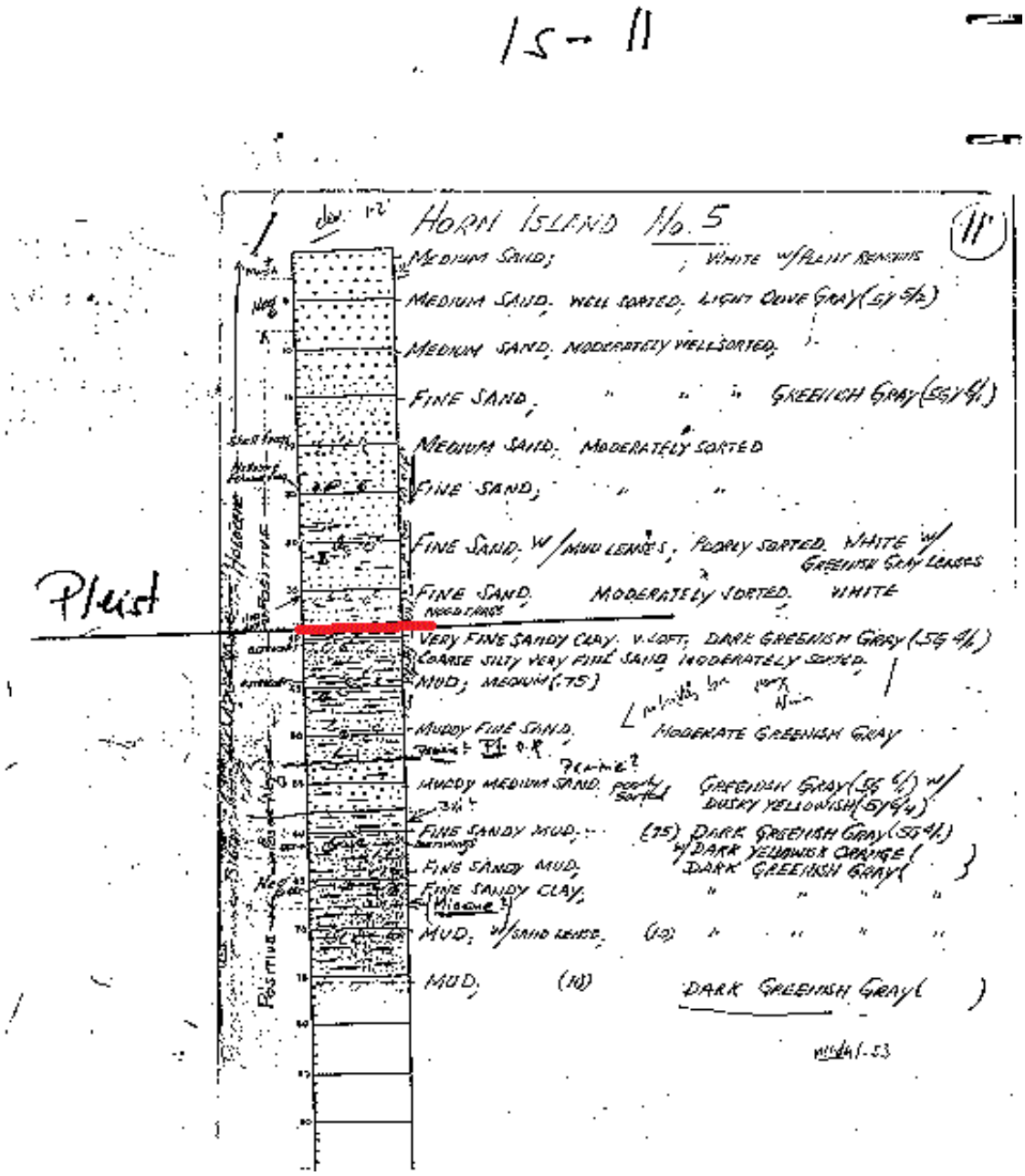

Figure A.14 Mississippi Sound core log BI11 provided by the MDEQ. Red line shows Pleistocene-Holocene contact.

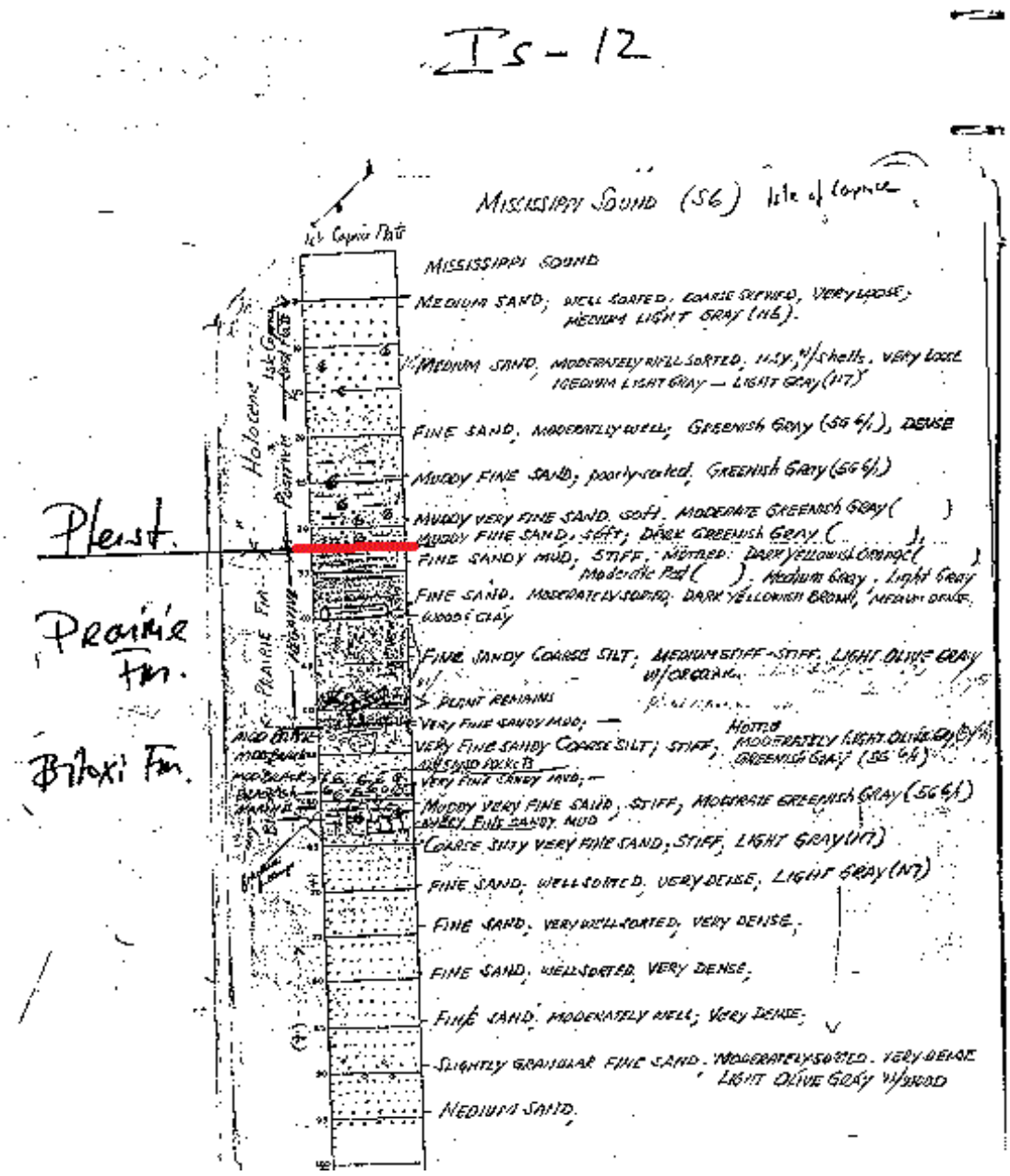

Figure A.15 Mississippi Sound core log BI12 provided by the MDEQ. Red line shows Pleistocene-Holocene contact.

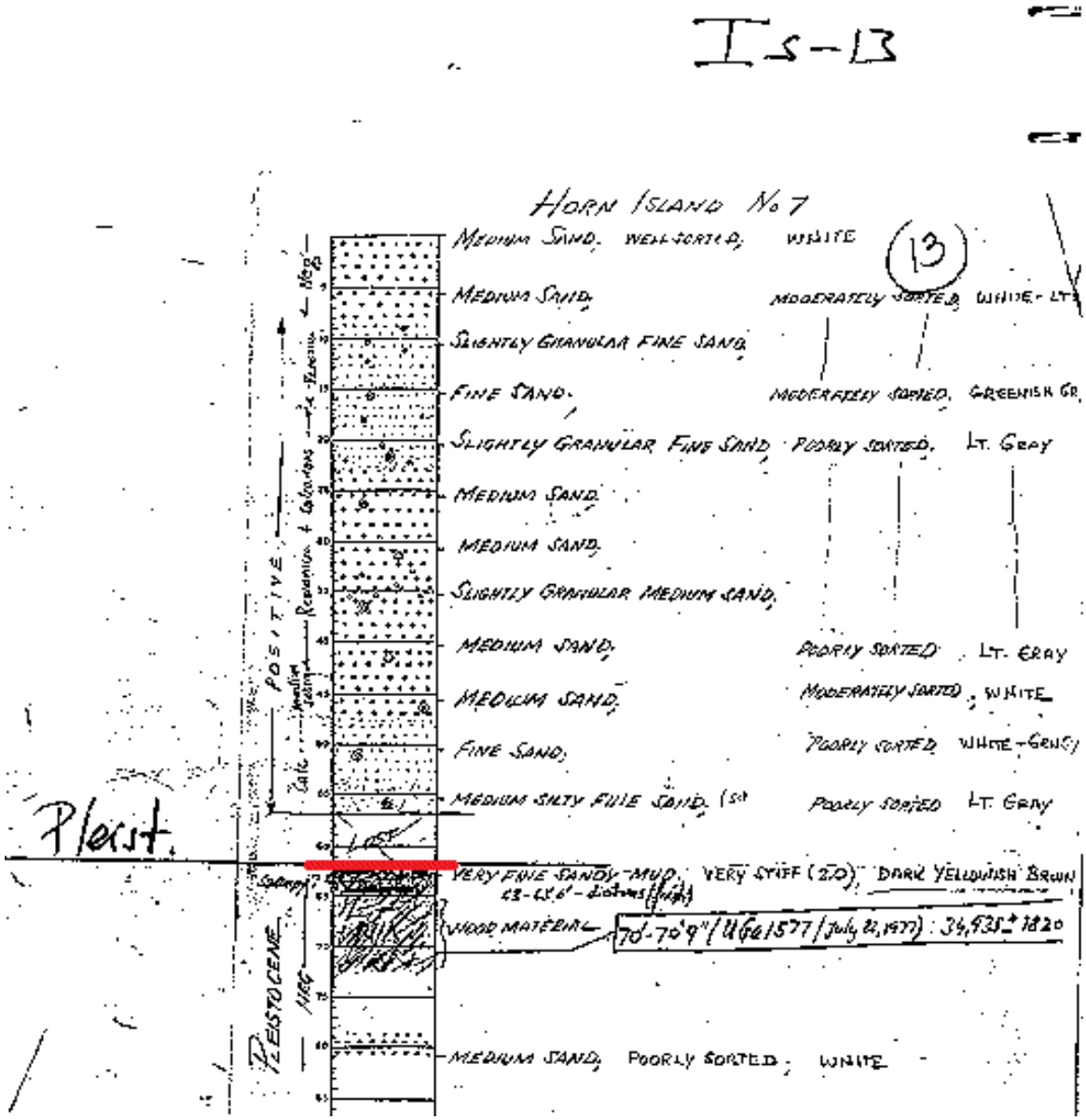

Figure A.16 Mississippi Sound core log BI13 provided by the MDEQ. Red line shows Pleistocene-Holocene contact.

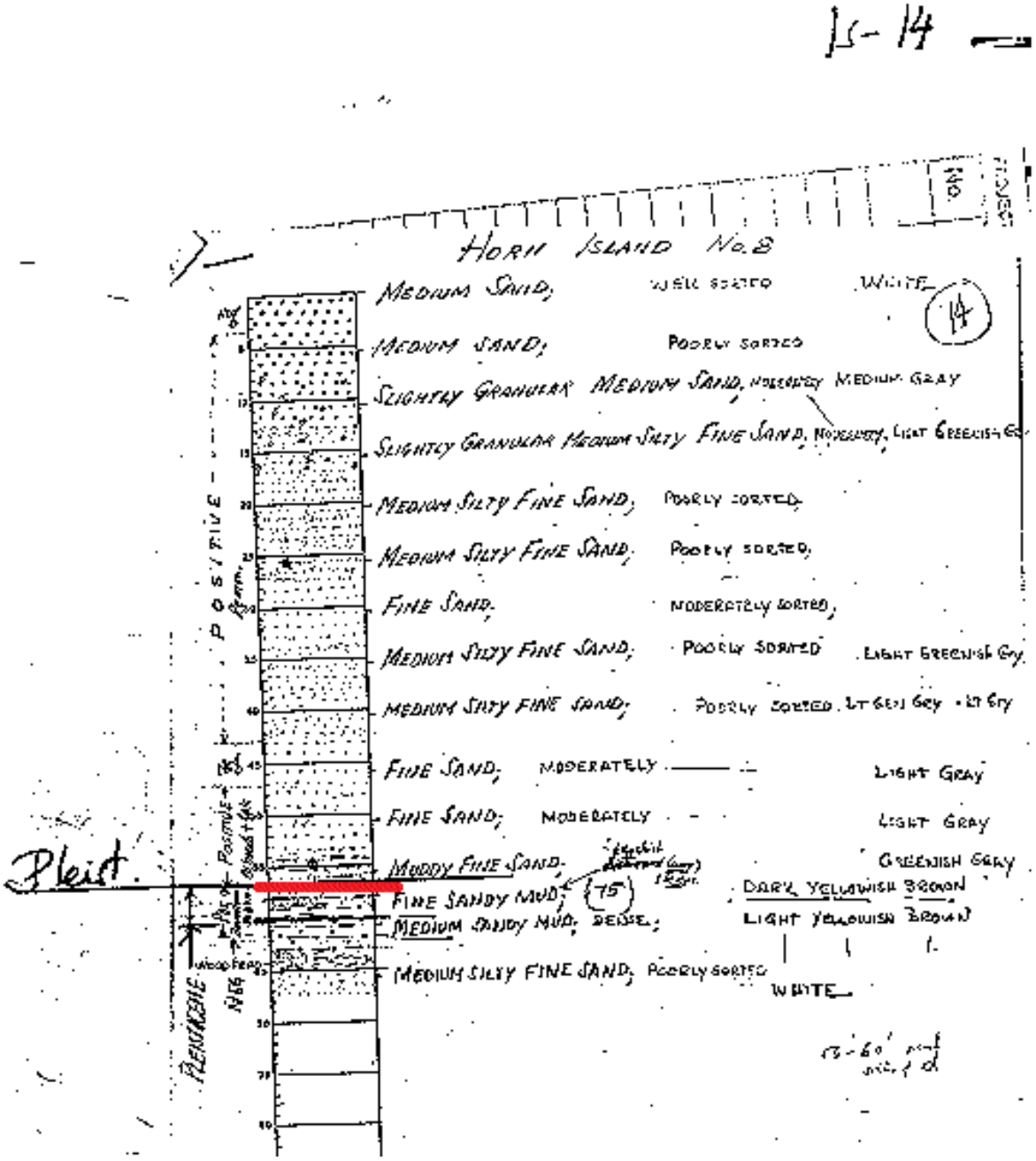

Figure A.17 Mississippi Sound core log BI14 provided by the MDEQ. Red line shows Pleistocene-Holocene contact.

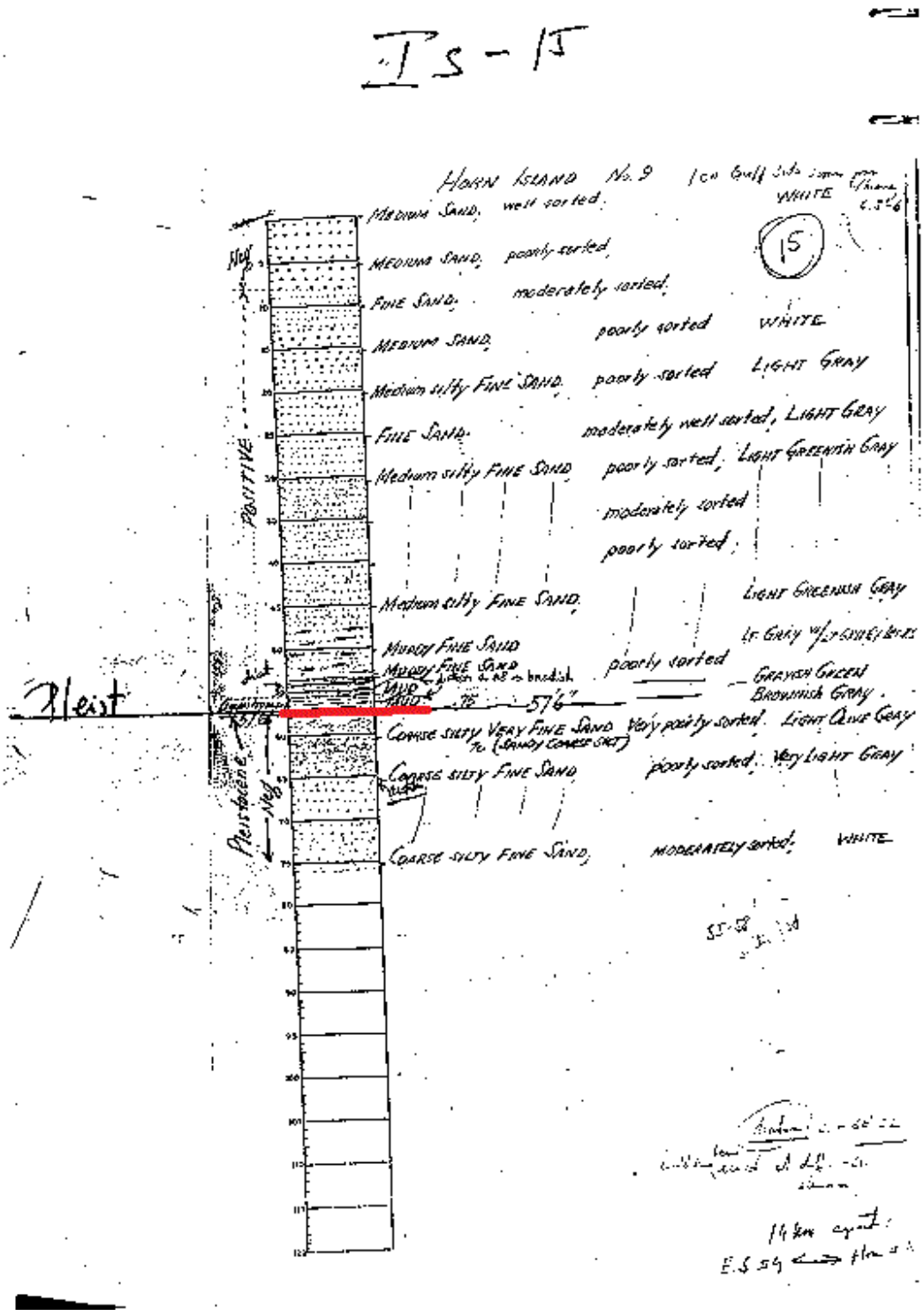

Figure A.18 Mississippi Sound core log BI15 provided by the MDEQ. Red line shows Pleistocene-Holocene contact.

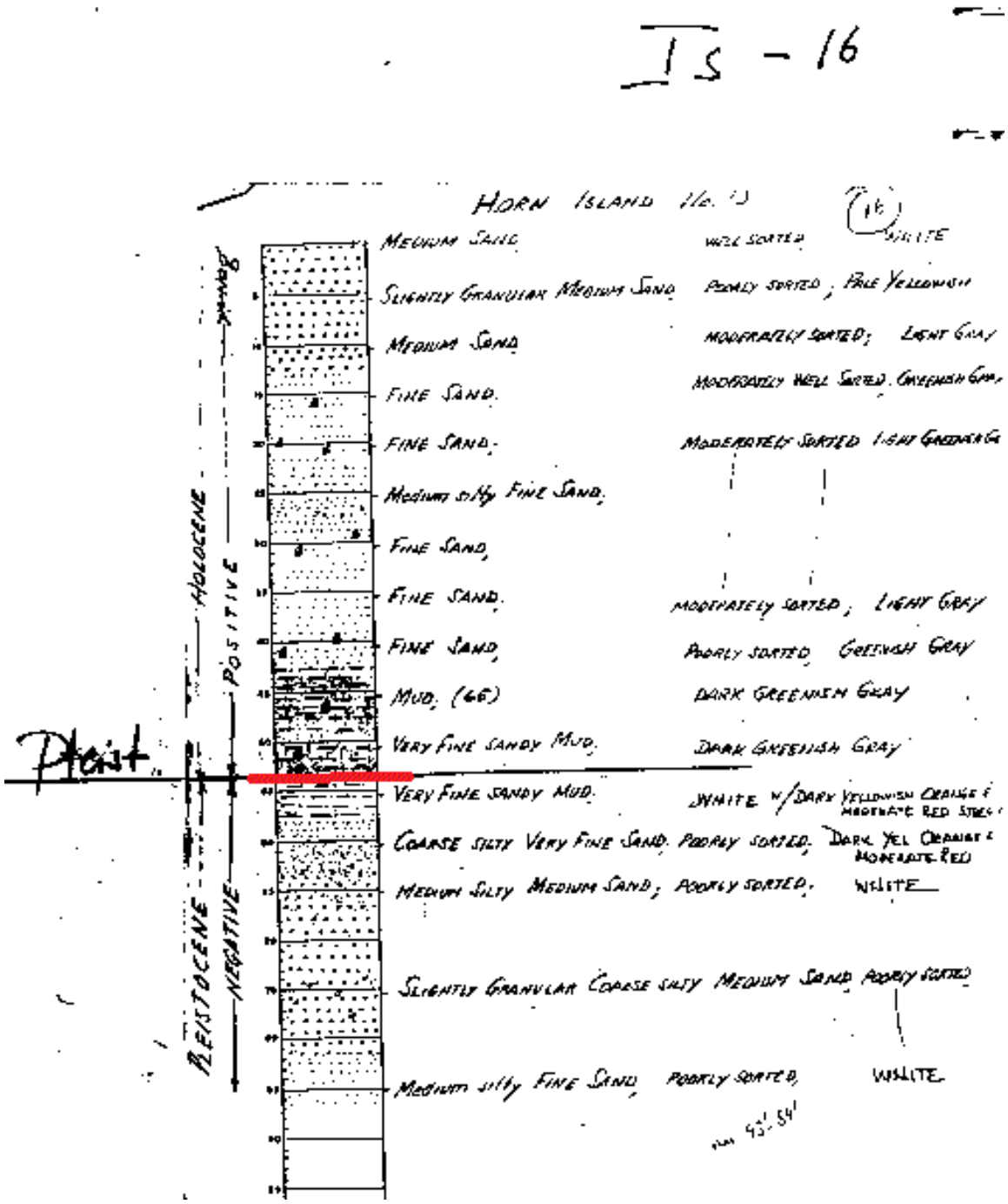

Figure A.19 Mississippi Sound core log BI16 provided by the MDEQ. Red line shows Pleistocene-Holocene contact.

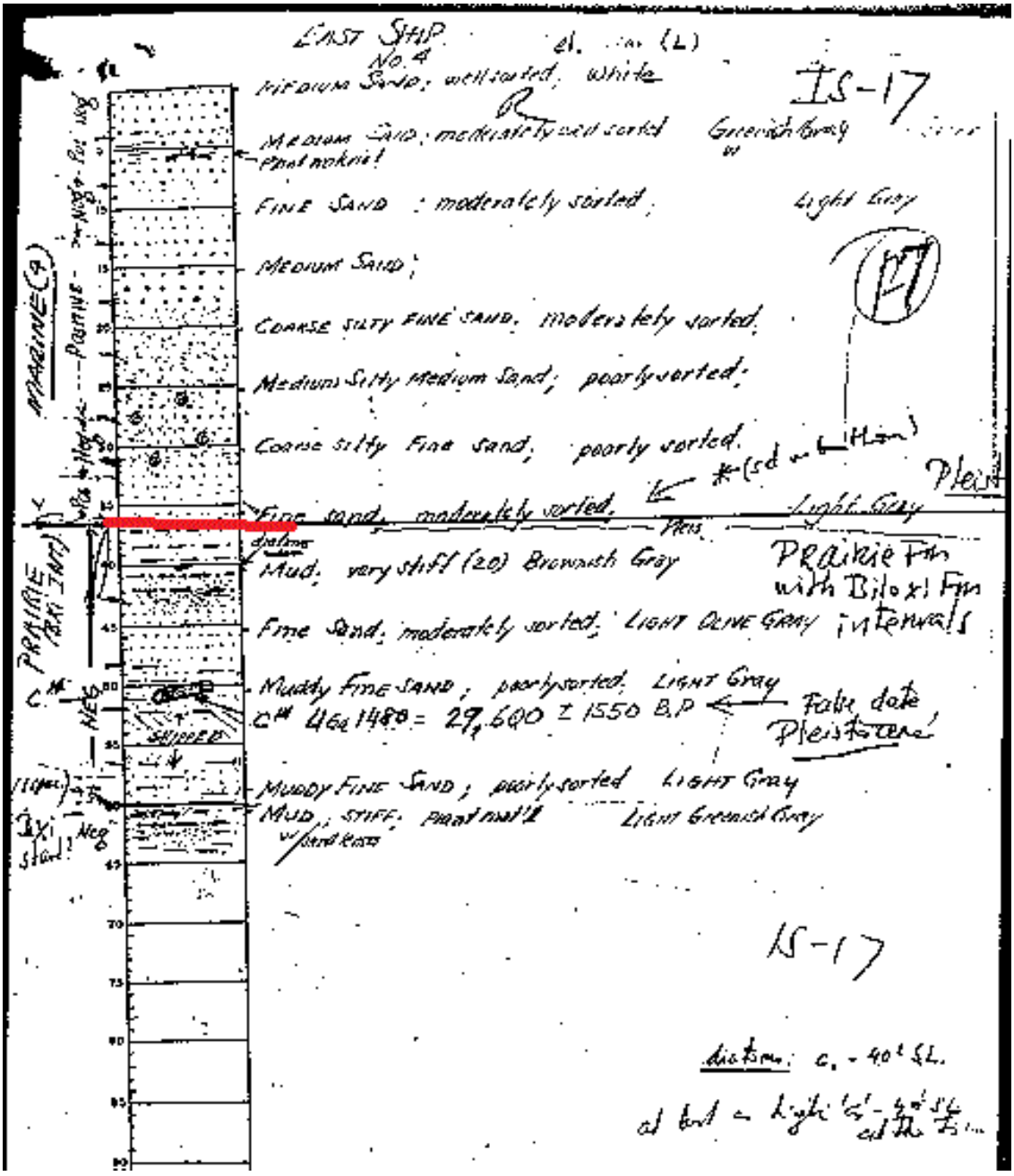

Figure A.20 Mississippi Sound core log BI17 provided by the MDEQ. Red line shows Pleistocene-Holocene contact.

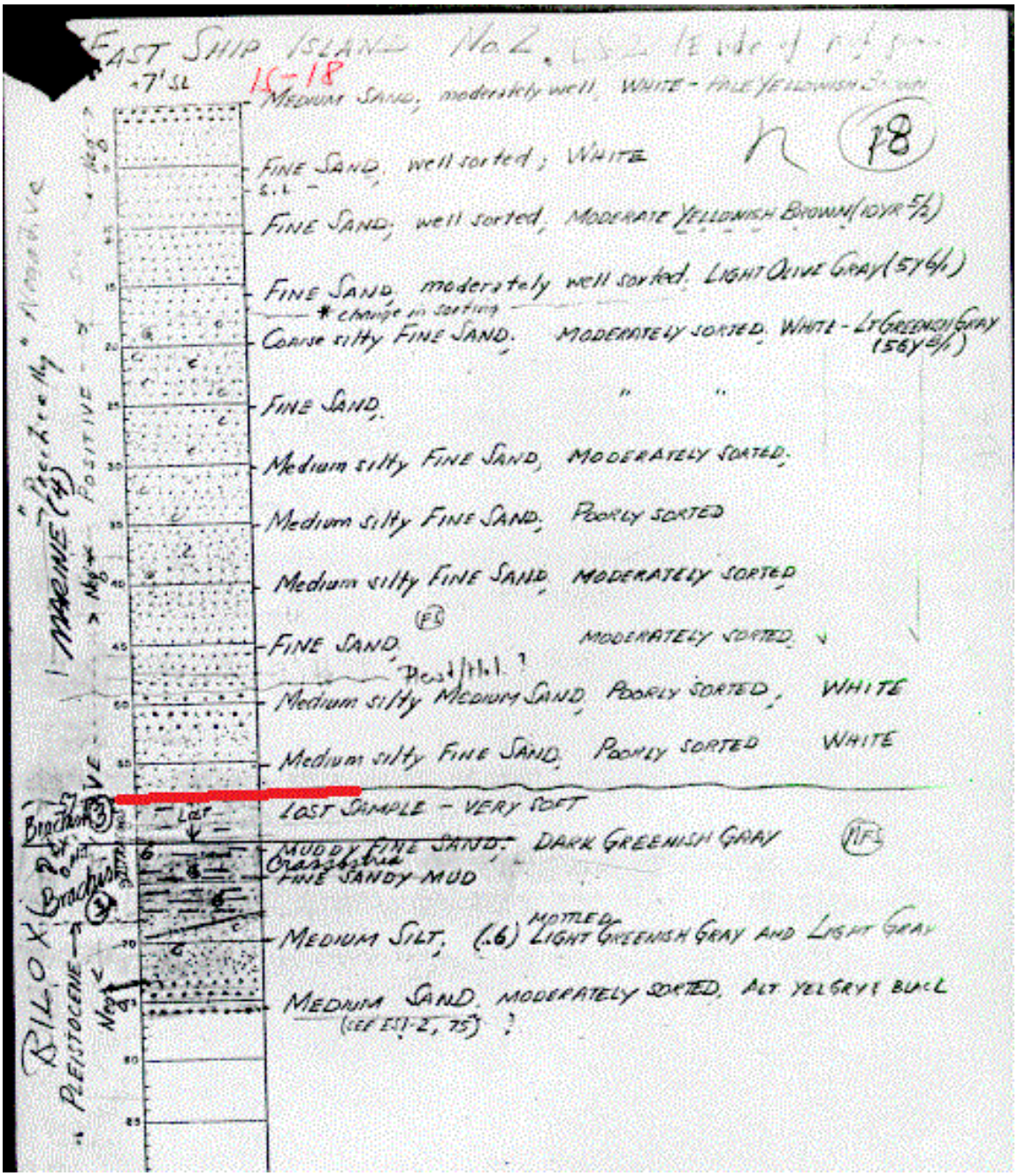

Figure A.21 Mississippi Sound core log BI18 provided by the MDEQ. Red line shows Pleistocene-Holocene contact.

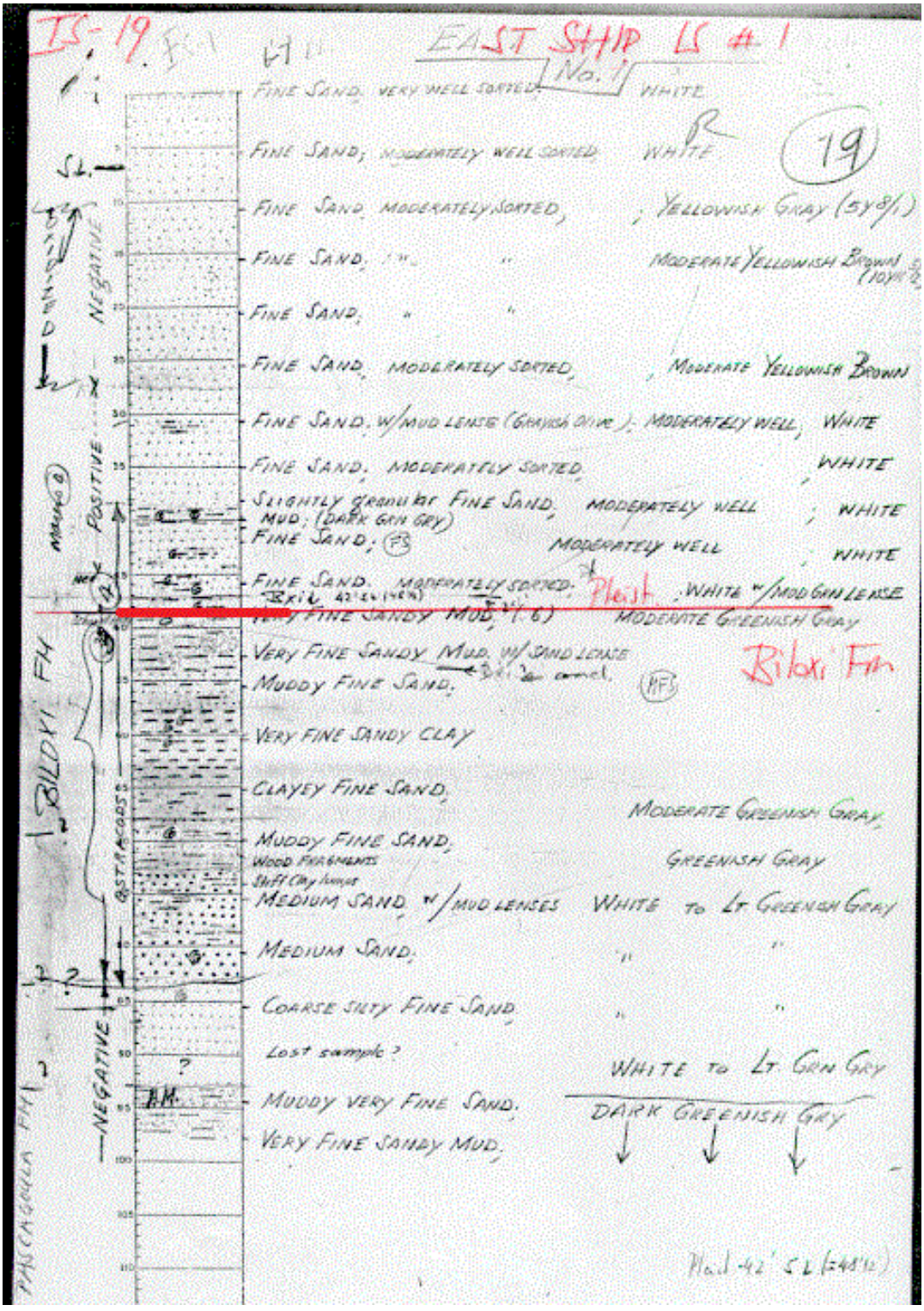

Figure A.22 Mississippi Sound core log BI19 provided by the MDEQ. Red line shows Pleistocene-Holocene contact.

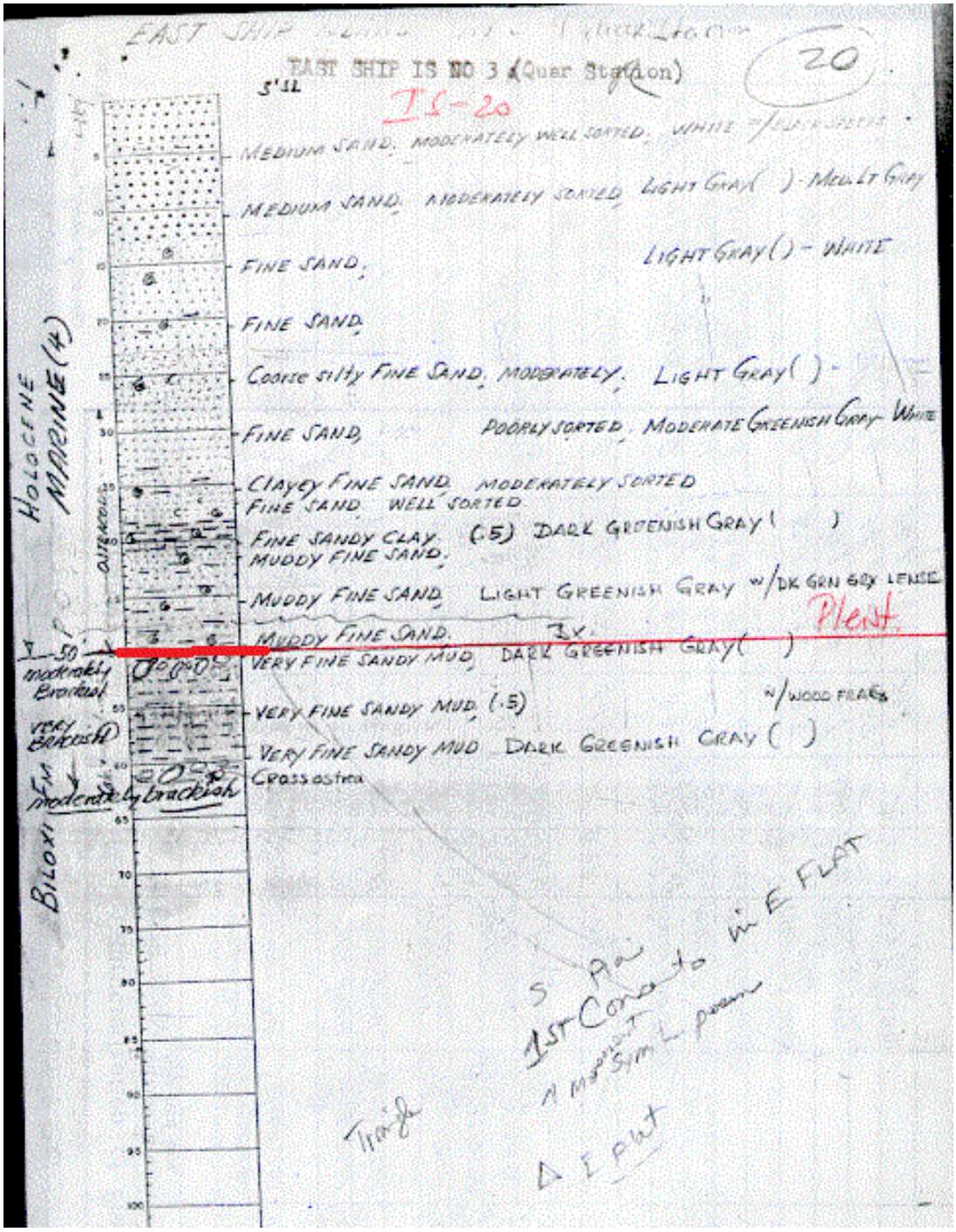

Figure A.23 Mississippi Sound core log BI20 provided by the MDEQ. Red line shows Pleistocene-Holocene contact.

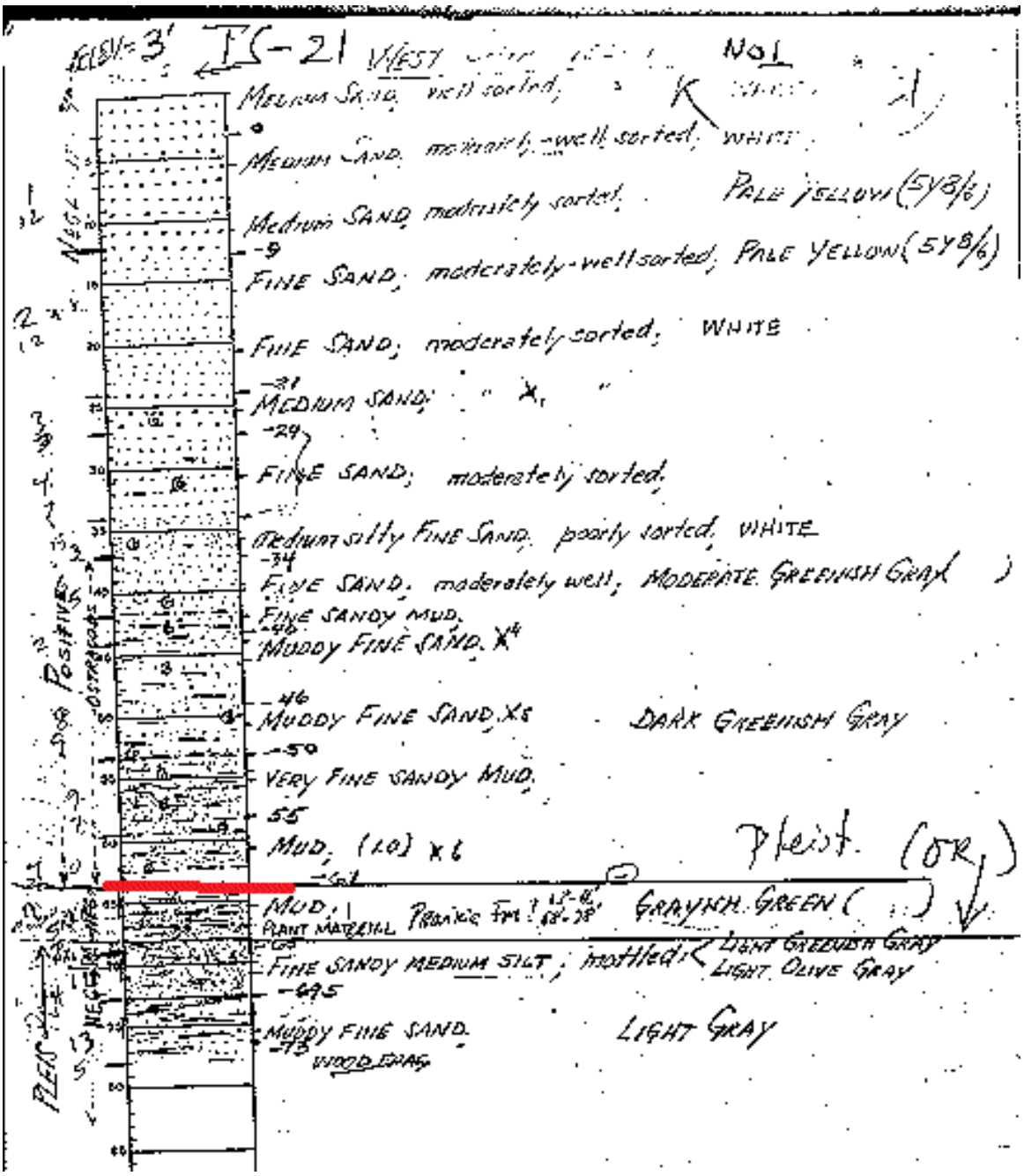

Figure A.24 Mississippi Sound core log BI21 provided by the MDEQ. Red line shows Pleistocene-Holocene contact.

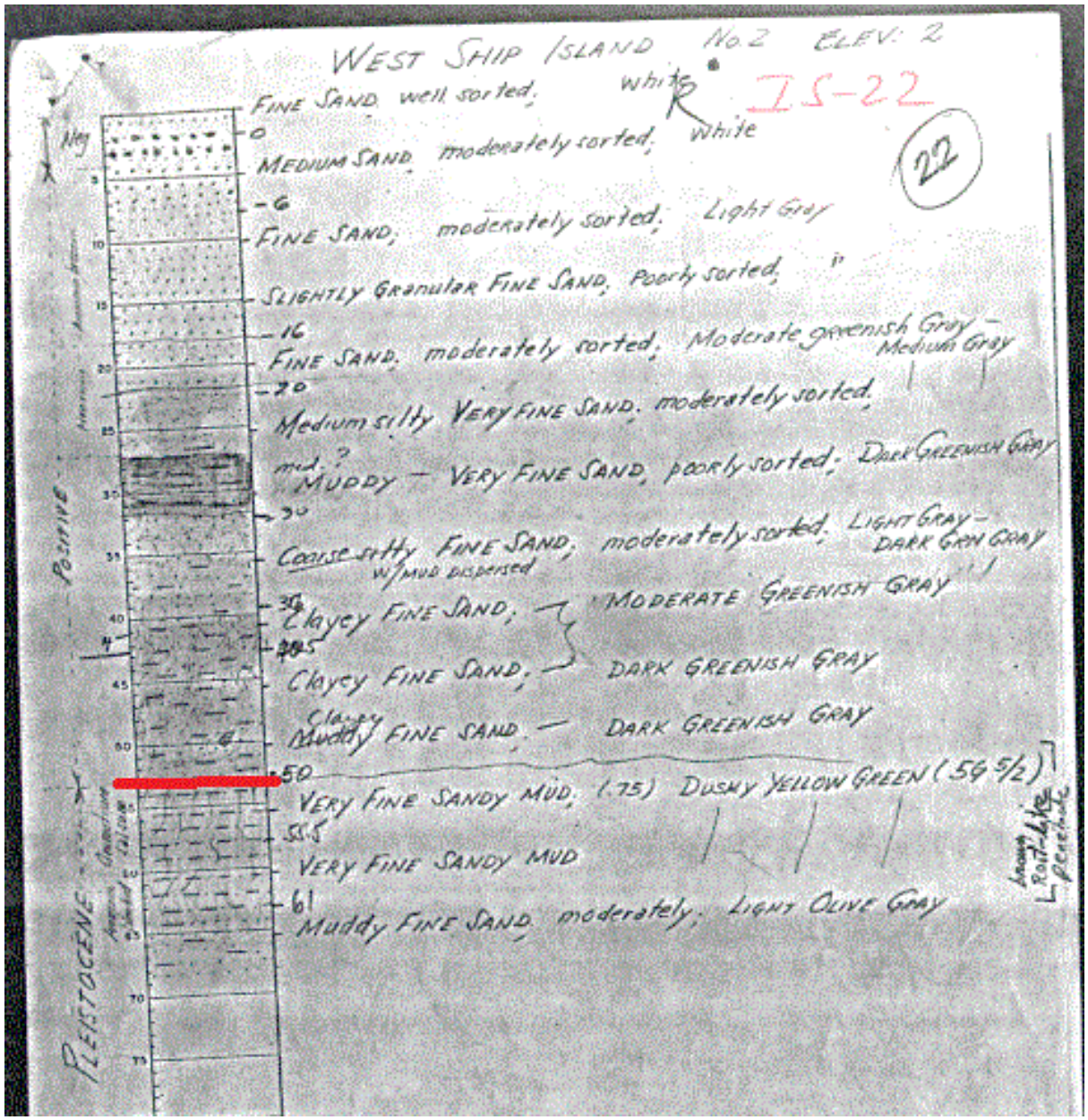

Figure A.25 Mississippi Sound core log BI22 provided by the MDEQ. Red line shows Pleistocene-Holocene contact.

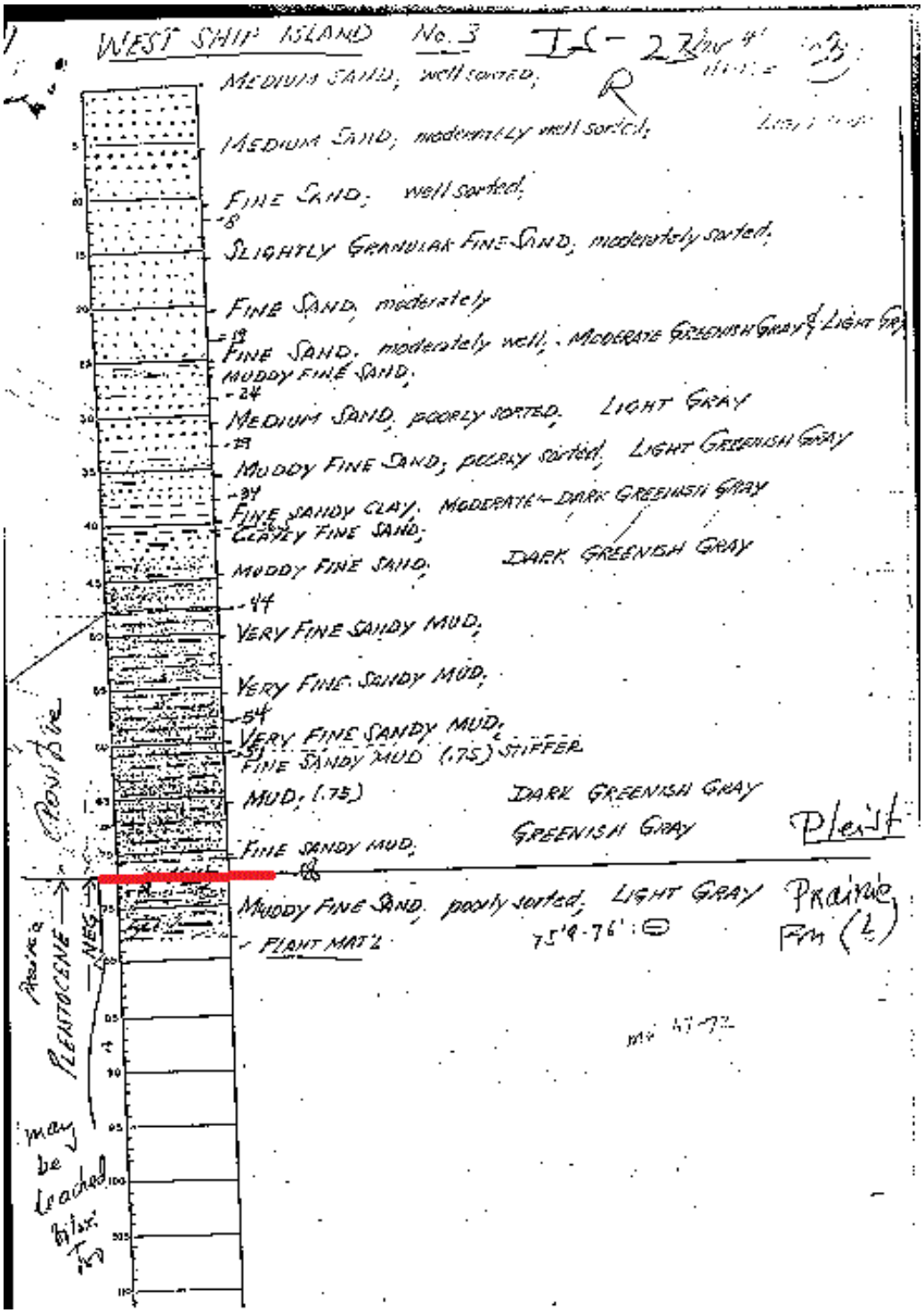

Figure A.26 Mississippi Sound core log BI23 provided by the MDEQ. Red line shows Pleistocene-Holocene contact.

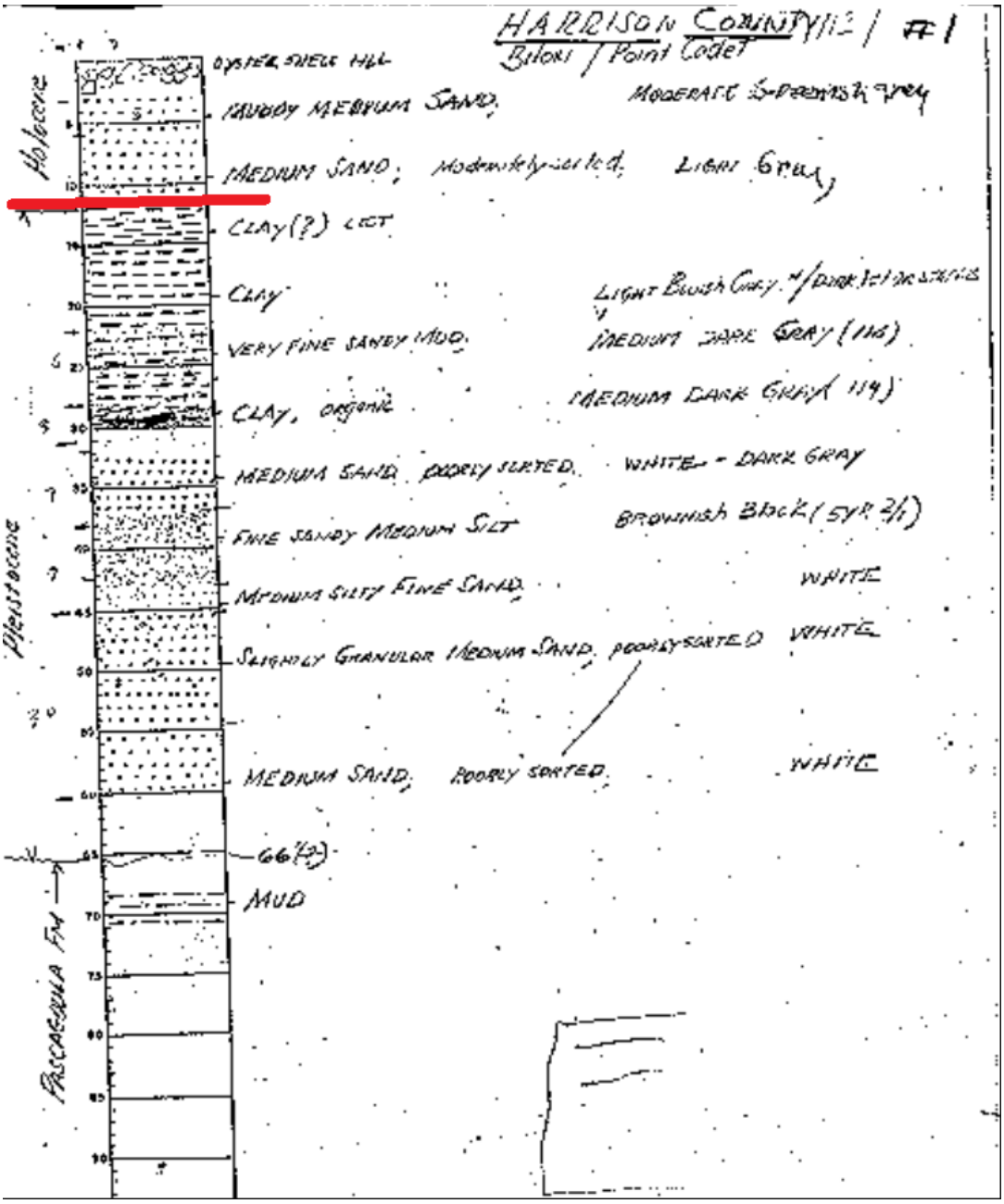

Figure A.27 Harrison County core log HR1 provided by the MDEQ. Red line shows Pleistocene-Holocene contact.

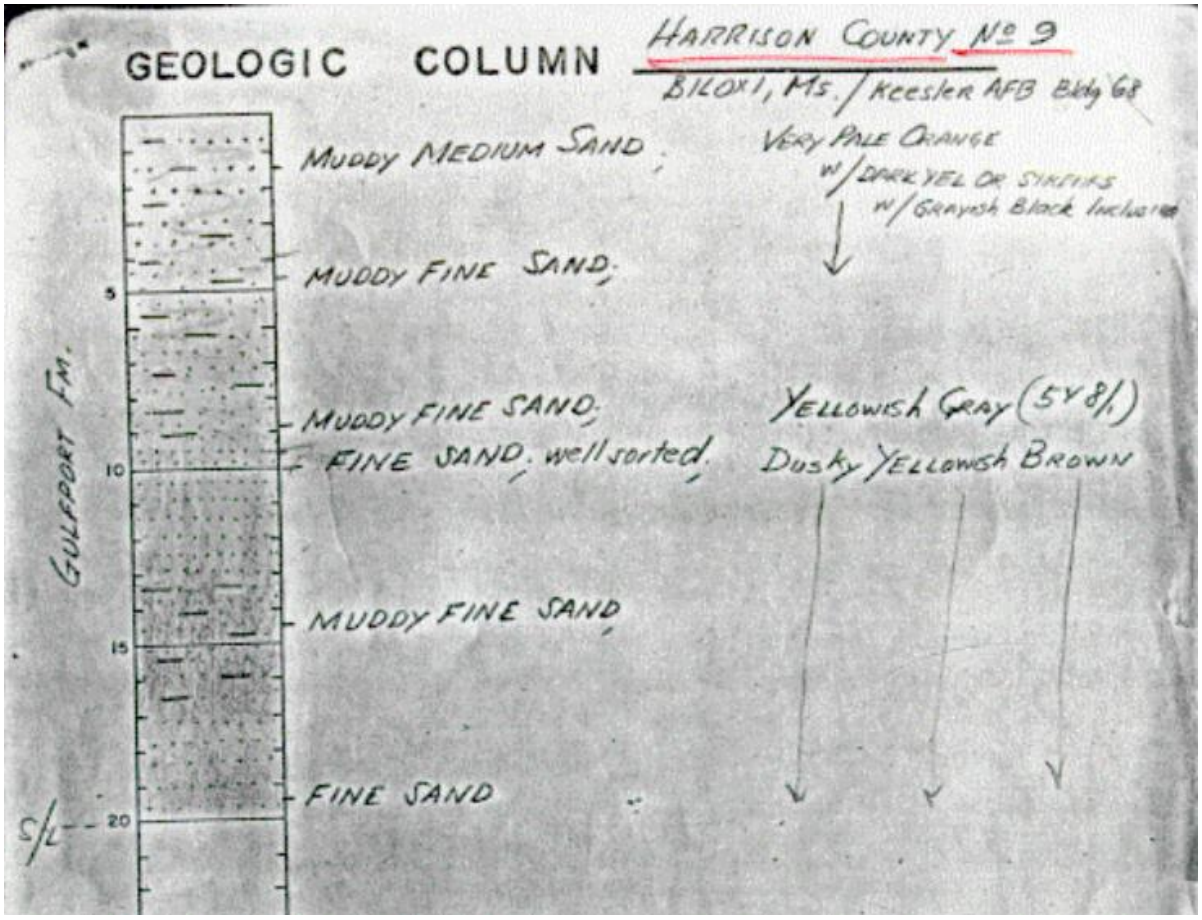

Figure A.28 Harrison County core log HR9 provided by the MDEQ. Pleistocene formations are at the surface.

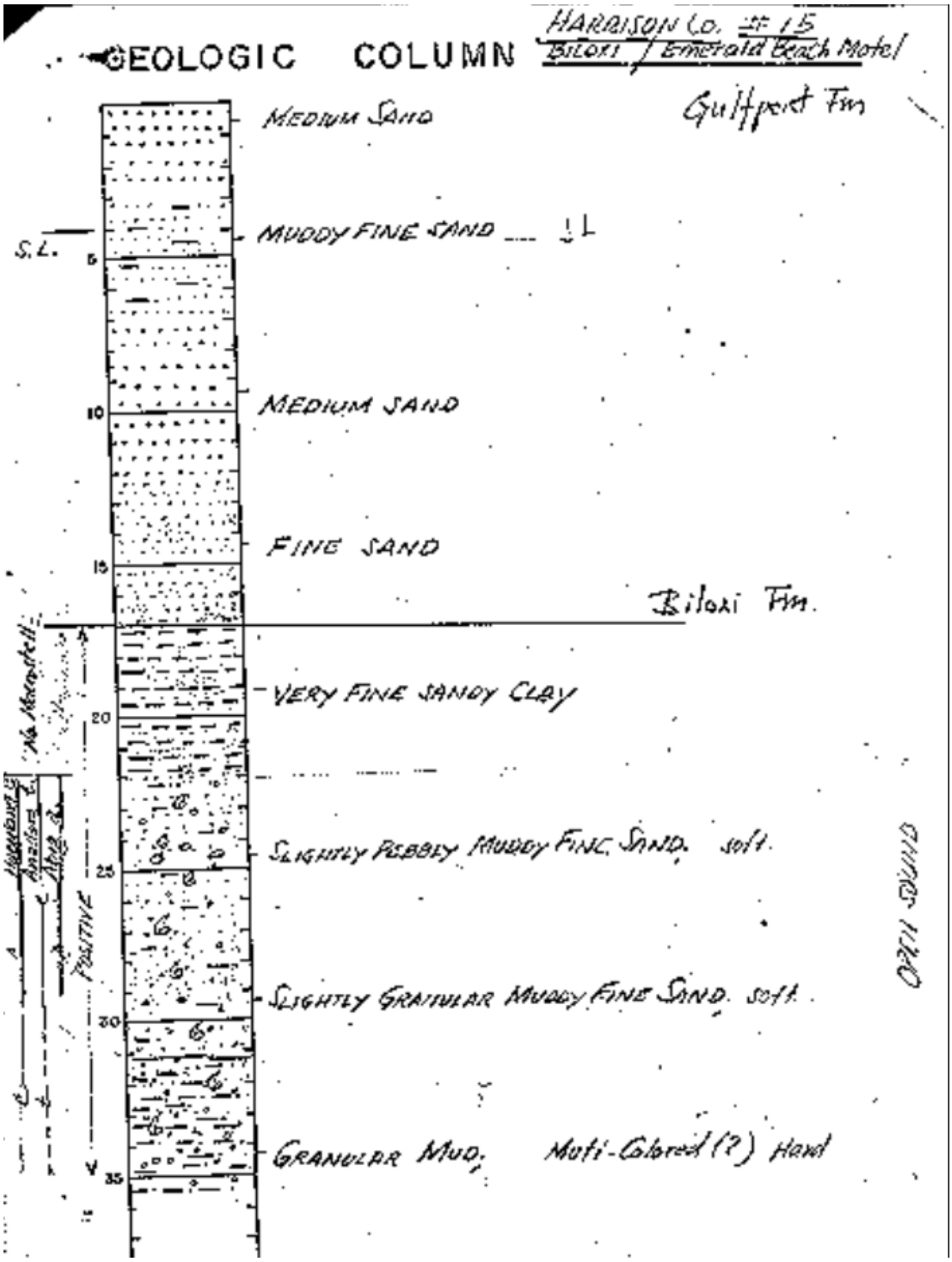

Figure A.29 Harrison County core log HR15 provided by the MDEQ. Pleistocene formations are at the surface.

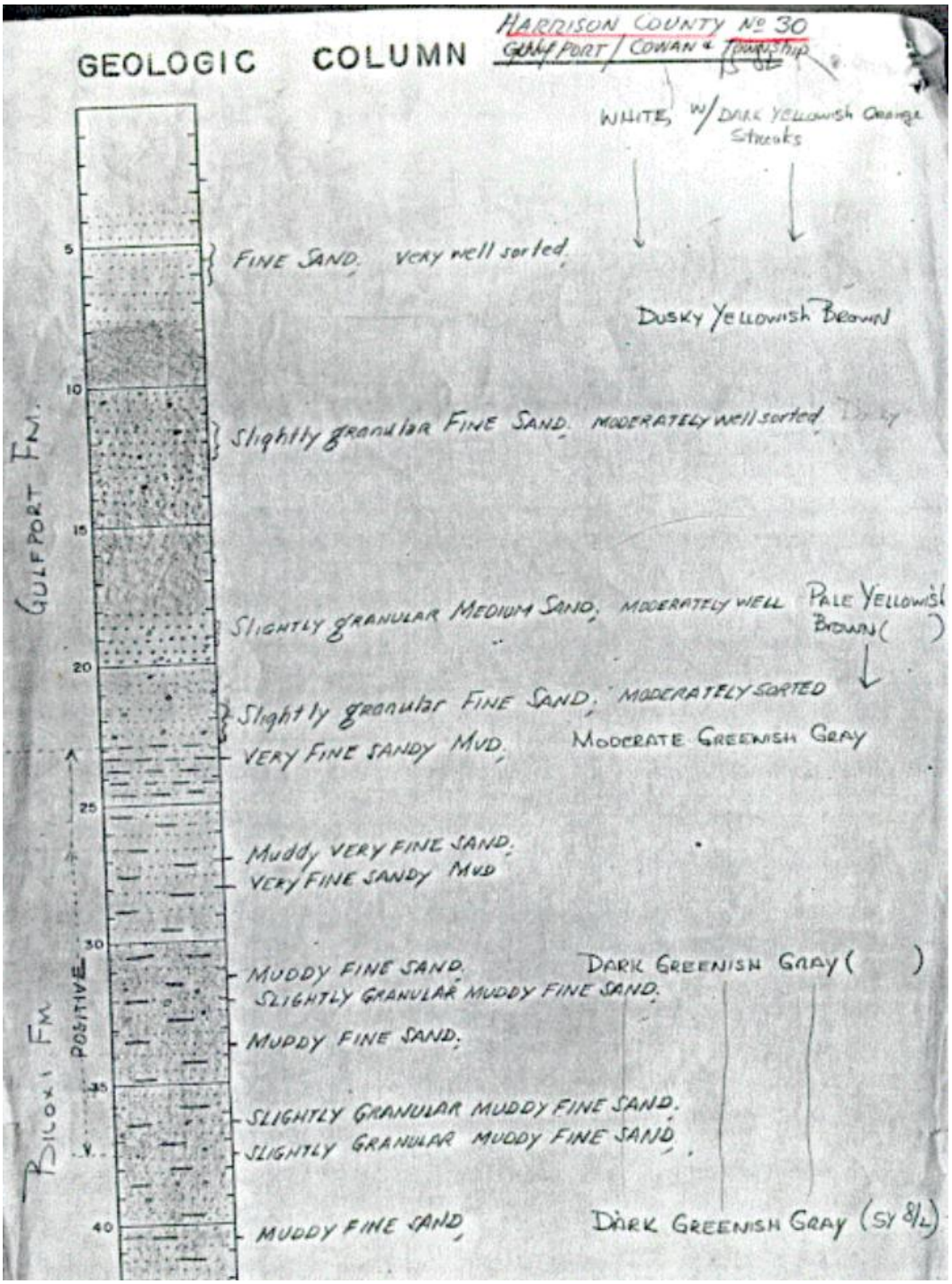

Figure A.30 Harrison County core log HR30 provided by the MDEQ. Pleistocene formations are at the surface.